

Unveiling Multi-Faceted Insights in Cancer Therapeutics

From Immunomodulation to Predictive Signatures

Doctoral thesis

to obtain a doctorate (MD/PhD)

from the Faculty of Medicine

of the University of Bonn

Fangfang Ge

from Henan/(PR) China

2023

Written with authorization of
the Faculty of Medicine of the University of Bonn

First reviewer: Prof. Dr. Ingo Schmidt-Wolf

Second reviewer: Prof. Dr. Ulrich Jaehde

Day of oral examination: 30.11.2023

From Department of Integrated Oncology, Center for Integrated Oncology (CIO) of
University Hospital Bonn

Director: Prof. Dr. med. Ingo Schmidt-Wolf

Table of Contents

	List of abbreviations	4
1.	Abstract	5
2.	Introduction and aims with references	7
2.1	Background	7
2.1.1	CIK cells	7
2.1.2	Hematologic malignancy and liver cancer	7
2.1.3	Oncologic and Non-oncologic drug	9
2.1.4	Long Noncoding RNA	10
2.2	Aims	11
2.3	References	12
3.	Publications	21
3.1	Publication 1: Cytokine-Induced Killer Cells in Combination with Heat Shock Protein 90 Inhibitors Functioning via the Fas/FasL Axis Provides Rationale for a Potential Clinical Benefit in Burkitt's lymphoma	21
3.2	Publication 2: Non-oncology drug (meticrane) shows anti-cancer ability in synergy with epigenetic inhibitors and appears to be involved passively in targeting cancer cells	37
3.3	Publication 3: Computational analysis of heat shock proteins and ferroptosis-associated lncRNAs to predict prognosis in acute myeloid leukemia patients	50
3.4	Publication 4: Immunoautophagy-Related Long Noncoding RNA (IAR-lncRNA) Signature Predicts Survival in Hepatocellular Carcinoma	60
4.	Discussion with references	72
4.1	Main findings	72
4.2	Further perspective	75
4.3	References	77
5.	Acknowledgement	80

List of abbreviations

CIK cell	cytokine-induced killer cell
NK cell	natural killer cell
NKG2D	natural killer group 2, member D
MICA/B	major histocompatibility complex class I polypeptide related sequence A and B
HSP	heat shock protein
17-DMAG	17-dimethylaminoethylamino-17 demethoxygeldanamycin
BL	Burkitt's lymphoma
PI3K	phosphoinositide 3-kinase
SYK	spleen tyrosine kinase
TCGA	the cancer genome atlas
KM curve	Kaplan–Meier curve
ICI	immune checkpoint inhibitor
HDAC	histone deacetylase
AML	acute myeloid leukemia
lncRNAs	long non-coding RNAs
TIDE	Tumor Immune Dysfunction and Exclusion
DNMT	DNA methyltransferase
IARlncRNA	immuno-autophagy-related long non-coding RNA
HCC	Hepatocellular carcinoma
ATG	autophagy-related genes
AIC	Akaike information criterion
FDR	false discovery rate

1. Abstract

Continual and dedicated endeavors are actively underway to advance the field of cancer immunotherapy, with a specific focus on enhancing the efficacy and applicability of various methodologies. One prominent avenue of research involves the ongoing refinement of cytokine-induced killer (CIK) cell therapy, a promising immunotherapeutic approach. CIK cells cytotoxicity against a variety of tumor target cells, potentially synergistic with surgery, chemotherapy, and radiotherapy. In the realm of addressing hematological malignancies and liver cancer, an enduring endeavor persists to uncover novel therapeutic modalities with the intent of attaining enhanced clinical outcomes. This pursuit is driven by the aspiration to curtail instances of recurrence and to efficaciously manage cases post-recurrence. Our research comprises two distinct components. The first pertains to the assessment of both the efficacy and underlying mechanisms associated with the combination of Cytokine-Induced Killer (CIK) cells and anti-tumor agents encompassing HSP90 inhibitors (namely, 17-DMAG and Ganetespib) as well as non-anti-tumor agents (such as meticrane) for the treatment of hematological malignancies and liver cancer. The second facet of our study involves the elucidation of non-coding RNA (long non-coding RNA, or lncRNA) profiles within the context of cancer. The primary objectives encompass prognostic prediction and the identification of potential therapeutic targets inherent to these intricate molecular signatures. In our publication, our results revealed that CIK cytotoxicity in Burkitt's lymphoma (BL) cells was augmented in combination with HSP90 inhibitors and we provide evidence that CIK cells combination with HSP90 inhibitors, target BL cells via the Fas–FasL axis rather than the NKG2D pathway. We also evaluated the antitumor properties of the diuretic drug meticrane against hematological malignancies and liver cancer, and its synergistic effect when combined with CIK cells and epigenetic drugs for cancer therapy. Meticrane exhibited notable anti-cancer properties in the contexts of both liver cancer and leukemia. Moreover, its application in conjunction with epigenetic agents displayed an inclination towards additive or synergistic interactions, thereby presenting a promising avenue for therapeutic enhancement against both

liver cancer and Hematological malignancies. However, it is noteworthy that no synergistic effect was observed when combined with Cytokine-Induced Killer (CIK) cells, as opposed to the independent utilization of CIK cells and meticrane in addressing Hematological malignancies and liver cancer. We utilized bioinformatic analysis to discern lncRNAs with plausible associations to the survival outcomes of cancer patients. Through this rigorous approach, we successfully identified a subset of lncRNAs that exhibit significant prognostic relevance within the context of cancer patients.

Collectively, the integrated approach involving the concurrent administration of Cytokine-Induced Killer (CIK) cells and HSP90 inhibitors presents a promising avenue for conferring tangible clinical advantages to individuals afflicted with Burkitt's lymphoma (BL). Furthermore, meticrane has demonstrated pronounced anti-cancer efficacy, and its conjunction with epigenetic agents has unveiled an inclination towards additive or synergistic responses in the treatment of liver cancer and leukemia. In addition, our research has contributed to the identification of long non-coding RNAs (lncRNAs) closely linked to prognostic considerations, thereby facilitating their potential deployment as predictive tools and therapeutic targets. This multifaceted exploration enriches our comprehension of cancer biology and broadens the horizons of therapeutic strategies.

2. Introduction

2.1 Background:

2.1.1. CIK cells

Comprising a heterogeneous blend of cell populations, cytokine-induced killing (CIK) cells encompass T cells (CD3+CD56-), NKT cells (CD3+CD56+), and NK cells (CD3-CD56+) (Ge et al., 2023). CIK cell therapy has gained notable prominence within the clinical landscape, as underscored by its substantial presence in over 80 clinical trials spanning an array of contexts, encompassing both solid tumors and hematologic malignancies (Sharma and Schmidt-Wolf, 2021). Since its inception in 1991, CIK cell therapy has been administered to more than 5,000 patients across 30 distinct tumor categories, either as standalone intervention or in tandem with supportive care, within the framework of clinical trials (Schmidt-Wolf et al., 1991; Zhang and Schmidt-Wolf, 2020). Moreover, noteworthy statistical enhancements were observed in terms of median progression-free survival and overall survival parameters, along with a significant elevation in 5-year survival rates, as ascertained from the CIK-based study. Owing to their remarkable attributes including MHC-unrestricted tumor lytic capabilities, facile propagation, prospective efficacy against diverse malignancies, and cost-effectiveness, CIK cell therapy has emerged as a prominent contender in the domain of cancer immunotherapy.

2.1.2 Hematologic malignancy and liver cancer

Hematologic malignancies (HM) include a variety of cancers of lymphoid and myeloid origin, such as acute myeloid leukemia (AML), acute lymphoblastic leukemia (ALL), chronic myeloid leukemia (CML), chronic lymphocytic leukemia (CLL), Hodgkin's lymphoma (HL), and non-Hodgkin's lymphoma (NHL), among others. Within the spectrum of hematologic malignancies, lymphoma constitutes a substantial proportion at approximately 40%, while acute myeloid leukemia (AML) represents a notable subset comprising around 10% (Klener et al., 2021). These conditions collectively contribute to a substantial disease landscape, with an estimated 1.2 million new cases of hematologic malignancies reported annually, culminating in approximately 690,000 fatalities (Song et

al., 2020). The most common form of acute leukemia in adults is acute myeloid leukemia (AML) (Shao et al., 2023). Targets for therapeutic intervention within AML encompass a multifaceted landscape spanning elements such as cell cycle regulators, epigenetic modulators, immune checkpoint regulators, metabolic pathways, and tumor cell surface antigens (Noh et al., 2020). Notably, AML holds distinction as the inaugural malignancy to achieve durable remission through allogeneic hematopoietic stem cell transplantation (HSCT), an exceptional therapeutic avenue that stands as the pinnacle of both anti-leukemic strategy and immunotherapy (Xuan and Liu, 2021; Yang et al., 2022). Nonetheless, the inherent toxicity associated with allogeneic HSCT often renders it an impractical option, particularly in the context of elderly patients. This underlines the imperative for immunotherapeutic approaches endowed with precision mechanisms of action, designed to mitigate toxicities while maintaining clinical efficacy. Burkitt's lymphoma (BL) represents a highly aggressive subtype of B-cell non-Hodgkin's lymphoma (NHL), distinguished by the translocation and subsequent dysregulation of the proto-oncogene MYC. BL manifests rapid disease progression and demonstrates a pronounced resistance to conventional chemotherapy regimens. While it is considered a chemosensitive malignancy and one of the early cancers amenable to chemotherapy-driven cure, it is essential to recognize that despite a relatively favorable 5-year overall survival (OS) rate ranging from 75% to 85%, the corresponding 3-year progression-free survival (PFS) and OS metrics stand at 64%, representing a moderate prognosis (Crombie and LaCasce, 2021). Nevertheless, it is noteworthy that certain patient subgroups face elevated treatment-related mortality (TRM) and heightened relapse risks. In light of these clinical complexities, there exists an imperative for the development of novel therapeutic strategies in the realm of Burkitt's lymphoma. This necessity is particularly pronounced for patients who are either unsuitable candidates for intensive therapeutic regimens or who grapple with relapsed disease, thereby underscoring the urgency of innovative treatment modalities.

Hepatocellular carcinoma (HCC), or liver cancer, constitutes a substantial component of the global cancer burden (McGlynn et al., 2021). In recent decades, there has been an observable escalation in the incidence of this ailment across several nations. Despite ranking as the sixth most prevalent form of primary cancer, liver cancer stands as the fourth principal contributor to cancer-associated mortality on a global scale (Li et al.,

2021). It is noteworthy that in the year 2018, the worldwide liver cancer mortality rate was estimated at 8.5 per 100,000 individuals (Shi et al., 2021). Immunotherapy has substantial attention as a therapeutic avenue, emerging as a consequential option beyond the realms of surgery, radiotherapy, and chemotherapy, and in certain cases, even advancing to the forefront as a first-line intervention across diverse malignancies (Oura et al., 2021). This shift underscores the intricate interplay of factors encompassing tumor heterogeneity, dynamic alterations in the tumor microenvironment (TME), the emergence of drug resistance, hypervascularity, hypoxia, and the often formidable side effects associated with traditional therapies. In the specific context of hepatocellular carcinoma (HCC), monotherapies involving immune checkpoint inhibitors (ICIs) or adoptive cell therapies (ACT) have encountered challenges in meeting pivotal clinical benchmarks, such as tumor size reduction and robust anti-tumor responses (Murciano-Goroff et al., 2020; Tagliamonte et al., 2020; Sangro et al., 2021). This necessitates a judicious approach in the selection of treatment regimens that holds the potential to enhance therapeutic efficacy.

While recent decades have witnessed significant strides in the domain of anticancer therapies, leading to notable enhancements in survival rates, it remains imperative to acknowledge that these therapeutic interventions often entail cytotoxic repercussions and subsequent enduring complexities. Such ramifications place a considerable strain on both patients and the healthcare infrastructure. Consequently, the imperative for more advanced and refined treatment modalities becomes increasingly urgent. In recent times, an increasing body of evidence has come to the fore, underscoring the auspicious correlation between cytokine-induced killer (CIK) cells and their efficacy against hematological malignancies and liver cancer (Schmeel et al., 2014; Lee et al., 2015; Pittari et al., 2015; Luo et al., 2016; Yang et al., 2018; Dalla Pietà et al., 2021; Yuan et al., 2021). These insights not only underscore the significance of comprehending the intricate mechanisms and pertinent targets underlying CIK cell therapy within the framework of disease development, progression, and therapeutic interventions, but also accentuate the imperative for the continued exploration and thorough investigation of this domain.

2.1.3 Oncologic and Non-oncologic drug

The augmentation of tumor eradication can be achieved through the synergistic interplay of cytokine-induced killer (CIK) cells in tandem with chemotherapy (Choi et al., 2022; F et al., 2022; Wu et al., 2023). The discernible role of heightened heat shock protein 90 (HSP90) expression in potentially instigating cancer development has been acknowledged (Barrott and Haystead, 2013; Kryeziu et al., 2019). A wealth of investigations has elucidated that HSP90 client proteins assume pivotal roles in the orchestration of diverse cellular functions. These encompass intricate processes such as signal transduction, protein trafficking, chromatin remodeling, autophagy, and the regulation of cell proliferation and survival (Terasawa et al., 2005; Whitesell and Lindquist, 2005; Tsutsumi et al., 2009; Zuehlke and Johnson, 2010; Miyata et al., 2013). A prevalence of HSP90 overexpression has been noted across a diverse spectrum of malignancies, prompting investigations into the modulation of its activity as a strategic measure in combating cancer. Therefore, HSP90 inhibitors are also widely used in cancer treatment. While anticancer/chemotherapy agents exhibit the capability to eradicate malignant cells, their action often comes at the cost of detrimental effects on healthy cells, giving rise to a range of associated adverse events. Consequently, the exploration of non-oncological pharmaceuticals and drugs originally intended for disparate medical conditions has surfaced as a promising avenue in the quest for potential therapeutic interventions against cancer (Papapetropoulos and Szabo, 2018; Zhang et al., 2020).

2.1.4 Long Noncoding RNA

Long noncoding RNAs (lncRNAs), form a separate category of RNA molecules that exceed 200 nucleotides in length, characterized by their marked heterogeneity, assume a pivotal regulatory role in modulating gene expression through an array of intricate mechanisms. Their distinct expression patterns in neoplastic settings are intricately linked to the transition from normative cellular states to malignant transformations. Certain lncRNAs have been substantiated in their contribution to fundamental processes such as proliferation, growth, or the sustained survival of cancerous cells (Ghafouri-Fard et al., 2023; Salman et al., 2023; Zhang et al., 2023). Due to their multifarious functional implications across numerous malignancies, lncRNAs have garnered considerable attention. lncRNAs operate not only as pivotal oncogenes or tumor suppressors, participating in a myriad of intricate signaling pathways, but also emerge as noteworthy

predictive markers within diverse cancer typologies, encompassing acute myeloid leukemia (AML) and Hepatocellular Carcinoma (Wong et al., 2018; Huang et al., 2020; Qin et al., 2020; Goyal et al., 2021; Chen et al., 2022, 35790864; Eptaminitaki et al., 2022; Li et al., 2022b).

2.2 Aims:

Currently, there exists a well-defined signaling pathway and molecular mechanism elucidating the association between CIK cells and cancer. This dissertation aims at the following: firstly, to investigate the efficacy and underlying mechanisms of oncology and Non oncology drug in synergy with CIK cell immunotherapy for the treatment of hematological malignancies and liver cancer. Secondly, to employ bioinformatics analyses to discern long non-coding RNAs (lncRNAs) potentially associated with survival outcomes in cancer patients and seeks to identify additional lncRNAs in cancers to improve the prediction of cancer patient prognosis and discover potential cancer targets.

2.3 References

- Barrott, J. J., and Haystead, T. A. J. (2013). Hsp90, an unlikely ally in the war on cancer. *FEBS J* 280, 1381–1396. doi: 10.1111/febs.12147.
- Chen, M., Zhang, C., Liu, W., Du, X., Liu, X., and Xing, B. (2022). Long noncoding RNA LINC01234 promotes hepatocellular carcinoma progression through orchestrating aspartate metabolic reprogramming. *Mol Ther* 30, 2354–2369. doi: 10.1016/j.ymthe.2022.02.020.
- Choi, J. H., Nam, G. H., Hong, J.-M., Cho, I. R., Paik, W. H., Ryu, J. K., et al. (2022). Cytokine-Induced Killer Cell Immunotherapy Combined With Gemcitabine Reduces Systemic Metastasis in Pancreatic Cancer: An Analysis Using Preclinical Adjuvant Therapy-Mimicking Pancreatic Cancer Xenograft Model. *Pancreas* 51, 1251–1257. doi: 10.1097/MPA.0000000000002176.
- Crombie, J., and LaCasce, A. (2021). The treatment of Burkitt lymphoma in adults. *Blood* 137, 743–750. doi: 10.1182/blood.2019004099.
- Dalla Pietà, A., Cappuzzello, E., Palmerini, P., Ventura, A., Visentin, A., Astori, G., et al. (2021). Innovative therapeutic strategy for B-cell malignancies that combines obinutuzumab and cytokine-induced killer cells. *J Immunother Cancer* 9, e002475. doi: 10.1136/jitc-2021-002475.
- Eptaminitaki, G. C., Stellas, D., Bonavida, B., and Baritaki, S. (2022). Long non-coding RNAs (lncRNAs) signaling in cancer chemoresistance: From prediction to druggability. *Drug Resist Updat* 65, 100866. doi: 10.1016/j.drug.2022.100866.
- F, F., N, Y., and N, R. (2022). Cytokine-induced killer cells mediated pathways in the treatment of colorectal cancer. *Cell communication and signaling: CCS* 20. doi: 10.1186/s12964-022-00836-0.
- Fan, X.-Y., Wang, P.-Y., Zhang, C., Zhang, Y.-L., Fu, Y., Zhang, C., et al. (2017). All-trans retinoic acid enhances cytotoxicity of CIK cells against human lung adenocarcinoma by upregulating MICA and IL-2 secretion. *Sci Rep* 7, 16481. doi: 10.1038/s41598-017-16745-z.

- Ge, F., Wang, Y., Sharma, A., Yang, Y., Liu, H., Essler, M., et al. (2023). Cytokine-Induced Killer Cells in Combination with Heat Shock Protein 90 Inhibitors Functioning via the Fas/FasL Axis Provides Rationale for a Potential Clinical Benefit in Burkitt's lymphoma. *Int J Mol Sci* 24, 12476. doi: 10.3390/ijms241512476.
- Ghafouri-Fard, S., Ahmadi Teshnizi, S., Hussien, B. M., Taheri, M., and Zali, H. (2023). A review on the role of GHET1 in different cancers. *Pathol Res Pract* 247, 154545. doi: 10.1016/j.prp.2023.154545.
- Goyal, B., Yadav, S. R. M., Awasthee, N., Gupta, S., Kunnumakkara, A. B., and Gupta, S. C. (2021). Diagnostic, prognostic, and therapeutic significance of long non-coding RNA MALAT1 in cancer. *Biochim Biophys Acta Rev Cancer* 1875, 188502. doi: 10.1016/j.bbcan.2021.188502.
- Huang, Z., Zhou, J.-K., Peng, Y., He, W., and Huang, C. (2020). The role of long noncoding RNAs in hepatocellular carcinoma. *Mol Cancer* 19, 77. doi: 10.1186/s12943-020-01188-4.
- Kennedy, L. B., and Salama, A. K. S. (2020). A review of cancer immunotherapy toxicity. *CA Cancer J Clin* 70, 86–104. doi: 10.3322/caac.21596.
- Klener, P., Sovilj, D., Renesova, N., and Andera, L. (2021). BH3 Mimetics in Hematologic Malignancies. *Int J Mol Sci* 22, 10157. doi: 10.3390/ijms221810157.
- Kryeziu, K., Bruun, J., Guren, T. K., Sveen, A., and Lothe, R. A. (2019). Combination therapies with HSP90 inhibitors against colorectal cancer. *Biochim Biophys Acta Rev Cancer* 1871, 240–247. doi: 10.1016/j.bbcan.2019.01.002.
- Laport, G. G., Sheehan, K., Baker, J., Armstrong, R., Wong, R. M., Lowsky, R., et al. (2011). Adoptive immunotherapy with cytokine-induced killer cells for patients with relapsed hematologic malignancies after allogeneic hematopoietic cell transplantation. *Biol Blood Marrow Transplant* 17, 1679–1687. doi: 10.1016/j.bbmt.2011.05.012.

- Lee, J. H., Lee, J.-H., Lim, Y.-S., Yeon, J. E., Song, T.-J., Yu, S. J., et al. (2015). Adjuvant immunotherapy with autologous cytokine-induced killer cells for hepatocellular carcinoma. *Gastroenterology* 148, 1383-1391.e6. doi: 10.1053/j.gastro.2015.02.055.
- Li, C., Tu, J., Han, G., Liu, N., and Sheng, C. (2022a). Heat shock protein 90 (Hsp90)/Histone deacetylase (HDAC) dual inhibitors for the treatment of azoles-resistant *Candida albicans*. *Eur J Med Chem* 227, 113961. doi: 10.1016/j.ejmech.2021.113961.
- Li, G., Liu, Y., Zhang, Y., Xu, Y., Zhang, J., Wei, X., et al. (2022b). A Novel Ferroptosis-Related Long Non-Coding RNA Prognostic Signature Correlates With Genomic Heterogeneity, Immunosuppressive Phenotype, and Drug Sensitivity in Hepatocellular Carcinoma. *Front Immunol* 13, 929089. doi: 10.3389/fimmu.2022.929089.
- Li, X., Ramadori, P., Pfister, D., Seehawer, M., Zender, L., and Heikenwalder, M. (2021). The immunological and metabolic landscape in primary and metastatic liver cancer. *Nat Rev Cancer* 21, 541–557. doi: 10.1038/s41568-021-00383-9.
- Liu, Y., and Geng, X. (2022). Long non-coding RNA (lncRNA) CYTOR promotes hepatocellular carcinoma proliferation by targeting the microRNA-125a-5p/LASP1 axis. *Bioengineered* 13, 3666–3679. doi: 10.1080/21655979.2021.2024328.
- Luo, Y., Zeng, H.-Q., Shen, Y., Zhang, P., Lou, S.-F., Chen, L., et al. (2016). Allogeneic hematopoietic stem cell transplantation following donor CIK cell infusion: A phase I study in patients with relapsed/refractory hematologic malignancies. *Leuk Res* 48, 6–10. doi: 10.1016/j.leukres.2016.06.006.
- McGlynn, K. A., Petrick, J. L., and El-Serag, H. B. (2021). Epidemiology of Hepatocellular Carcinoma. *Hepatology* 73 Suppl 1, 4–13. doi: 10.1002/hep.31288.
- Miyata, Y., Nakamoto, H., and Neckers, L. (2013). The therapeutic target Hsp90 and cancer hallmarks. *Curr Pharm Des* 19, 347–365. doi: 10.2174/138161213804143725.

- Murciano-Goroff, Y. R., Warner, A. B., and Wolchok, J. D. (2020). The future of cancer immunotherapy: microenvironment-targeting combinations. *Cell Res* 30, 507–519. doi: 10.1038/s41422-020-0337-2.
- Noh, J.-Y., Seo, H., Lee, J., and Jung, H. (2020). Immunotherapy in Hematologic Malignancies: Emerging Therapies and Novel Approaches. *Int J Mol Sci* 21, 8000. doi: 10.3390/ijms21218000.
- Nwangwu, C. A., Weiher, H., and Schmidt-Wolf, I. G. H. (2017). Increase of CIK cell efficacy by upregulating cell surface MICA and inhibition of NKG2D ligand shedding in multiple myeloma. *Hematol Oncol* 35, 719–725. doi: 10.1002/hon.2326.
- Oura, K., Morishita, A., Tani, J., and Masaki, T. (2021). Tumor Immune Microenvironment and Immunosuppressive Therapy in Hepatocellular Carcinoma: A Review. *Int J Mol Sci* 22, 5801. doi: 10.3390/ijms22115801.
- Papapetropoulos, A., and Szabo, C. (2018). Inventing new therapies without reinventing the wheel: the power of drug repurposing. *Br J Pharmacol* 175, 165–167. doi: 10.1111/bph.14081.
- Pittari, G., Filippini, P., Gentilcore, G., Grivel, J.-C., and Rutella, S. (2015). Revving up Natural Killer Cells and Cytokine-Induced Killer Cells Against Hematological Malignancies. *Front Immunol* 6, 230. doi: 10.3389/fimmu.2015.00230.
- Qin, G., Tu, X., Li, H., Cao, P., Chen, X., Song, J., et al. (2020). Long Noncoding RNA p53-Stabilizing and Activating RNA Promotes p53 Signaling by Inhibiting Heterogeneous Nuclear Ribonucleoprotein K deSUMOylation and Suppresses Hepatocellular Carcinoma. *Hepatology* 71, 112–129. doi: 10.1002/hep.30793.
- Ramaiah, M. J., Tangutur, A. D., and Manyam, R. R. (2021). Epigenetic modulation and understanding of HDAC inhibitors in cancer therapy. *Life Sci* 277, 119504. doi: 10.1016/j.lfs.2021.119504.

- Riley, R. S., June, C. H., Langer, R., and Mitchell, M. J. (2019). Delivery technologies for cancer immunotherapy. *Nat Rev Drug Discov* 18, 175–196. doi: 10.1038/s41573-018-0006-z.
- Roca, M. S., Moccia, T., Iannelli, F., Testa, C., Vitagliano, C., Minopoli, M., et al. (2022). HDAC class I inhibitor domatinostat sensitizes pancreatic cancer to chemotherapy by targeting cancer stem cell compartment via FOXM1 modulation. *J Exp Clin Cancer Res* 41, 83. doi: 10.1186/s13046-022-02295-4.
- Salman, I. T., Abulsoud, A. I., Abo-Elmatty, D. M., Fawzy, A., Mesbah, N. M., and Saleh, S. M. (2023). The long non-coding RNA ZFAS1 promotes colorectal cancer progression via miR200b/ZEB1 axis. *Pathol Res Pract* 247, 154567. doi: 10.1016/j.prp.2023.154567.
- Sangro, B., Sarobe, P., Hervás-Stubbs, S., and Melero, I. (2021). Advances in immunotherapy for hepatocellular carcinoma. *Nat Rev Gastroenterol Hepatol* 18, 525–543. doi: 10.1038/s41575-021-00438-0.
- Schmeel, F. C., Schmeel, L. C., Gast, S.-M., and Schmidt-Wolf, I. G. H. (2014). Adoptive immunotherapy strategies with cytokine-induced killer (CIK) cells in the treatment of hematological malignancies. *Int J Mol Sci* 15, 14632–14648. doi: 10.3390/ijms150814632.
- Schmidt-Wolf, I. G., Negrin, R. S., Kiem, H. P., Blume, K. G., and Weissman, I. L. (1991). Use of a SCID mouse/human lymphoma model to evaluate cytokine-induced killer cells with potent antitumor cell activity. *J Exp Med* 174, 139–149. doi: 10.1084/jem.174.1.139.
- Shao, R., Li, Z., Xin, H., Jiang, S., Zhu, Y., Liu, J., et al. (2023). Biomarkers as targets for CAR-T/NK cell therapy in AML. *Biomark Res* 11, 65. doi: 10.1186/s40364-023-00501-9.
- Sharma, A., and Schmidt-Wolf, I. G. H. (2021). 30 years of CIK cell therapy: recapitulating the key breakthroughs and future perspective. *J Exp Clin Cancer Res* 40, 388. doi: 10.1186/s13046-021-02184-2.

- Shi, J.-F., Cao, M., Wang, Y., Bai, F.-Z., Lei, L., Peng, J., et al. (2021). Is it possible to halve the incidence of liver cancer in China by 2050? *Int J Cancer* 148, 1051–1065. doi: 10.1002/ijc.33313.
- Song, Y., Himmel, B., Öhrmalm, L., and Gyarmati, P. (2020). The Microbiota in Hematologic Malignancies. *Curr Treat Options Oncol* 21, 2. doi: 10.1007/s11864-019-0693-7.
- Tagliamonte, M., Mauriello, A., Cavalluzzo, B., Ragone, C., Manolio, C., Petrizzo, A., et al. (2020). Tackling hepatocellular carcinoma with individual or combinatorial immunotherapy approaches. *Cancer Lett* 473, 25–32. doi: 10.1016/j.canlet.2019.12.029.
- Tang, C., Wang, X., Jin, Y., and Wang, F. (2022). Recent advances in HDAC-targeted imaging probes for cancer detection. *Biochim Biophys Acta Rev Cancer* 1877, 188788. doi: 10.1016/j.bbcan.2022.188788.
- Terasawa, K., Minami, M., and Minami, Y. (2005). Constantly updated knowledge of Hsp90. *J Biochem* 137, 443–447. doi: 10.1093/jb/mvi056.
- Tsutsumi, S., Beebe, K., and Neckers, L. (2009). Impact of heat-shock protein 90 on cancer metastasis. *Future Oncol* 5, 679–688. doi: 10.2217/fon.09.30.
- Wang, D., Zeng, T., Lin, Z., Yan, L., Wang, F., Tang, L., et al. (2020a). Long non-coding RNA SNHG5 regulates chemotherapy resistance through the miR-32/DNAJB9 axis in acute myeloid leukemia. *Biomed Pharmacother* 123, 109802. doi: 10.1016/j.biopha.2019.109802.
- Wang, X., Waschke, B. C., Woolaver, R. A., Chen, S. M. Y., Chen, Z., and Wang, J. H. (2020b). HDAC inhibitors overcome immunotherapy resistance in B-cell lymphoma. *Protein Cell* 11, 472–482. doi: 10.1007/s13238-020-00694-x.
- Wang, Y., Li, W., Chen, X., Li, Y., Wen, P., and Xu, F. (2019). MIR210HG predicts poor prognosis and functions as an oncogenic lncRNA in hepatocellular carcinoma. *Biomed Pharmacother* 111, 1297–1301. doi: 10.1016/j.biopha.2018.12.134.

- Whitesell, L., and Lindquist, S. L. (2005). HSP90 and the chaperoning of cancer. *Nat Rev Cancer* 5, 761–772. doi: 10.1038/nrc1716.
- Wong, N. K., Huang, C.-L., Islam, R., and Yip, S. P. (2018). Long non-coding RNAs in hematological malignancies: translating basic techniques into diagnostic and therapeutic strategies. *J Hematol Oncol* 11, 131. doi: 10.1186/s13045-018-0673-6.
- Wu, C.-C., Pan, M.-R., Shih, S.-L., Shiau, J.-P., Wu, C.-C., Chang, S.-J., et al. (2023). Combination of FAK inhibitor and cytokine-induced killer cell therapy: An alternative therapeutic strategy for patients with triple-negative breast cancer. *Biomed Pharmacother* 163, 114732. doi: 10.1016/j.biopha.2023.114732.
- Wu, F., Wei, H., Liu, G., and Zhang, Y. (2021a). Bioinformatics Profiling of Five Immune-Related lncRNAs for a Prognostic Model of Hepatocellular Carcinoma. *Front Oncol* 11, 667904. doi: 10.3389/fonc.2021.667904.
- Wu, X., Sharma, A., Oldenburg, J., Weiher, H., Essler, M., Skowasch, D., et al. (2021b). NKG2D Engagement Alone Is Sufficient to Activate Cytokine-Induced Killer Cells While 2B4 Only Provides Limited Coactivation. *Front Immunol* 12, 731767. doi: 10.3389/fimmu.2021.731767.
- Wu, X., Zhang, Y., Li, Y., and Schmidt-Wolf, I. G. H. (2020). Increase of Antitumoral Effects of Cytokine-Induced Killer Cells by Antibody-Mediated Inhibition of MICA Shedding. *Cancers (Basel)* 12, 1818. doi: 10.3390/cancers12071818.
- Xuan, L., and Liu, Q. (2021). Maintenance therapy in acute myeloid leukemia after allogeneic hematopoietic stem cell transplantation. *J Hematol Oncol* 14, 4. doi: 10.1186/s13045-020-01017-7.
- Yang, G., Wang, X., Huang, S., Huang, R., Wei, J., Wang, X., et al. (2022). Generalist in allogeneic hematopoietic stem cell transplantation for MDS or AML: Epigenetic therapy. *Front Immunol* 13, 1034438. doi: 10.3389/fimmu.2022.1034438.
- Yang, T., Zhang, W., Wang, L., Xiao, C., Wang, L., Gong, Y., et al. (2018). Co-culture of dendritic cells and cytokine-induced killer cells effectively suppresses liver cancer

- stem cell growth by inhibiting pathways in the immune system. *BMC Cancer* 18, 984. doi: 10.1186/s12885-018-4871-y.
- Yuan, H., Ren, G., Liu, K., and Zhao, Z. (2021). Effect of Incorporating Polyvinyl Alcohol Fiber on the Mechanical Properties of EICP-Treated Sand. *Materials (Basel)* 14, 2765. doi: 10.3390/ma14112765.
- Zhang, H., Ma, B., Li, N., Zhang, L., Xu, J., Zhang, S., et al. (2023). SNHG1, a KLF4-upregulated gene, promotes glioma cell survival and tumorigenesis under endoplasmic reticulum stress by upregulating BIRC3 expression. *J Cell Mol Med* 27, 1806–1819. doi: 10.1111/jcmm.17779.
- Zhang, L., Ke, W., Hu, P., Li, Z., Geng, W., Guo, Y., et al. (2022). N6-Methyladenosine-Related lncRNAs Are Novel Prognostic Markers and Predict the Immune Landscape in Acute Myeloid Leukemia. *Front Genet* 13, 804614. doi: 10.3389/fgene.2022.804614.
- Zhang, Y., and Schmidt-Wolf, I. G. H. (2020). Ten-year update of the international registry on cytokine-induced killer cells in cancer immunotherapy. *J Cell Physiol* 235, 9291–9303. doi: 10.1002/jcp.29827.
- Zhang, Z., Zhou, L., Xie, N., Nice, E. C., Zhang, T., Cui, Y., et al. (2020). Overcoming cancer therapeutic bottleneck by drug repurposing. *Signal Transduct Target Ther* 5, 113. doi: 10.1038/s41392-020-00213-8.
- Zhao, C., Wang, Y., Tu, F., Zhao, S., Ye, X., Liu, J., et al. (2021). A Prognostic Autophagy-Related Long Non-coding RNA (ARlncRNA) Signature in Acute Myeloid Leukemia (AML). *Front Genet* 12, 681867. doi: 10.3389/fgene.2021.681867.
- Zhu, Y., He, J., Li, Z., and Yang, W. (2023). Cuproptosis-related lncRNA signature for prognostic prediction in patients with acute myeloid leukemia. *BMC Bioinformatics* 24, 37. doi: 10.1186/s12859-023-05148-9.

Zuehlke, A., and Johnson, J. L. (2010). Hsp90 and co-chaperones twist the functions of diverse client proteins. *Biopolymers* 93, 211–217. doi: 10.1002/bip.21292.

3. Publications

3.1 Publication 1: Cytokine-Induced Killer Cells in Combination with Heat Shock Protein 90 Inhibitors Functioning via the Fas/FasL Axis Provides Rationale for a Potential Clinical Benefit in Burkitt's Lymphoma

Fangfang Ge¹, Yulu Wang¹, Amit Sharma^{1,2}, Yu Yang³, Hongde Liu³, Markus Essler⁴, Ulrich Jaehde⁵ and Ingo G. H. Schmidt-Wolf^{1,*}

¹Department of Integrated Oncology, Center for Integrated Oncology (CIO), University Hospital of Bonn, 53127 Bonn, Germany; gefangfang3@gmail.com (F.G.); yuluwang3@gmail.com (Y.W.); amit.sharma@ukbonn.de (A.S.)

²Department of Neurosurgery, University Hospital Bonn, 53127 Bonn, Germany

³State Key Laboratory of Bioelectronics, School of Biological Science & Medical Engineering, Southeast University, Nanjing 210096, China; 220212221@seu.edu.cn (Y.Y.); liuhongde@seu.edu.cn (H.L.)

⁴Department of Nuclear Medicine, University Hospital Bonn, 53127 Bonn, Germany; markus.essler@ukbonn.de

⁵Department of Clinical Pharmacy, Institute of Pharmacy, University of Bonn, 53121 Bonn, Germany;



Article

Cytokine-Induced Killer Cells in Combination with Heat Shock Protein 90 Inhibitors Functioning via the Fas/FasL Axis Provides Rationale for a Potential Clinical Benefit in Burkitt's lymphoma

Fangfang Ge ¹, Yulu Wang ¹, Amit Sharma ^{1,2} , Yu Yang ³, Hongde Liu ³ , Markus Essler ⁴, Ulrich Jaehde ⁵ and Ingo G. H. Schmidt-Wolf ^{1,*}

¹ Department of Integrated Oncology, Center for Integrated Oncology (CIO), University Hospital of Bonn, 53127 Bonn, Germany; gefangfang3@gmail.com (F.G.); yuluwang3@gmail.com (Y.W.); amit.sharma@ukbonn.de (A.S.)

² Department of Neurosurgery, University Hospital Bonn, 53127 Bonn, Germany

³ State Key Laboratory of Bioelectronics, School of Biological Science & Medical Engineering, Southeast University, Nanjing 210096, China; 220212221@seu.edu.cn (Y.Y.); liuhongde@seu.edu.cn (H.L.)

⁴ Department of Nuclear Medicine, University Hospital Bonn, 53127 Bonn, Germany; markus.essler@ukbonn.de

⁵ Department of Clinical Pharmacy, Institute of Pharmacy, University of Bonn, 53121 Bonn, Germany; u.jaehde@uni-bonn.de

* Correspondence: ingo.schmidt-wolf@ukbonn.de; Tel.: +49-(0)-228-287-17050

Abstract: Constant efforts are being made to develop methods for improving cancer immunotherapy, including cytokine-induced killer (CIK) cell therapy. Numerous heat shock protein (HSP) 90 inhibitors have been assessed for antitumor efficacy in preclinical and clinical trials, highlighting their individual prospects for targeted cancer therapy. Therefore, we tested the compatibility of CIK cells with HSP90 inhibitors using Burkitt's lymphoma (BL) cells. Our analysis revealed that CIK cytotoxicity in BL cells was augmented in combination with independent HSP90 inhibitors 17-DMAG (17-dimethylaminoethylamino-17-demethoxygeldanamycin) and ganetespib. Interestingly, CIK cell cytotoxicity did not diminish after blocking with NKG2D (natural killer group 2, member D), which is a prerequisite for their activation. Subsequent analyses revealed that the increased expression of Fas on the surface of BL cells, which induces caspase 3/7-dependent apoptosis, may account for this effect. Thus, we provide evidence that CIK cells, either alone or in combination with HSP90 inhibitors, target BL cells via the Fas–FasL axis rather than the NKG2D pathway. In the context of clinical relevance, we also found that high expression of HSP90 family genes (*HSP90AA1*, *HSP90AB1*, and *HSP90B1*) was significantly associated with the reduced overall survival of BL patients. In addition to HSP90, genes belonging to the Hsp40, Hsp70, and Hsp110 families have also been found to be clinically significant for BL survival. Taken together, the combinatorial therapy of CIK cells with HSP90 inhibitors has the potential to provide clinical benefits to patients with BL.

Keywords: CIK cell; HSP90 inhibitor; Burkitt's lymphoma; Fas–FasL; apoptosis



Citation: Ge, F.; Wang, Y.; Sharma, A.; Yang, Y.; Liu, H.; Essler, M.; Jaehde, U.; Schmidt-Wolf, I.G.H.

Cytokine-Induced Killer Cells in Combination with Heat Shock Protein 90 Inhibitors Functioning via the Fas/FasL Axis Provides Rationale for a Potential Clinical Benefit in Burkitt's lymphoma. *Int. J. Mol. Sci.* **2023**, *24*, 12476. <https://doi.org/10.3390/ijms241512476>

Academic Editor: Akiyoshi Takami

Received: 8 July 2023

Revised: 26 July 2023

Accepted: 2 August 2023

Published: 5 August 2023



Copyright: © 2023 by the authors. Licensee MDPI, Basel, Switzerland. This article is an open access article distributed under the terms and conditions of the Creative Commons Attribution (CC BY) license (<https://creativecommons.org/licenses/by/4.0/>).

1. Introduction

Despite having an unprecedented understanding of cancer today [1–3], it remains one of the leading causes of death. Certainly, there have been a number of efforts to improve treatment options for cancer, most notably by exploring various inhibitors (most recently HSP90 C-terminal inhibitors) in order to understand the molecular and cellular determinants harboring any clinical relevance [4–6]. Since it has been recognized that the overexpression of HSP90 plays a potential role in the development of cancer, researchers have begun to modulate its activity to combat cancer [7–9]. Interestingly, HSP90 overexpression has been observed in numerous cancers, including breast, urinary, ovarian, lung, colon, esophageal, ovarian, endometrial, bone, and prostate cancers [10,11]. HSP90

encompasses various isoforms that exhibit distinct accumulation patterns within cellular compartments. Among the prominent cytoplasmic variants, *HSP90AA1* and *HSP90AB1* have been observed to not only localize in the cytoplasm but also in the nucleus. On the other hand, *HSP90B1*-GRP94 predominantly targets the endoplasmic reticulum lumen, where it plays a role in the unfolded protein response [12]. Another significant HSP90 isoform, TNF-receptor-associated protein-1 (TRAP1), primarily functions as a mitochondrial protein, contributing to mitochondrial integrity, apoptosis regulation, and protection against oxidative stress [13,14]. *HSP90AA1*, *HSP90AB1*, and *HSP90B1* have been associated with a poor prognosis of tumors [15], and upregulation of TRAP1 promotes the growth and progression of various cancers [16].

Burkitt's lymphoma (BL), a rare but extremely aggressive B-cell non-Hodgkin's lymphoma that is usually diagnosed in children and adolescents, seems to be somewhat unique. Valbuena et al. reported moderate to strong cytoplasmic expression levels of HSP90 in all BL cases [17]. Giulino-Roth et al. reported that primary BL tumors overexpress HSP90, and that its inhibition exerts antitumor effects both in vitro and in vivo [18]. These authors found that the inhibition of HSP90 targets multiple components of PI3K/AKT/mTOR signaling, underscoring the importance of this pathway in BL. By characterizing the molecular consequences of HSP90 inhibition in BL cells, Walter et al. provided evidence that SYK is a client protein of HSP90, and that the BCR signaling-dependent phosphorylation of Hsp90 is required for this interaction [19]. Based on these findings, Poole et al. speculated that the MYC-HSP90 axis may be critical for tumor maintenance in BL and may represent a novel therapeutic strategy [20]. These authors showed that the MYC oncogene is a client protein of HSP90 in BL, and that its inhibition using pharmacological inhibitors causes MYC transcription switching and protein destabilization. Overall, HSP90 appears to be a critical component of BL; however, chemotherapy remains the mainstay of BL treatment in the clinic. The use of immunotherapies for BL has also been reported [21,22]; however, their success rates have not been fully elucidated. Notably, the success rates in refractory/relapsed BL cases are extremely low; therefore, there is an urgent need to identify new options. Strikingly, cytokine-induced killer (CIK) cell therapy, which has been successful for 30 years in treating various cancers, has never been tested for BL [23–26].

Being a mixture of cells, CIK cells include T cells (CD3+CD56⁻), NKT cells (CD3+CD56⁺), and NK cells (CD3⁻CD56⁺). CIK cells can significantly lyse cancer cells in an MHC-unrestricted manner by activating NK cell receptors [27]. Alongside directly killing tumor cells, CIK cells can also regulate immune function by releasing various cytokines. Evidence has shown that after stimulation by tumor cells, the amount of proinflammatory cytokines, such as tumor necrosis factor (TNF)- α , IFN- γ , and IL-2, released by CIK cells were significantly increased [28], and these cytokines potentiate systemic antitumor activity. The first clinical trial of CIK cells in lymphoma was reported by Schmidt-Wolf et al. in 1999 [29]. Subsequently, 17 clinical trials have been conducted for the treatment of lymphoma owing to the proven safety of CIK cell therapy [30].

Therefore, in this study, we assessed the compatibility of CIK cells with HSP90 inhibitors (17-DMAG and ganetespib) in diverse BL cell lines. In addition to highlighting the possible mechanism behind their favorable synergistic effect, we discussed the clinical significance of the expression patterns of the HSP90 family (including *HSP90AA1*, *HSP90AB1*, and *HSP90B1*) and nine other heat shock proteins (HSPs) in the survival of patients with BL. To our knowledge, this is the first study to use foreground CIK cell therapy as a potential treatment option for patients with BL.

2. Results

2.1. HSP90 Inhibitors Showed Synergistic Effect with CIK Cells in Burkitt's Lymphoma Cells

First, we investigated the viability of BL cells (specifically BL41 and Raji cells) using two independent HSP90 inhibitors (17-DMAG and ganetespib). An optimal concentration of 17-DMAG (0.1 μ M) and ganetespib (20 nM) was used for further experiments based on the co-culture experiments (Figure 1A). Thereafter, the subtypes of CIK cells were

examined (day 14), and NKT cells (CD3+CD56+, 27.66% \pm 4.573%), T cells (CD3+CD56-, 71.85% \pm 4.607%), and NK cells (CD3-CD56+, 0.7% \pm 0.2%) were identified (Figure 1B). Considering that NKG2D and CD8 were mainly expressed on NKT and T cells, we also examined their individual proportions, as shown in Figure 1B. In the context of synergy, significant results were obtained with Raji cells, while the combined effect of DMSO with CIK cells (25.46% \pm 0.2301%, $p = 0.0002$) and the isolated 17-DMAG (15.38% \pm 5.007%, $p < 0.0001$) treatment group demonstrated a lower efficacy compared to the combination of CIK cells with 17-DMAG (55.25% \pm 4.725%) (Figure 2A). Similar results, especially in BL41 cells, were obtained in that the cytotoxicity of CIK cells in combination with 17-DMAG (27.91% \pm 4.176%) was significantly higher than that of the controls, such as the DMSO in combination with CIK cells (13.6% \pm 0.7162%, $p = 0.0008$) and isolated 17-DMAG (4.317% \pm 0.8552%, $p < 0.0001$) (Figure 2A) groups. In addition, the above findings were confirmed with ganetespib, as the results showed that ganetespib in combination with CIK cells (51.47% \pm 2.357%) significantly increased the cytotoxicity against Raji cells compared to the controls, ganetespib alone (12.33% \pm 1.911%, $p < 0.0001$), and DMSO in combination with CIK cells (24.90% \pm 3.954%, $p < 0.0001$) (Figure 2B). Similarly, for BL41 cells, the cytotoxicity of CIK cells in combination with ganetespib (72.12% \pm 5.537%) was higher than that of the controls, isolated ganetespib (16.37% \pm 5.272, $p < 0.0001$) treatment, and DMSO in combination with CIK cells (11.19 \pm 1.295, $p < 0.0001$) (Figure 2B). This indicates that both HSP90 inhibitors, 17-DMAG and ganetespib, have synergistic effects with CIK cells against BL cell lines.

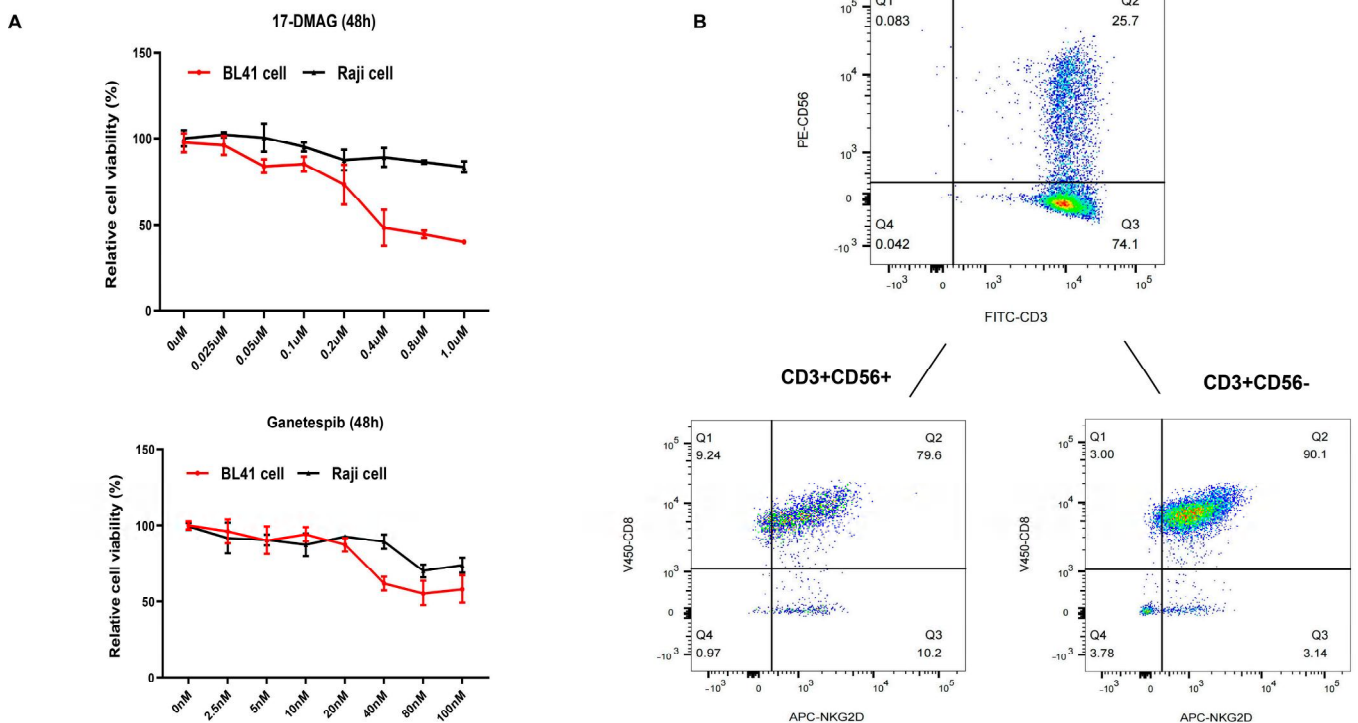


Figure 1. (A) Cell viability of Burkitt's lymphoma (BL) cells was assessed following treatment with HSP90 inhibitors. Subsequently, the optimal concentration of HSP90 inhibitors was determined (17-DMAG-0.1 μ M and ganetespib-20 μ M, respectively). The presented data represent the mean \pm standard deviation (SD) of triplicates per experimental condition. (B) Phenotype of day 14 CIK cells. The figure shows data from one representative from four donors.

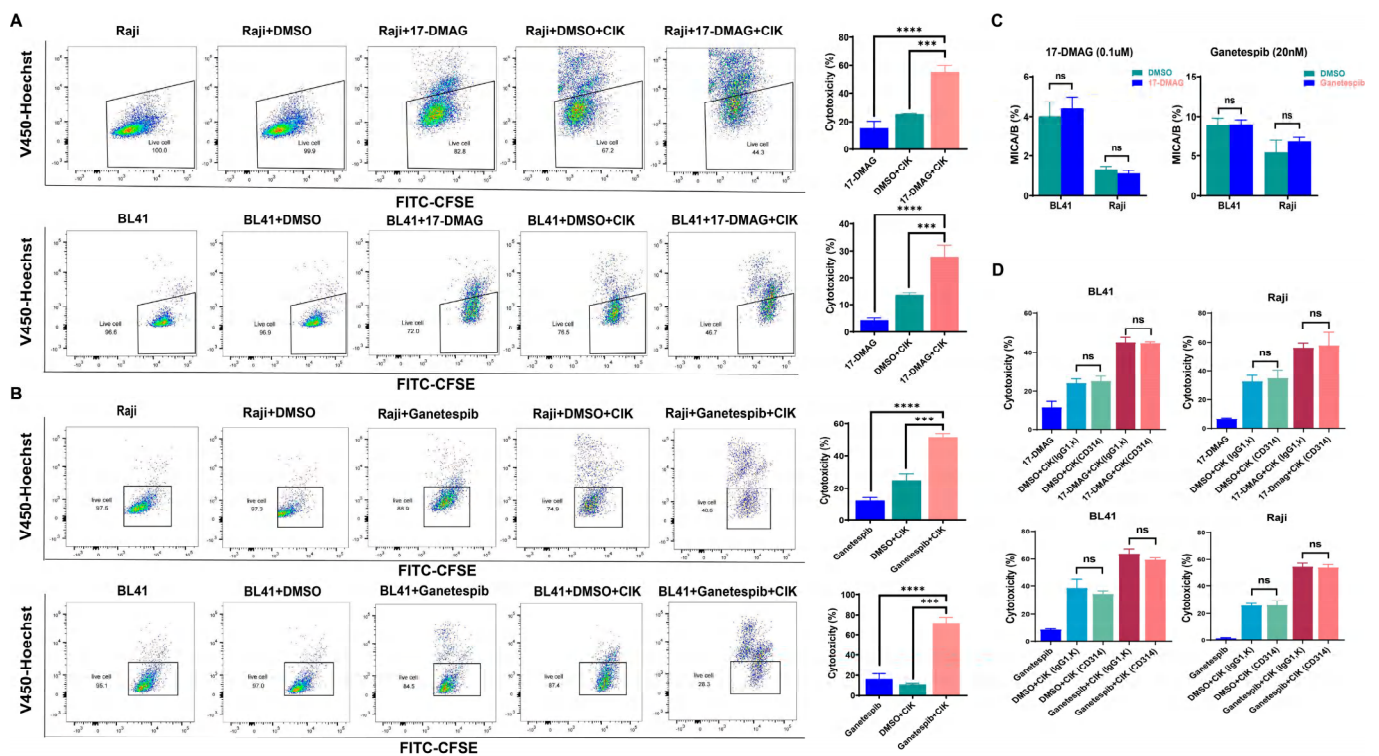


Figure 2. Cytotoxicity of CIK cells treated with/without 17-DMAG (A) and ganetespib (B) against Raji and BL41 cells. Analyses were performed on different donors ($n = 3$) and values are expressed as mean \pm SD. Analyses were performed using the Student's t -test. (C) MICA/B expression on the surface of Raji and BL41 cells after treatment with 17-DMAG and ganetespib. Each bar represents the mean \pm SD of a representative donor. (D) Cytotoxicity of CIK cells treated with/without two HSP90 inhibitors against Burkitt's lymphoma cell lines with/without NKG2D blocking (CIK cells were completely blocked before co-culture with Raji and BL41 cells). Cytotoxicity assays were conducted on CIK cells between days 14 and 16. CIK cells and BL cell lines were co-cultured with or without HSP90 inhibitors for 24 h at an E/T ratio of 10:1. Analyses were performed on 3 donors and one of them has been indicated. Data analysis was performed using the one-way ANOVA. *** $p < 0.001$, **** $p < 0.0001$, ns: not significant.

2.2. Cytotoxic Effect of CIK Cells Synergizing with HSP90 Is Independent of the NKD2D/NKG2DL Axis

Given that the NKG2D/NKG2DL axis plays an important role in the anticancer properties of CIK cells, MICA/B is the major NKG2D ligand on the surface of tumors. Therefore, we evaluated MICA/B expression on the surface of BL cells (Raji and BL-41) and investigated any possible alterations induced by HSP90 inhibitors (Figure 2C). Interestingly, we found that BL cells treated with 17-DMAG and ganetespib did not show altered MICA/B expression levels compared to the controls. Moreover, no effect on the cytotoxicity of CIK cells was observed when an anti-human CD314 (NKG2D) antibody was used to block the NKG2D/NKG2DL axis between the CIK and BL cells (Figure 2D). Importantly, we observed similar effects similar to those of ganetespib (Figure 2D). This suggests that the NKD2D/NKG2DL axis does not contribute to the cytotoxic effect of CIK cells in synergy with HSP90 inhibitors in BL.

2.3. CIK Cells Combined with HSP90 Inhibitors Primarily Induced Apoptosis in BL

Next, we investigated the possible activation of apoptosis induced by CIK cells and/or HSP90 inhibitors in BL cells. It was found that early apoptosis significantly increased in Raji cells and 17-DMAG combined with CIK cells ($18.767\% \pm 1.966\%$) compared with 17-DMAG ($6.893\% \pm 1.7\%$, $p < 0.0001$) and CIK cells ($11.867\% \pm 1.457\%$, $p = 0.0003$) (Figure 3A). Interestingly, equally significant results were found for BL41 cells when 17-DMAG was com-

combined with CIK cells ($32.667\% \pm 2.857\%$) compared to the control groups, 17-DMAG ($6.343\% \pm 0.184\%$, $p < 0.0001$), and CIK cells ($12.67\% \pm 3.247\%$, $p < 0.0001$) (Figure 3A). As a proof of concept, we also tested ganetespib and found comparable results to 17-DMAG. In Raji cells, an increase in early apoptosis was observed when ganetespib was co-cultured with CIK cells ($54.8\% \pm 3.818\%$), compared with ganetespib alone ($8.533\% \pm 1.443\%$, $p < 0.0001$) and CIK cells ($28.85\% \pm 2.616\%$, $p < 0.0001$) (Figure 3B). Ganetespib and CIK cells ($23.067\% \pm 1.358\%$) also exhibited increased early apoptosis in BL cells compared to ganetespib alone ($14.233\% \pm 0.351\%$, $p < 0.0001$) and CIK cells ($8.833\% \pm 1.609\%$, $p < 0.0001$) (Figure 3B). Thus, the combination of HSP90 inhibitors with CIK cells has demonstrated the ability to enhance late apoptosis in Burkitt's lymphoma (BL), particularly with ganetespib. In Raji cells, a notable increase in late apoptosis was observed when ganetespib was combined with CIK cells (32.75 ± 3.182), compared to the individual treatments of ganetespib (7.857 ± 0.49 , $p < 0.0001$) and CIK cells (23.167 ± 2.747 , $p = 0.0052$) (Figure 3B). Similarly, significant results were obtained with BL41 cells, where the combination of ganetespib and CIK cells ($16.7\% \pm 2.946\%$) demonstrated a substantial increase in late apoptosis compared to the control groups, ganetespib alone ($4.5\% \pm 0.298$, $p < 0.0001$), and CIK cells alone ($3.54\% \pm 0.233\%$, $p < 0.0001$) (Figure 3B). Thus, CIK cells, in combination with HSP90 inhibitors, were responsible for inducing early apoptosis in BL cells.

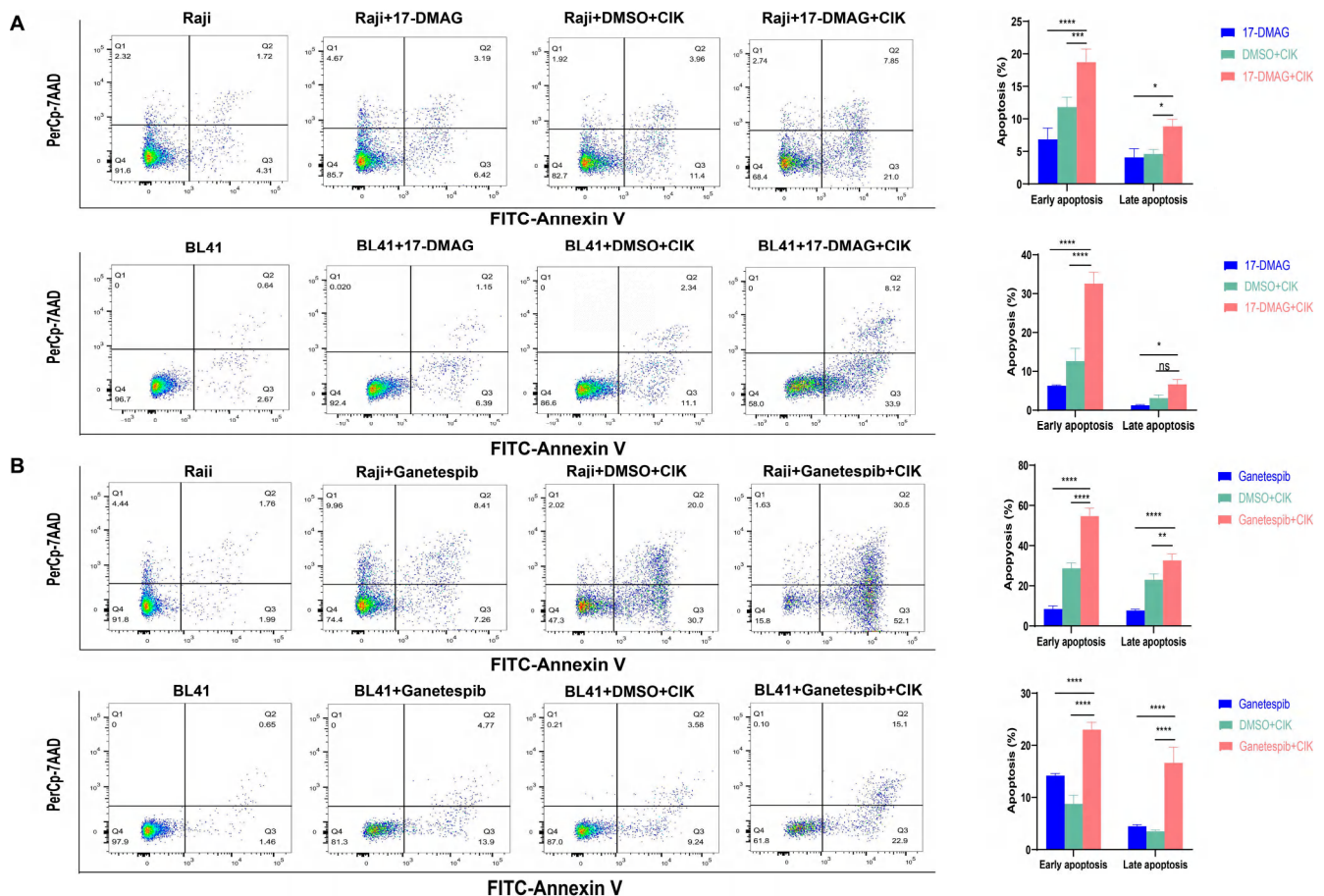


Figure 3. Apoptosis in Raji and BL 41 cells co-cultured with/without CIK cells treated with 17-DMAG (A) and ganetespib (B). In the apoptosis experiment involving BL cell lines, we utilized CIK cells at days 14–16, co-cultured with or without HSP90 inhibitors for 24 h, with an E/T ratio of 5:1. Each bar represents the mean \pm SD of a triplicate measurement, and these data are representative of three independent experiments. Data analysis was conducted using the two-way ANOVA. * $p < 0.05$, ** $p < 0.01$, *** $p < 0.001$, **** $p < 0.0001$, ns: not significant.

2.4. Increased Expression of Fas May Lead to the Induction of Caspase 3/7-Dependent Apoptosis in BL Cells via HSP90 Inhibitors

In addition to NKG2D/NKG2D, Fas/FasL is considered an alternative pathway for the cytotoxicity of CIK cells, leading to apoptosis; therefore, we examined Fas expression on the surfaces of BL cells. Interestingly, we found that after treatment with 17-DMAG, the percentage of Fas expression in BL41 cells significantly increased ($p = 0.0003$) (Figure 4A). After confirming that Fas was expressed in almost all Raji cells, we then assessed the MFI (mean fluorescence intensity) values and confirmed the significantly increased effect of 17-DMAG ($p = 0.0426$) (Figure 4A). Similar results were observed when ganetespib was administered (as shown in Figure 4B). Notably, a significant increase in caspase-3/7-activated apoptotic cells was observed in BL41 and Raji cells when CIK cells were combined with 17-DMAG compared to 17-DMAG ($p = 0.0004$ and $p = 0.002$, respectively) and CIK cells ($p = 0.0088$ and $p = 0.0123$, respectively) alone (Figure 4C). Ganetespib, in co-culture with CIK cells, also supported the increase in caspase-3/7-activated apoptotic cells in BL41 and Raji cells compared to the ganetespib ($p = 0.0012$ and $p = 0.0008$, respectively) and CIK cell groups ($p = 0.0112$ and $p = 0.0191$, respectively) (Figure 4D). This suggests that the increased expression of Fas on the BL cell surface may lead to caspase 3/7-dependent apoptosis induction via HSP90 inhibitors.

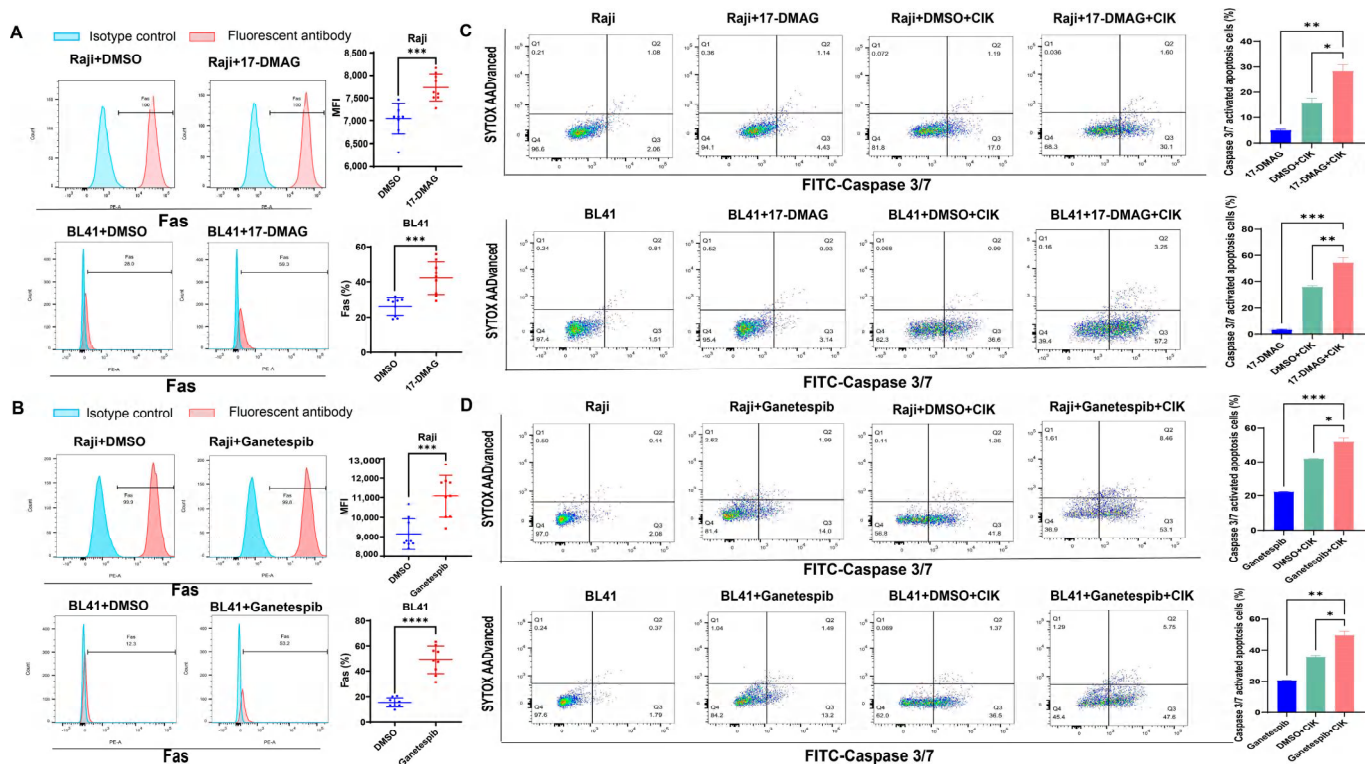


Figure 4. Fas expression on the surface of BL41 and Raji cells treated with/without 17-DMAG (A) and ganetespib (B). Fas expression was measured using flow cytometry following treatment with or without HSP90 inhibitors for 48 h. Each bar represents the mean \pm SD of three independent experiments. Data analysis was conducted using the Student's *t*-test. Caspase 3/7-activated apoptotic cells on BL41 and Raji cells treated with/without the 17-DMAG (C) and ganetespib (D) combination of CIK cells for 12 h, with an E/T of 2.5:1. These data are representative of three independent experiments and analysis was performed using the one-way ANOVA. * $p < 0.05$, ** $p < 0.01$, *** $p < 0.001$, **** $p < 0.0001$.

2.5. High Expression of HSP90 Genes Is Significantly Associated with Reduced Overall Survival in BL Patients

Considering that HSP90 is not the only HSP involved in cancer, we next investigated the prognostic ability of HSP90 and other HSP-related genes ($n = 84$) using the TCGA dataset for BL. We first performed a log-rank test (Mantel–Haenszel) to detect significant differences in patient survival depending on HSP gene expression (low and high expression groups). Importantly, we found that the high expression of HSP90 genes (namely *HSP90AA1*, *HSP90AB1*, and *HSP90B1*) was significantly associated with reduced overall survival in the KM-plotter cohort ($p = 0.015$; $p = 0.046$; and $p = 0.031$, respectively) (Figure 5). In addition to the HSP90 genes, several other HSP genes, including *HSPA1B*, *HSPA4*, *HSPA9*, *HSPA14*, *HYOU1*, *HSPB11*, *MKKS*, *DNAJA1*, *DNAJA3*, *DNAJA4*, *DNAJB6*, *DNAJB9*, *DNAJB11*, *DNAJC2*, *DNAJC15*, *DNAJC17*, *DNAJC19*, and *CCT8* were also found to be clinically significant for BL survival ($p \leq 0.05$) (Figure 6 and Supplementary Table S1). Thus, these findings strengthen the importance of our preclinical model (CIK cells and HSP90) for BL and prompts a more in-depth investigation of other HSP candidates.

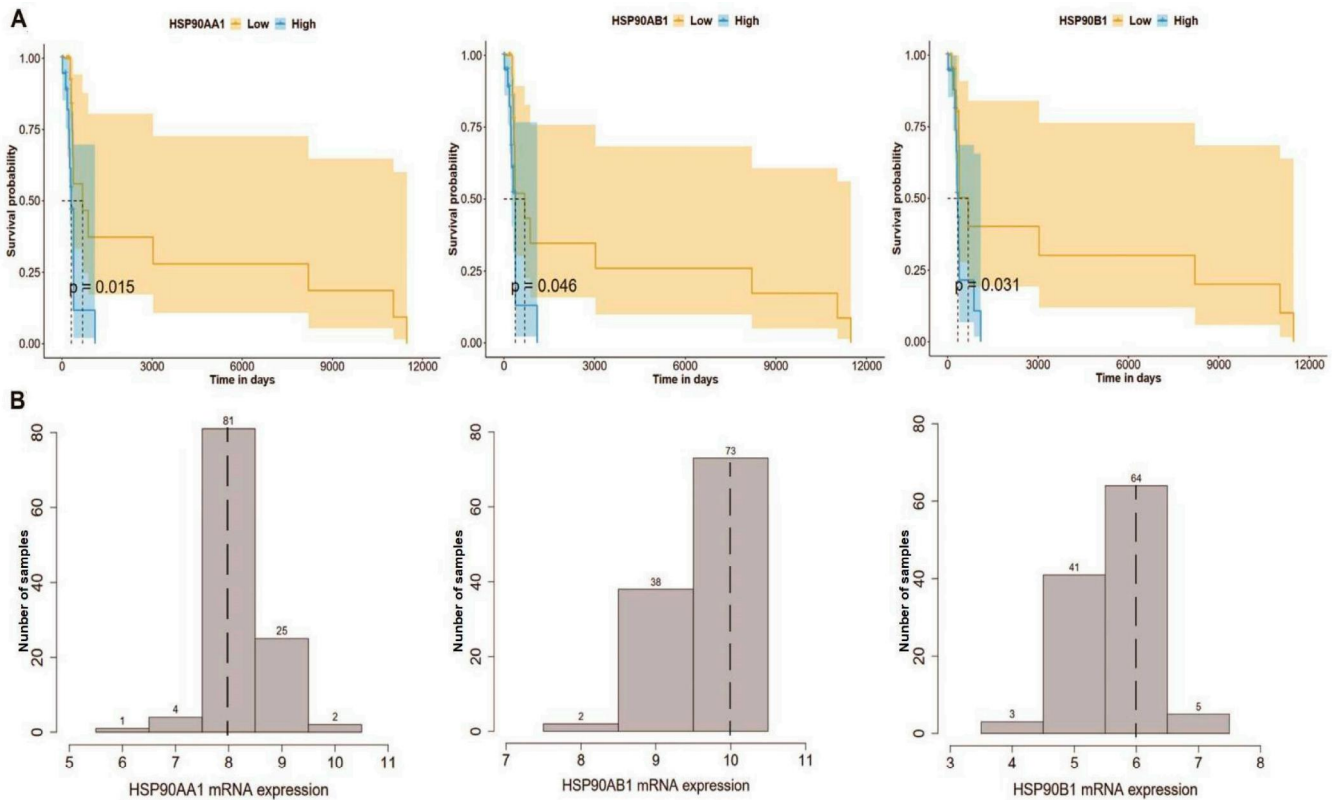


Figure 5. Expression of three HSP90 genes (*HSP90AA1*, *HSP90AB1*, and *HSP90B1*) predicts the survival of Burkitt's lymphoma patients. **(A)** Kaplan–Meier survival curve based on overall survival based on gene expression in a cohort of TCGA Burkitt's lymphoma patients, 95% confidence interval and the p -value (logarithmic rank test, Mantel–Haenszel). **(B)** Distribution of three HSP90s expression in the TCGA Burkitt's lymphoma dataset. The dotted lines indicate the median gene expression used as a cutoff to normalize the mRNA data, which were then log₂ processed.

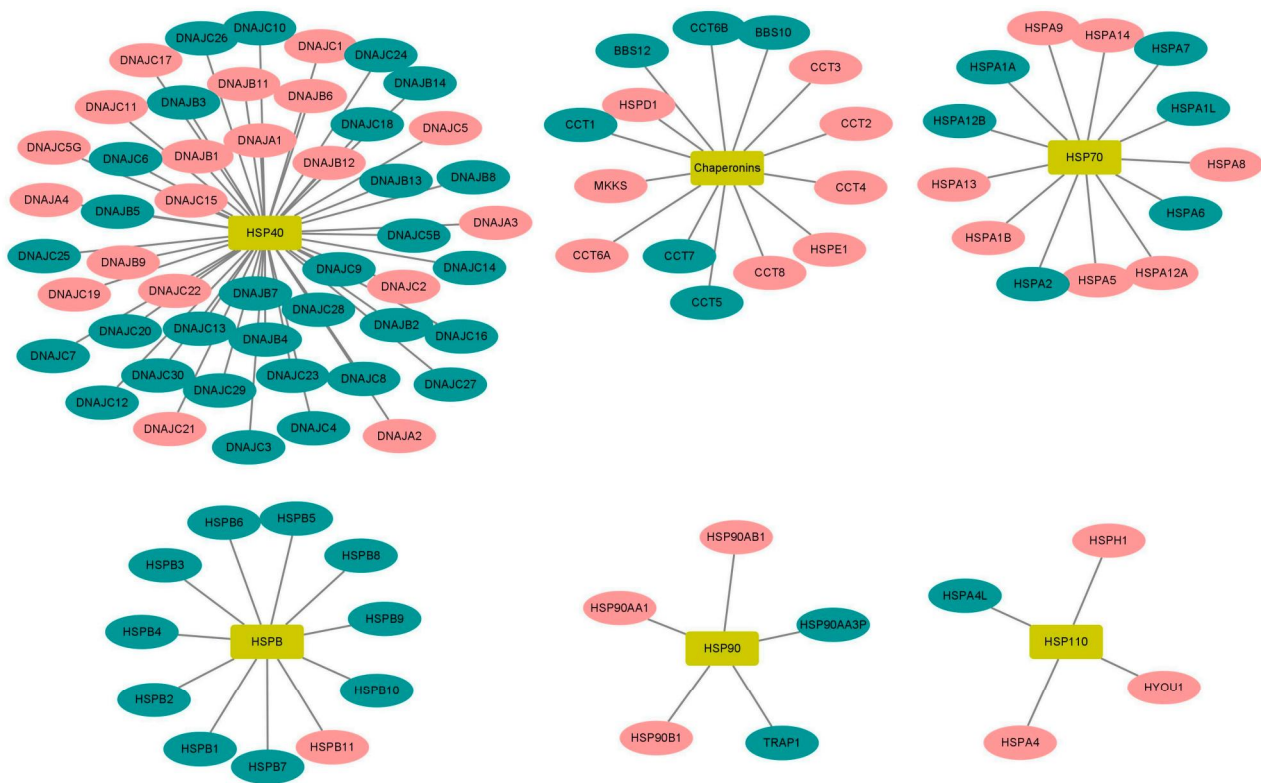


Figure 6. Association of 96 genes encoding heat shock proteins with overall survival of Burkitt's lymphoma patients from the KM plotter. The red color represents the genes that are related with survival, while the green color denotes the genes that are not related with survival.

3. Discussion

Although cancer immunotherapy has become the mainstay of cancer treatment, a minority of cancer patients still do not respond to it. Consequently, researchers and clinicians are currently identifying and investigating alternative and combined treatment modalities. Immune checkpoint inhibitors (ICI) have been very successful in this context, but the ability of heat shock proteins (HSPs), especially HSP90, to trigger the immune system against tumor cells has also been of particular interest. HSP90 inhibitors have been successfully assessed across a wide range of preclinical/clinical cancers, including gliomas [31], breast cancer [32], lung cancer [33], prostate cancer [34], and colorectal cancer [35]. Furthermore, HSP90 has been implicated in hematological malignancies, including acute myeloid leukemia [36], mantle cell lymphoma [37], acute lymphoblastic leukemia [38], T-cell leukemia [39], and chronic lymphocytic leukemia [40]. Interestingly, the outcomes of clinical trials involving HSP90 in various cancer types (including hematological malignancies) have been encouraging [41–46]. Surprisingly, HSP90 has never been tested with cytokine-induced killer (CIK) cell therapy, which has recently turned 30 years old and has been shown to be successful across various hematological malignancies, including B-cell malignancies [47], multiple myeloma [48], and acute myeloid leukemia [49]. Considering that Burkitt's lymphoma (BL) continues to be a challenging hematological malignancy, we investigated whether the synergy of HSP90 and CIK cells could pave the way for a potential treatment. To widen our analysis, we used both EBV-negative (BL41) and EBV-positive (Raji) cell lines in this first preclinical study.

To address this, we first checked the viability of BL cells (BL41 and Raji) using two independent HSP90 inhibitors (17-DMAG and ganetespib) with CIK cells and confirmed a synergistic effect in all combinations. It has been well established that the NKG2D/NKG2DL axis plays an important role in the anticancer properties of CIK cells, and MICA/B is the major NKG2D ligand on the surface of tumors [50]. Next, we assessed MICA/B expression on the surface of BL cells and evaluated possible changes induced by HSP90 inhibitors. The

results clearly showed that neither HSP90 inhibitor had an effect on MICA/B expression levels in BL cells. In addition, when anti-human CD314 (NKG2D) antibody was used to block the NKG2D/NKG2DL axis between the CIK cells and BL cells, no effect was apparent. In particular, CIK cells, in combination with HSP90 inhibitors, induced early apoptosis in BL cells. A study on the combination therapy of HSP90 inhibitors for colorectal cancer indicated that HSP90 can enhance immunotherapy through the Fas/FasL axis between cancer cells and T cells, HSP90 was able to improve immunotherapy through cancer cells and the T cell Fas/FasL axis [35]. It was further evident that the increased expression of Fas on the surface of BL cells resulted in the induction of caspase 3/7-dependent apoptosis. Thus, it is possible that the Fas/FasL pathway, rather than the NKG2D/NKG2DL pathway, serves as an alternative mechanism for CIK cell cytotoxicity (with HSP90) in BL.

Using TCGA datasets for BL, we examined the prognostic ability of HSP90 and found that high expression levels of the HSP90 family (specifically *HSP90AA1*, *HSP90AB1*, and *HSP90B1*) were significantly associated with reduced overall survival. This suggests that the HSP90-CIK cell combination may serve as an alternative treatment strategy for BL. However, it cannot be excluded that other HSP-related genes (in addition to HSP90) may also have an importance in BL. Therefore, we evaluated the expression of all HSP-related genes ($n = 84$), and nine of them, including *HSPA1B*, *HSPA8*, *HSPB11*, *DNAJA3*, *DNAJB9*, *DNAJC11*, *DNAJC17*, *DNAJC19*, and *DNAJC22*, were found to be clinically significant for BL survival. Importantly, a few of them have already been implicated in different cancers, such as AML [51], gastric cancer [52], colon cancer [53], lung cancer [54,55], liver cancer [56], B-cell lymphoma [57] and breast cancer [58]. Taken together, HSPs are closely associated with BL, and their suitability for CIK cells has been warranted.

It is also worth mentioning that we used first-generation (17-DMAG) and second-generation (ganetespib) HSP90 inhibitors as a combination strategy with CIK cells, and the future availability of dual inhibitors (such as HSP90-HDAC [59]) may further contribute to defining the cytotoxic efficacy of CIK cells in BL. The cytotoxic ability of CIK cells has been successfully demonstrated in several clinical studies. The functional aspect of the cytotoxicity of CIK cells via the NKG2D/NKG2DL signaling pathway and/or Fas/FasL signaling has also been widely discussed in the literature. However, the exact and alternative modes of functioning for these cells is still unclear, and the involvement of other mechanisms cannot be ruled out. Particularly, in the context of BL, our study is the first attempt to show that HSP90 inhibitors can enhance the cytotoxic effect of CIK cells via the Fas/FasL signaling pathway, which consequently activates caspase3/7-dependent apoptosis. Certainly, further experiments, especially *in vivo*, can help to gain further insight into the deeper mechanisms, but at the preclinical level, our study is the first attempt to investigate the suitability of cancer immunotherapy of CIK cells together with HSP90 in Burkitt's lymphoma.

4. Materials and Methods

4.1. Cell Lines and Cell Culture

The Burkitt's lymphoma lines (Raji and BL41) were cultured in RPMI-1640 (Pan-Biotech, Aidenbach, Bavaria, Germany) medium supplemented with 10% FBS (Sigma-Aldrich Chemie GmbH, Munich, Germany) and 1% penicillin/streptomycin (P/S) (Gibco, Schwerte, Germany) at 37 °C and 5% CO₂. Both cell lines were purchased from DSMZ (Braunschweig, Germany) and detected as mycoplasma-free using a Mycoplasma Detection Kit (Thermo Fisher Scientific, Darmstadt, Germany).

4.2. Reagents

The antibodies (FITC-CD3, PE-CD56, APC-NKG2D, BV421-CD8, and APC-MICA/B) and their respective isotype antibodies were purchased from BioLegend (San Diego, CA, USA). The Annexin V-FITC -7AAD (7-Amino-Actinomycin D) kit was also purchased from BioLegend (San Diego, CA, USA). The HSP90 inhibitors 17-DMAG and ganetespib (STA-9090) were purchased from Selleckchem (Boston, MA, USA). These HSP90 inhibitors

were dissolved in DMSO and stored at $-80\text{ }^{\circ}\text{C}$ at a concentration of 50 mM (please note that the control DMSO concentration of 17-DMAG was 0.1‰, and that the control DMSO concentration of ganetespib was 0.02‰). The FxCycle™ Violet stain and CellTrace™ CFSE Cell Proliferation Kit (Invitrogen, Thermo Fisher Scientific, Eugene, OR, USA) were used to distinguish tumor cells from CIK cells using flow cytometry. Hoechst 34580 (Merck, Sigma, Darmstadt, Germany) was added prior to flow cytometry to stain the dead cells. The CellEvent™ Caspase-3/7 Green flow cytometry assay kit was purchased from Invitrogen (Thermo Fisher Scientific Inc., Waltham, MA, USA).

4.3. Generation of Cytokine-Induced Killer (CIK) Cells

CIK cells were generated according to a previously described protocol [60]. Briefly, peripheral blood mononuclear cells (PBMCs) were isolated from the blood of healthy donors (blood bank of the University Hospital Bonn, Bonn, Germany) through gradient centrifugation using Pancoll (Aidenbach, Bavaria, Germany). PBMCs were cultured at $2 \times 10^6/\text{mL}$ in a 75 cm^2 flask, and 1000 U/mL of IFN- γ (ImmunoTools GmbH, Aidenbach, Bavaria, Germany) was added 2 h later. On the second day, monocytes were removed, and 100 U/mL of IL-1 β (ImmunoTools GmbH, Aidenbach, Bavaria, Germany), 600 U/mL of IL-2 (ImmunoTools GmbH, Aidenbach, Bavaria, Germany) and 50 ng/mL of anti-CD3 (Thermo Fisher Scientific, CA, USA) were added. CIK cells were then cultured in RPMI-1640 medium (Pan-Biotech, Aidenbach, Bavaria, Germany), and supplemented with 10% FBS (Sigma-Aldrich Chemie GmbH, Munich, Germany), 2.5% HEPES (Gibco, Thermo Fisher Scientific, Inc.), and 1% penicillin/streptomycin (P/S) (Gibco, Schwerte, Germany) at $37\text{ }^{\circ}\text{C}$, 5% CO_2 , and humidified atmosphere. Subcultures were obtained every 3 days at $0.5\text{--}1 \times 10^6$ cells/mL in fresh medium containing 600 U/mL of IL-2. After two weeks of *in vivo* expansion, CIK cells were collected for the experiments.

4.4. CCK8 Assay

Cell viability was assessed using the Cell Counting Kit-8 (CCK8, Dojindo Molecular Technologies, Inc., Rockville, MD, USA) assay. Raji and BL41 cells were seeded at a density of 1×10^4 cells per well in a U-bottom Nunclon™ 96-well plate and exposed to a range of concentrations of 17-DMAG and ganetespib for 48 h. Subsequently, 10 μL of CCK-8 working solution was added to each well and incubated for 2–4 h. Absorbance at 450 nm and 650 nm was measured using a Fluostar OPTIMA microplate reader (BMG Labtech, Ortenberg, Germany).

4.5. Phenotype Expression of CIK Cells

Mature CIK cells (at day 14) were used to confirm their phenotype using flow cytometry. The CIK cells were stained with PE-CD56, FITC-CD3, APC-NKG2D, BV421-CD8, and their corresponding isotype antibodies. 7AAD was used to stain the dead cells. Samples were acquired using flow cytometry (FACS Canto II, BD Biosciences, Heidelberg, Germany).

4.6. Cytotoxicity of CIK Cells

Tumor cells (1×10^6) were labeled with 1 μM CFSE in 1 mL DPBS and incubated for 15 min at $37\text{ }^{\circ}\text{C}$ in darkness. The cells were then washed twice with 10 mL culture medium to remove any excess CFSE dye. Subsequently, 2×10^4 tumor cells per well were co-cultured with a medium containing either 17-DMAG (0.1 μM) or ganetespib (20 nM) in a $37\text{ }^{\circ}\text{C}$, 5% CO_2 incubator for 24 h. Afterward, CIK cells were added while maintaining the E:T ratio of 10:1. To perform NKG2D blocking experiments, CIK cells were pretreated with purified anti-human CD314 (clone 1D11, BioLegend, Koblenz, Germany) or isotype mouse IgG1 κ (10 $\mu\text{g}/\text{mL}$) for 30 min. Following pre-treatment, CIK cells were co-cultured with tumor cells for 20–24 h. Dead cells were then labeled with Hoechst 34580 and analyzed using flow cytometry. The CFSE-labeled cells were identified as tumor cells, whereas the other cells were identified as CIK cells. The formula used to calculate cytotoxicity was described as the following: Cytotoxicity (%) = $(\text{CT} - \text{TE})/\text{CT} \times 100$. CT: tumor live cells

with CFSE. TE denotes live tumor cells with CFSE following treatment with HSP90 inhibitor or/and CIK cells.

4.7. MICA/B Expression

Raji and BL41 cells were seeded at a density of 2×10^4 cells per well in 48-well plates with complete medium containing 17-DMAG (0.1 μM) or ganetespib (20 nM) at a total volume of 300 μL per well for 48 h. The cells were then collected and washed twice with DPBS to remove any remaining medium. To assess MICA/B expression, cells were stained with an APC-MICA/B antibody and analyzed using flow cytometry; viable cells were labeled with Hoechst.

4.8. The Apoptosis of Burkitt's Lymphoma Cells

To analyze the apoptosis of BL cells, 1×10^6 Raji and BL41 cells in 1ml DPBS were labeled with 0.5 μM violet dye for marking tumor cells under the conditions of 37 °C in darkness for 15 min. The cells were then washed twice with 10 mL culture medium to remove any excess dye. Subsequently, 2×10^4 cells per well were seeded in 48-well plates (with a total volume of 300 μL) and co-cultured with HSP90 inhibitors (experimental group) or DMSO (control group) for 24 h. The appropriate number of CIK cells were then added to maintain an E:T ratio of 5:1 for 20–24 h. Afterward, the cells were washed with Annexin V buffer and stained with FITC-Annexin V antibody and 7AAD dye for 15 min.

4.9. Caspase 3/7 Activity

To label the tumor cells, Raji and BL41 cells (1×10^6) were incubated with 0.5 μM violet dye in 1 mL DPBS at 37 °C for 15 min in an incubator. The cells were washed twice with 10 mL culture medium to eliminate excess dye and then seeded at a density of 1×10^4 cells per well in 96-well plates with or without HSP90 inhibitors for 36 h. Next, CIK cells were added at an E:T ratio of 2.5:1. To evaluate caspase3/7 activity, the CellEvent™ Caspase-3/7 Green Flow Cytometry Assay Kit was utilized to stain the tumor cells with 0.5 μM CellEvent™ Caspase-3/7 Green Detection Reagent and 1 μM SYTOX™ AADvanced™ Dead Cell Stain at room temperature for 1 h and 5 min, respectively. The percentage of activated caspase-3/7 cells was determined using flow cytometry.

4.10. Fas Expression

Raji and BL41 cells (2×10^4 cells per well) were seeded in 48-well plates and treated with HSP90 inhibitors at 37 °C and 5% CO₂ for 48 h. After washing with PBS twice, the cells were stained with PE-CD95 for 30 min. Hoechst 34580 was then added, following which flow cytometry measurements were taken.

4.11. Correlation of HSP Genes with BL Patients

The BL dataset was downloaded from the TCGA database (<https://portal.gdc.cancer.gov/projects/CGCI-BLGSP> (accessed on 26 March 2023), Project ID: CGCI-BLGSP). The log-rank test (Mantel–Haenszel) was used to detect significant differences in patient survival according to HSP expression (low and high expression groups). The cut-off value for each gene was the median expression.

4.12. Statistical Analysis

Flow cytometry datasets were analyzed using FlowJo V10.6 (LLC, Ashland, OR, USA). Statistical analyses were performed and figures were prepared using GraphPad Prism software (version 9.0; GraphPad Software, San Diego, CA, USA), including the one-way or two-way analysis of variance (ANOVA) with the Bonferroni test and Student's *t*-test. Bioinformatics analyses were performed using R statistical software (version 4.1.1). Statistical significance was set at $p < 0.05$. * $p < 0.05$, ** $p < 0.01$, *** $p < 0.001$, **** $p < 0.0001$.

Supplementary Materials: The following supporting information can be downloaded at: <https://www.mdpi.com/article/10.3390/ijms241512476/s1>.

Author Contributions: Conceptualization: F.G. and I.G.H.S.-W. Methodology: F.G., Y.W., Y.Y. and H.L. Investigation: F.G. and Y.W. Validation: F.G. and Y.Y. Formal analysis: F.G., Y.W. and A.S. Data curation: F.G. and Y.Y. Writing—original draft preparation: F.G. Writing—review and editing: I.G.H.S.-W., Y.W., A.S., H.L., M.E. and U.J. Visualization: F.G., Y.W. and A.S. Supervision: I.G.H.S.-W. Project administration: I.G.H.S.-W. All authors have read and agreed to the published version of the manuscript.

Funding: This research received no external funding.

Institutional Review Board Statement: Not applicable.

Informed Consent Statement: Not applicable.

Data Availability Statement: Not applicable.

Conflicts of Interest: The authors declare no conflict of interest.

Abbreviations

CIK cell: cytokine-induced killer cell; NK cell: natural killer cell; NKT cell: natural killer T cell; NKG2D: natural killer group 2, member D; NKG2DL: NKG2D ligand; MICA/B: major histocompatibility complex class I polypeptide-related sequence A and B; HSP: heat shock protein; 17-DMAG: 17-dimethylaminoethylamino-17-demethoxygeldanamycin; DMSO: dimethyl sulfoxide; BL: Burkitt's lymphoma; PI3K: phosphoinositide 3-kinase; SYK: spleen tyrosine kinase; TNF: tumor necrosis factor; IFN- γ : interferon- γ ; IL-2: interleukin-2; 7AAD: 7-amino-actinomycin D; TCGA: the cancer genome atlas; KM curve: Kaplan–Meier curve; ICI: immune checkpoint inhibitor; and HDAC: histone deacetylase.

References

- Li, H.; Luo, K.; Sharma, A.; Sun, X. Prognostic gene expression signature revealed the involvement of mutational pathways in cancer genome. *J. Cancer* **2020**, *11*, 4510–4520. [[CrossRef](#)]
- Sharma, A.; Liu, H.; Herwig-Carl, M.C.; Chand Dakal, T.; Schmidt-Wolf, I.G.H. Epigenetic Regulatory Enzymes: Mutation Prevalence and Coexistence in Cancers. *Cancer Investig.* **2021**, *39*, 257–273. [[CrossRef](#)] [[PubMed](#)]
- Dhabhai, B.; Sharma, A.; Maciaczyk, J.; Dakal, T.C. X-Linked Tumor Suppressor Genes Act as Presumed Contributors in the Sex Chromosome–Autosome Crosstalk in Cancers. *Cancer Investig.* **2022**, *40*, 103–110. [[CrossRef](#)] [[PubMed](#)]
- Jhaveri, K.; Ochiana, S.O.; Dunphy, M.P.; Gerecitano, J.F.; Corben, A.D.; Peter, R.I.; Janjigian, Y.Y.; Gomes-DaGama, E.M.; Koren, J.; Modi, S.; et al. Heat shock protein 90 inhibitors in the treatment of cancer: Current status and future directions. *Expert Opin. Investig. Drugs* **2014**, *23*, 611–628. [[CrossRef](#)]
- Li, Y.; Zhang, T.; Schwartz, S.J.; Sun, D. New developments in Hsp90 inhibitors as anti-cancer therapeutics: Mechanisms, clinical perspective and more potential. *Drug Resist. Updat.* **2009**, *12*, 17–27. [[CrossRef](#)]
- Amatya, E.; Blagg, B.S.J. Recent advances toward the development of Hsp90 C-terminal inhibitors. *Bioorg. Med. Chem. Lett.* **2023**, *80*, 129111. [[CrossRef](#)]
- Birbo, B.; Madu, E.E.; Madu, C.O.; Jain, A.; Lu, Y. Role of HSP90 in Cancer. *Int. J. Mol. Sci.* **2021**, *22*, 10317. [[CrossRef](#)]
- Barrott, J.J.; Haystead, T.A.J. Hsp90, an unlikely ally in the war on cancer. *FEBS J.* **2013**, *280*, 1381–1396. [[CrossRef](#)] [[PubMed](#)]
- Garg, G.; Khandelwal, A.; Blagg, B.S.J. Anticancer Inhibitors of Hsp90 Function: Beyond the Usual Suspects. *Adv. Cancer Res.* **2016**, *129*, 51–88. [[CrossRef](#)] [[PubMed](#)]
- Li, Z.-N.; Luo, Y. HSP90 inhibitors and cancer: Prospects for use in targeted therapies (Review). *Oncol. Rep.* **2023**, *49*, 6. [[CrossRef](#)]
- Chatterjee, S.; Burns, T.F. Targeting Heat Shock Proteins in Cancer: A Promising Therapeutic Approach. *Int. J. Mol. Sci.* **2017**, *18*, 1978. [[CrossRef](#)]
- Hoter, A.; El-Sabban, M.E.; Naim, H.Y. The HSP90 Family: Structure, Regulation, Function, and Implications in Health and Disease. *Int. J. Mol. Sci.* **2018**, *19*, 2560. [[CrossRef](#)] [[PubMed](#)]
- Schneider, R.; Linka, R.M.; Reinke, H. HSP90 affects the stability of BMAL1 and circadian gene expression. *J. Biol. Rhythms.* **2014**, *29*, 87–96. [[CrossRef](#)] [[PubMed](#)]
- Coskunpinar, E.; Akkaya, N.; Yildiz, P.; Oltulu, Y.M.; Aynaci, E.; Isbir, T.; Yaylim, I. The significance of HSP90AA1, HSP90AB1 and HSP90B1 gene polymorphisms in a Turkish population with non-small cell lung cancer. *Anticancer Res.* **2014**, *34*, 753–757. [[PubMed](#)]

15. Liu, K.; Kang, M.; Li, J.; Qin, W.; Wang, R. Prognostic value of the mRNA expression of members of the HSP90 family in non-small cell lung cancer. *Exp. Ther. Med.* **2019**, *17*, 2657–2665. [[CrossRef](#)] [[PubMed](#)]
16. Wengert, L.A.; Backe, S.J.; Bourbouliia, D.; Mollapour, M.; Woodford, M.R. TRAP1 Chaperones the Metabolic Switch in Cancer. *Biomolecules* **2022**, *12*, 786. [[CrossRef](#)] [[PubMed](#)]
17. Valbuena, J.R.; Rassidakis, G.Z.; Lin, P.; Atwell, C.; Georgakis, G.V.; Younes, A.; Jones, D.; Medeiros, L.J. Expression of heat-shock protein-90 in non-Hodgkin's lymphomas. *Mod. Pathol.* **2005**, *18*, 1343–1349. [[CrossRef](#)] [[PubMed](#)]
18. Giulino-Roth, L.; van Besien, H.J.; Dalton, T.; Totonchy, J.E.; Rodina, A.; Taldone, T.; Bolaender, A.; Erdjument-Bromage, H.; Sadek, J.; Chadburn, A.; et al. Inhibition of Hsp90 Suppresses PI3K/AKT/mTOR Signaling and Has Antitumor Activity in Burkitt Lymphoma. *Mol. Cancer Ther.* **2017**, *16*, 1779–1790. [[CrossRef](#)]
19. Walter, R.; Pan, K.-T.; Doebele, C.; Comoglio, F.; Tomska, K.; Bohnenberger, H.; Young, R.M.; Jacobs, L.; Keller, U.; Bönig, H.; et al. HSP90 promotes Burkitt lymphoma cell survival by maintaining tonic B-cell receptor signaling. *Blood* **2017**, *129*, 598–608. [[CrossRef](#)]
20. Poole, C.J.; Zheng, W.; Lee, H.; Young, D.; Lodh, A.; Chadli, A.; van Riggelen, J. Targeting the MYC Oncogene in Burkitt Lymphoma through HSP90 Inhibition. *Cancers* **2018**, *10*, 448. [[CrossRef](#)]
21. Wu, J.; Cao, Y.; Zhang, Q.; Liu, W.; Zhou, X.; Ming, X.; Meng, F.; Zhang, Y.; Li, C.; Huang, L.; et al. Chimeric Antigen Receptor-Modified T Cell Immunotherapy for Relapsed and Refractory Adult Burkitt Lymphoma. *Front. Immunol.* **2022**, *13*, 879983. [[CrossRef](#)] [[PubMed](#)]
22. Zayac, A.S.; Olszewski, A.J. Burkitt lymphoma: Bridging the gap between advances in molecular biology and therapy. *Leuk Lymphoma* **2020**, *61*, 1784–1796. [[CrossRef](#)]
23. Sharma, A.; Schmidt-Wolf, I.G.H. 30 years of CIK cell therapy: Recapitulating the key breakthroughs and future perspective. *J. Exp. Clin. Cancer Res.* **2021**, *40*, 388. [[CrossRef](#)]
24. Schmidt-Wolf, I.G.; Negrin, R.S.; Kiem, H.P.; Blume, K.G.; Weissman, I.L. Use of a SCID mouse/human lymphoma model to evaluate cytokine-induced killer cells with potent antitumor cell activity. *J. Exp. Med.* **1991**, *174*, 139–149. [[CrossRef](#)]
25. Schmidt-Wolf, I.G.; Lefterova, P.; Mehta, B.A.; Fernandez, L.P.; Huhn, D.; Blume, K.G.; Weissman, I.L.; Negrin, R.S. Phenotypic characterization and identification of effector cells involved in tumor cell recognition of cytokine-induced killer cells. *Exp. Hematol.* **1993**, *21*, 1673–1679.
26. Schmidt-Wolf, I.G.; Lefterova, P.; Johnston, V.; Huhn, D.; Blume, K.G.; Negrin, R.S. Propagation of large numbers of T cells with natural killer cell markers. *Br. J. Haematol.* **1994**, *87*, 453–458. [[CrossRef](#)]
27. Pievani, A.; Belussi, C.; Klein, C.; Rambaldi, A.; Golay, J.; Introna, M. Enhanced killing of human B-cell lymphoma targets by combined use of cytokine-induced killer cell (CIK) cultures and anti-CD20 antibodies. *Blood* **2011**, *117*, 510–518. [[CrossRef](#)] [[PubMed](#)]
28. Linn, Y.C.; Wang, S.M.; Hui, K.M. Comparative gene expression profiling of cytokine-induced killer cells in response to acute myeloid leukemic and acute lymphoblastic leukemic stimulators using oligonucleotide arrays. *Exp. Hematol.* **2005**, *33*, 671–681. [[CrossRef](#)] [[PubMed](#)]
29. Schmidt-Wolf, I.G.; Finke, S.; Trojaneck, B.; Denkena, A.; Lefterova, P.; Schwella, N.; Heuft, H.G.; Prange, G.; Korte, M.; Takeya, M.; et al. Phase I clinical study applying autologous immunological effector cells transfected with the interleukin-2 gene in patients with metastatic renal cancer, colorectal cancer and lymphoma. *Br. J. Cancer* **1999**, *81*, 1009–1016. [[CrossRef](#)]
30. Zhang, Y.; Sharma, A.; Weiher, H.; Schmid, M.; Kristiansen, G.; Schmidt-Wolf, I.G.H. Clinical Studies on Cytokine-Induced Killer Cells: Lessons from Lymphoma Trials. *Cancers* **2021**, *13*, 6007. [[CrossRef](#)]
31. Wei, S.; Yin, D.; Yu, S.; Lin, X.; Savani, M.R.; Du, K.; Ku, Y.; Wu, D.; Li, S.; Liu, H.; et al. Antitumor Activity of a Mitochondrial-Targeted HSP90 Inhibitor in Gliomas. *Clin. Cancer Res.* **2022**, *28*, 2180–2195. [[CrossRef](#)]
32. Lang, J.E.; Forero-Torres, A.; Yee, D.; Yau, C.; Wolf, D.; Park, J.; Parker, B.A.; Chien, A.J.; Wallace, A.M.; Murthy, R.; et al. Safety and efficacy of HSP90 inhibitor ganetespib for neoadjuvant treatment of stage II/III breast cancer. *NPJ Breast Cancer* **2022**, *8*, 128. [[CrossRef](#)] [[PubMed](#)]
33. Niu, M.; Zhang, B.; Li, L.; Su, Z.; Pu, W.; Zhao, C.; Wei, L.; Lian, P.; Lu, R.; Wang, R.; et al. Targeting HSP90 Inhibits Proliferation and Induces Apoptosis Through AKT1/ERK Pathway in Lung Cancer. *Front. Pharmacol.* **2021**, *12*, 724192. [[CrossRef](#)] [[PubMed](#)]
34. Rice, M.A.; Kumar, V.; Tailor, D.; Garcia-Marques, F.J.; Hsu, E.-C.; Liu, S.; Bermudez, A.; Kanchustambham, V.; Shankar, V.; Inde, Z.; et al. SU086, an inhibitor of HSP90, impairs glycolysis and represents a treatment strategy for advanced prostate cancer. *Cell Rep. Med.* **2022**, *3*, 100502. [[CrossRef](#)] [[PubMed](#)]
35. Kryeziu, K.; Bruun, J.; Guren, T.K.; Sveen, A.; Lothe, R.A. Combination therapies with HSP90 inhibitors against colorectal cancer. *Biochim. Biophys. Acta Rev. Cancer* **2019**, *1871*, 240–247. [[CrossRef](#)]
36. Lancet, J.E.; Gojo, I.; Burton, M.; Quinn, M.; Tighe, S.M.; Kersey, K.; Zhong, Z.; Albitar, M.X.; Bhalla, K.; Hannah, A.L.; et al. Phase I study of the heat shock protein 90 inhibitor alvespimycin (KOS-1022, 17-DMAG) administered intravenously twice weekly to patients with acute myeloid leukemia. *Leukemia* **2010**, *24*, 699–705. [[CrossRef](#)]
37. Lee, J.; Zhang, L.L.; Wu, W.; Guo, H.; Li, Y.; Sukhanova, M.; Venkataraman, G.; Huang, S.; Zhang, H.; Alikhan, M.; et al. Activation of MYC, a bona fide client of HSP90, contributes to intrinsic ibrutinib resistance in mantle cell lymphoma. *Blood Adv.* **2018**, *2*, 2039–2051. [[CrossRef](#)]

38. Diamanti, P.; Cox, C.V.; Moppett, J.P.; Blair, A. Dual targeting of Hsp90 in childhood acute lymphoblastic leukaemia. *Br. J. Haematol.* **2016**, *180*, 147–149. [[CrossRef](#)]
39. Ikebe, E.; Shimosaki, S.; Hasegawa, H.; Iha, H.; Tsukamoto, Y.; Wang, Y.; Sasaki, D.; Imaizumi, Y.; Miyazaki, Y.; Yanagihara, K.; et al. TAS-116 (pimitespib), a heat shock protein 90 inhibitor, shows efficacy in preclinical models of adult T-cell leukemia. *Cancer Sci.* **2022**, *113*, 684–696. [[CrossRef](#)]
40. Chen, T.L.; Harrington, B.; Truxall, J.; Wasmuth, R.; Prouty, A.; Sloan, S.; Lehman, A.M.; Sampath, D.; Orlemans, E.; Baiocchi, R.A.; et al. Preclinical evaluation of the Hsp90 inhibitor SNX-5422 in ibrutinib resistant CLL. *J. Hematol Oncol.* **2021**, *14*, 36. [[CrossRef](#)]
41. Kawazoe, A.; Itahashi, K.; Yamamoto, N.; Kotani, D.; Kuboki, Y.; Taniguchi, H.; Harano, K.; Naito, Y.; Suzuki, M.; Fukutani, M.; et al. TAS-116 (Pimitespib), an Oral HSP90 Inhibitor, in Combination with Nivolumab in Patients with Colorectal Cancer and Other Solid Tumors: An Open-Label, Dose-Finding, and Expansion Phase Ib Trial (EPOC1704). *Clin. Cancer Res.* **2021**, *27*, 6709–6715. [[CrossRef](#)]
42. Gutierrez, M.; Guo, R.; Giaccone, G.; Liu, S.V.; Hao, Z.; Hilton, C.; Hinson, J.M.; Kris, M.G.; Orlemans, E.O.; Drilon, A. Phase 1 multicenter study of the HSP90 inhibitor SNX-5422 plus carboplatin and paclitaxel in patients with lung cancers. *Lung Cancer* **2021**, *162*, 23–28. [[CrossRef](#)] [[PubMed](#)]
43. Slovin, S.; Hussain, S.; Saad, F.; Garcia, J.; Picus, J.; Ferraldeschi, R.; Crespo, M.; Flohr, P.; Riisnaes, R.; Lin, C.; et al. Pharmacodynamic and Clinical Results from a Phase I/II Study of the HSP90 Inhibitor Onalespib in Combination with Abiraterone Acetate in Prostate Cancer. *Clin. Cancer Res.* **2019**, *25*, 4624–4633. [[CrossRef](#)] [[PubMed](#)]
44. McCaig, A.M.; Cosimo, E.; Leach, M.T.; Michie, A.M. Dasatinib inhibits B cell receptor signalling in chronic lymphocytic leukaemia but novel combination approaches are required to overcome additional pro-survival microenvironmental signals. *Br. J. Haematol.* **2011**, *153*, 199–211. [[CrossRef](#)]
45. Cavenagh, J.; Oakervee, H.; Baetiong-Caguioa, P.; Davies, F.; Gharibo, M.; Rabin, N.; Kurman, M.; Novak, B.; Shiraishi, N.; Nakashima, D.; et al. A phase I/II study of KW-2478, an Hsp90 inhibitor, in combination with bortezomib in patients with relapsed/refractory multiple myeloma. *Br. J. Cancer* **2017**, *117*, 1295–1302. [[CrossRef](#)] [[PubMed](#)]
46. Oki, Y.; Younes, A.; Knickerbocker, J.; Samaniego, F.; Nastoupil, L.; Hagemester, F.; Romaguera, J.; Fowler, N.; Kwak, L.; Westin, J. Experience with HSP90 inhibitor AU922 in patients with relapsed or refractory non-Hodgkin lymphoma. *Haematologica* **2015**, *100*, e272–e274. [[CrossRef](#)] [[PubMed](#)]
47. Dalla Pietà, A.; Cappuzzello, E.; Palmerini, P.; Ventura, A.; Visentin, A.; Astori, G.; Chierogato, K.; Mozzo, V.; Perbellini, O.; Tisi, M.C.; et al. Innovative therapeutic strategy for B-cell malignancies that combines obinutuzumab and cytokine-induced killer cells. *J. Immunother Cancer* **2021**, *9*, e002475. [[CrossRef](#)]
48. Stephan, D.; Weiher, H.; Schmidt-Wolf, I.G.H. CIK Cells and HDAC Inhibitors in Multiple Myeloma. *Int. J. Mol. Sci.* **2017**, *18*, 945. [[CrossRef](#)]
49. Linn, Y.C.; Lau, S.K.J.; Liu, B.H.; Ng, L.H.; Yong, H.X.; Hui, K.M. Characterization of the recognition and functional heterogeneity exhibited by cytokine-induced killer cell subsets against acute myeloid leukaemia target cell. *Immunology* **2009**, *126*, 423–435. [[CrossRef](#)]
50. Wu, X.; Sharma, A.; Oldenburg, J.; Weiher, H.; Essler, M.; Skowasch, D.; Schmidt-Wolf, I.G.H. NKG2D Engagement Alone Is Sufficient to Activate Cytokine-Induced Killer Cells While 2B4 Only Provides Limited Coactivation. *Front. Immunol.* **2021**, *12*, 731767. [[CrossRef](#)]
51. Li, J.; Ge, Z. High HSPA8 expression predicts adverse outcomes of acute myeloid leukemia. *BMC Cancer* **2021**, *21*, 475. [[CrossRef](#)]
52. Wang, S.-F.; Huang, K.-H.; Tseng, W.-C.; Lo, J.-F.; Li, A.F.-Y.; Fang, W.-L.; Chen, C.-F.; Yeh, T.-S.; Chang, Y.-L.; Chou, Y.-C.; et al. DNAJA3/Tid1 Is Required for Mitochondrial DNA Maintenance and Regulates Migration and Invasion of Human Gastric Cancer Cells. *Cancers* **2020**, *12*, 3463. [[CrossRef](#)] [[PubMed](#)]
53. Guan, Y.; Zhu, X.; Liang, J.; Wei, M.; Huang, S.; Pan, X. Upregulation of HSPA1A/HSPA1B/HSPA7 and Downregulation of HSPA9 Were Related to Poor Survival in Colon Cancer. *Front. Oncol.* **2021**, *11*, 749673. [[CrossRef](#)]
54. Guo, H.; Deng, Q.; Wu, C.; Hu, L.; Wei, S.; Xu, P.; Kuang, D.; Liu, L.; Hu, Z.; Miao, X.; et al. Variations in HSPA1B at 6p21.3 are associated with lung cancer risk and prognosis in Chinese populations. *Cancer Res.* **2011**, *71*, 7576–7586. [[CrossRef](#)]
55. Losmanova, T.; Zens, P.; Scherz, A.; Schmid, R.A.; Tschan, M.P.; Berezowska, S. Chaperone-Mediated Autophagy Markers LAMP2A and HSPA8 in Advanced Non-Small Cell Lung Cancer after Neoadjuvant Therapy. *Cells* **2021**, *10*, 2731. [[CrossRef](#)]
56. Yang, C.; Shao, Y.; Wang, X.; Wang, J.; Wang, P.; Huang, C.; Wang, W.; Wang, J. The Effect of the Histone Chaperones HSPA8 and DEK on Tumor Immunity in Hepatocellular Carcinoma. *Int. J. Mol. Sci.* **2023**, *24*, 2653. [[CrossRef](#)]
57. Winkler, R.; Mägdefrau, A.-S.; Piskor, E.-M.; Kleemann, M.; Beyrer, M.; Linke, K.; Hansen, L.; Schaffer, A.-M.; Hoffmann, M.E.; Poepsel, S.; et al. Targeting the MYC interaction network in B-cell lymphoma via histone deacetylase 6 inhibition. *Oncogene* **2022**, *41*, 4560–4572. [[CrossRef](#)]
58. Kim, H.-Y.; Kim, Y.-M.; Hong, S. DNAJB9 suppresses the metastasis of triple-negative breast cancer by promoting FBXO45-mediated degradation of ZEB1. *Cell Death Dis.* **2021**, *12*, 461. [[CrossRef](#)] [[PubMed](#)]

59. Wu, Y.-W.; Chao, M.-W.; Tu, H.-J.; Chen, L.-C.; Hsu, K.-C.; Liou, J.-P.; Yang, C.-R.; Yen, S.-C.; HuangFu, W.-C.; Pan, S.-L. A novel dual HDAC and HSP90 inhibitor, MPT0G449, downregulates oncogenic pathways in human acute leukemia in vitro and in vivo. *Oncogenesis* **2021**, *10*, 39. [[CrossRef](#)]
60. Li, Y.; Sharma, A.; Wu, X.; Weiher, H.; Skowasch, D.; Essler, M.; Schmidt-Wolf, I.G.H. A Combination of Cytokine-Induced Killer Cells With PD-1 Blockade and ALK Inhibitor Showed Substantial Intrinsic Variability Across Non-Small Cell Lung Cancer Cell Lines. *Front. Oncol.* **2022**, *12*, 713476. [[CrossRef](#)] [[PubMed](#)]

Disclaimer/Publisher's Note: The statements, opinions and data contained in all publications are solely those of the individual author(s) and contributor(s) and not of MDPI and/or the editor(s). MDPI and/or the editor(s) disclaim responsibility for any injury to people or property resulting from any ideas, methods, instructions or products referred to in the content.

3.2 Publication 2: Non-oncology drug (meticrane) shows anti-cancer ability in synergy with epigenetic inhibitors and appears to be involved passively in targeting cancer cells

Yulu Wang¹ , Amit Sharma^{1,2}, **Fangfang Ge**¹ , Peng Chen¹ , Yu Yang³ , Hongjia Liu³ , Hongde Liu³ , Chunxia Zhao⁴ , Lovika Mittal ⁵ , Shailendra Asthana ⁵ and Ingo G. H. Schmidt-Wolf ¹ *

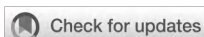
¹ Department of Integrated Oncology, Center for Integrated Oncology (CIO), University Hospital Bonn, Bonn, Germany

²Department of Neurosurgery, University Hospital Bonn, Bonn, Germany

³State Key Laboratory of Bioelectronics, School of Biological Science and Medical Engineering, Southeast University, Nanjing, China

⁴School of Nursing, Nanchang University, Nanchang, China

⁵Translational Health Science and Technology Institute (THSTI), NCR Biotech Science Cluster, Faridabad, Haryana, India



OPEN ACCESS

EDITED BY

Balasubramanyam Karanam,
Tuskegee University, United States

REVIEWED BY

Ihtisham Bukhari,
Fifth Affiliated Hospital of Zhengzhou
University, China
Guohui Sun,
Beijing University of Technology, China

*CORRESPONDENCE

Ingo G. H. Schmidt-Wolf
✉ ingo.schmidt-wolf@ukbonn.de

RECEIVED 02 February 2023

ACCEPTED 05 May 2023

PUBLISHED 19 May 2023

CITATION

Wang Y, Sharma A, Ge F, Chen P, Yang Y,
Liu H, Liu H, Zhao C, Mittal L, Asthana S
and Schmidt-Wolf IG (2023)
Non-oncology drug (meticrane)
shows anti-cancer ability in synergy
with epigenetic inhibitors and appears
to be involved passively in
targeting cancer cells.
Front. Oncol. 13:1157366.
doi: 10.3389/fonc.2023.1157366

COPYRIGHT

© 2023 Wang, Sharma, Ge, Chen, Yang, Liu,
Liu, Zhao, Mittal, Asthana and Schmidt-Wolf.
This is an open-access article distributed
under the terms of the [Creative Commons
Attribution License \(CC BY\)](https://creativecommons.org/licenses/by/4.0/). The use,
distribution or reproduction in other
forums is permitted, provided the original
author(s) and the copyright owner(s) are
credited and that the original publication in
this journal is cited, in accordance with
accepted academic practice. No use,
distribution or reproduction is permitted
which does not comply with these terms.

Non-oncology drug (meticrane) shows anti-cancer ability in synergy with epigenetic inhibitors and appears to be involved passively in targeting cancer cells

Yulu Wang¹, Amit Sharma^{1,2}, Fangfang Ge¹, Peng Chen¹,
Yu Yang³, Hongjia Liu³, Hongde Liu³, Chunxia Zhao⁴,
Lovika Mittal⁵, Shailendra Asthana⁵
and Ingo G. H. Schmidt-Wolf^{1*}

¹Department of Integrated Oncology, Center for Integrated Oncology (CIO), University Hospital Bonn, Bonn, Germany, ²Department of Neurosurgery, University Hospital Bonn, Bonn, Germany, ³State Key Laboratory of Bioelectronics, School of Biological Science and Medical Engineering, Southeast University, Nanjing, China, ⁴School of Nursing, Nanchang University, Nanchang, China, ⁵Translational Health Science and Technology Institute (THSTI), NCR Biotech Science Cluster, Faridabad, Haryana, India

Emerging evidence suggests that chemotherapeutic agents and targeted anticancer drugs have serious side effects on the healthy cells/tissues of the patient. To overcome this, the use of non-oncology drugs as potential cancer therapies has been gaining momentum. Herein, we investigated one non-oncology drug named meticrane (a thiazide diuretic used to treat essential hypertension), which has been reported to indescribably improve the therapeutic efficacy of anti-CTLA4 in mice with AB1 HA tumors. In our hypothesis-driven study, we tested anti-cancer potential meticrane in hematological malignance (leukemia and multiple myeloma) and liver cancer cell lines. Our analysis showed that: 1) Meticrane induced alteration in the cell viability and proliferation in leukemia cells (Jurkat and K562 cells) and liver cancer (SK-hep-1), however, no evidence of apoptosis was detectable. 2) Meticrane showed additive/synergistic effects with epigenetic inhibitors (DNMT1/5AC, HDACs/CUDC-101 and HDAC6/ACY1215). 3) A genome-wide transcriptional analysis showed that meticrane treatment induces changes in the expression of genes associated with non-cancer associated pathways. Of importance, differentially expressed genes showed favorable correlation with the survival-related genes in the cancer genome. 4) We also performed molecular docking analysis and found considerable binding affinity scores of meticrane against PD-L1, TIM-3, CD73, and HDACs. Additionally, we tested its suitability for immunotherapy against cancers, but meticrane showed no response to the cytotoxicity of cytokine-induced killer (CIK) cells. To our knowledge, our study is the first attempt to identify and experimentally confirm the anti-cancer potential of meticrane, being also the first to test the suitability of any non-oncology drug

in CIK cell therapy. Beyond that, we have expressed some concerns confronted during testing meticrane that also apply to other non-oncology drugs when considered for future clinical or preclinical purposes. Taken together, meticrane is involved in some anticancer pathways that are passively targeting cancer cells and may be considered as compatible with epigenetic inhibitors.

KEYWORDS

meticrane, CIK cells, non-oncology drug, epigenetics, cancer

Introduction

It has been well established that while anti-cancer/chemotherapy drugs kill cancer cells, they can also damage the healthy cells, causing a plethora of side effects. To avoid this collateral damage, special attention has been paid to the concept of testing non-oncology drugs, prompting the strategy of “drug repurposing,” i.e., drugs already approved for other diseases being identified as potential cancer therapies (1, 2). One of the best examples demonstrating the use of non-oncology drug repurposing is metformin, a classic anti-diabetic drug, that has been under intense investigation across multiple cancer types (3, 4). Of interest is a recent article summarizing several small molecule non-oncology drugs with therapeutic potential in cancer and discussing their putative targets and key pathways relevant to cancer treatment (5).

Notwithstanding all this new progress, it is still too early to definitively assess the success of these proposed potential drugs, although early indications point to positive results. Pushpakom and colleagues recently discussed the challenges being faced by the repurposing community and recommended some innovative ways to address them (6). As a broader concept, the testing of selective (computationally/dockings, high throughput screenings) non-oncology drugs in diverse cancer models, and how they may respond to individual epi(genomic) characteristics remain to be carefully evaluated. In particular, if they can be well combined with other clinically proven drugs/active compounds for cancer. For instance, the combination of epigenetic drugs with chemotherapeutic regimens has proven to be a synergistically relevant as treatment approach (7, 8). More importantly, if the newly selective drug is compatible with cancer immunotherapy related approach.

Considering this, herein, we investigated one non-oncology drug named meticrane (a thiazide diuretic used to treat essential hypertension), which undescribably improved the therapeutic efficacy of anti-CTLA4 in AB1-HA tumor-bearing mice (9). In this hypothesis-driven study, we tested the anti-cancer potential meticrane in hematological malignance (leukemia and multiple myeloma) and liver cancer cell lines. We further extend our analyses by assessing the additive/synergistic potential of meticrane with two epigenetic inhibitors (DNMT1/5AC and HDAC/CUDC-101) in these cells, which was further supported

by the molecular docking analysis. Besides, we evaluated the compatibility of meticrane with cytokine-induced killer (CIK) cells, a clinically established effective adoptive immunotherapy approach. To our knowledge, our study is the first attempt to identify and experimentally confirm the anticancer potential of meticrane.

Materials and methods

Generation of PBMCs and CIKs

Both Peripheral Blood Mononuclear Cells (PBMCs) and Cytokine-induced killer (CIK) cells were generated, as described previously (10–13). To isolate PBMCs from healthy donors by gradient density centrifugation, Pancoll (Pan-Biotech, Aidenbach, Bavaria, Germany) was used. All donors included in our study were from the blood bank of the University Hospital Bonn. To generate CIK cells, fresh PBMCs were seeded at 3×10^6 cells/mL in a 75 cm² flask and 1000 U/ml IFN- γ (ImmunoTools GmbH, Aidenbach, Bavaria, Germany) was added after 2 hours. On the following day, 50 ng/ml anti-CD3 antibody (OKT, eBioscience, Thermo Fisher Scientific, Inc. San Diego, CA, USA), 600 U/ml IL-2 (ImmunoTools GmbH, Aidenbach, Bavaria, Germany) and 100 U/ml IL-1 β (ImmunoTools GmbH, Aidenbach, Bavaria, Germany) were supplemented. Both PBMCs and CIK cells were cultured in RPMI-1640 medium (Pan-Biotech, Aidenbach, Bavaria, Germany) supplemented with 10% FBS (Sigma-Aldrich Chemie GmbH, Munich, Germany) and 1% penicillin/streptomycin (P/S) (Gibco, Schwerte, Germany), at 37°C, 5% CO₂, and humidified atmosphere. CIK cells were subcultured every 2–3 days with fresh medium supplemented with 600U/ml IL-2 (1×10^6 cells/ml). On completion of 14 days of expansion, the CIK cells were collected for the experiments.

Cell culture, meticrane compound and epigenetic inhibitors

We utilized seven cell lines in this study. The cell lines K562, SK-hep-1, HepG2, and CCD18co were purchased from the American Type Culture Collection (ATCC, Manassas, Virginia,

USA). Whereas the cell lines Jurkat, U266 and OPM2 were acquired from the German Collection of Microorganisms and Cell Cultures (DSMZ, Braunschweig, Germany). We cultured K562, U266, Jurkat, and OPM2 in RPMI1640 medium (Pan-Biotech, Aidenbach, Bavaria, Germany) supplemented with 10% FBS (Sigma-Aldrich Chemie GmbH, Munich, Germany) and 1% penicillin/streptomycin (P/S) (Gibco, Schwerte, Germany). While SK-hep-1, HepG2, and CCD18co cells were maintained in EMEM medium (Pan-Biotech, Aidenbach, Bavaria, Germany) supplemented with 10% FBS (Sigma-Aldrich Chemie GmbH, Munich, Germany) and 1% penicillin/streptomycin (P/S) (Gibco, Schwerte, Germany). Meticrane (Sigma-Aldrich Chemie GmbH, Munich, Germany) was dissolved in DMSO and stored at -20°C at a concentration of 200mM. The HDAC inhibitor CUDC-101 (Selleck Chemicals GmbH, Munich, Germany) and the selective HDAC6 inhibitor ACY1215 (Cayman Chemical, Ann Arbor, Michigan, US) was dissolved in DMSO and stored at -20°C at a concentration of 50mM. Also, DNMT1 inhibitor 5-Azacytidine (5AC) (STEMCELL Technologies Germany GmbH, Cologne, Germany) was dissolved in DMSO and stored at -20°C at a concentration of 25mM.

Cell viability assay and cells number counting assay

In case of suspension cells (K562, U266, OPM2, Jurkat, and PBMCs), the cells were seeded in 96-well flat-bottom plates and then immediately mixed with compounds (meticrane, CUDC-101, 5AC and ACY1215). For adherent cells (SK-hep-1, HepG2, and CCD18co), the drugs were added 4 hours later allowing the cells to adhere first. Considering the different growth rates of tumor cells, 0.5×10^4 K562 cells, 2×10^4 U266 cells, 2×10^4 OPM2 cells, 10×10^4 PBMCs, 0.5×10^4 Jurkat cells, 0.25×10^4 CCD18co cells, 0.3×10^4 SK-hep-1 cells, and 0.3×10^4 HepG2 cells were seeded. CCK8 assay (Dojindo EU GmbH, Munich, Germany) was used to determine the cell viability according to its manufacturer's instructions. In addition, based on the CCK8 results, the combined effects of meticrane and HDAC inhibitors (CUDC101, 5AC and ACY1215) were evaluated using the formula, as described elsewhere (14):

Combination index Q

$$= KE(a + b)/(KEa + KEb - KEa \times KEb)$$

KE represents the killing effect of drugs on cells, while a and b represent drug a and drug b. KE(a+b) means the killing effect of combination drug a and drug b.

According to the combination index Q value, the combined effects of meticrane and epigenetic inhibitors on tumor cells were classified as antagonism (< 0.85), additive (0.85 - 1.15) or synergism (> 1.15). The live cell count was performed using the Canto II flow cytometer (BD Biosciences, Heidelberg, Germany). Hoechst 33258 (Cayman Chemical, Ann Arbor, Michigan, US) was used to stain dead cells, and then precision count beads (BioLegend GmbH, Koblenz, Germany) were used to count the number of live cells.

Cell proliferation and apoptosis assays

To assess cell proliferation, 0.25µM CFSE (Cell Trace carboxyfluorescein succinimidyl ester) (Thermo Fisher Scientific, Eugene, USA) was used to stain 1×10^6 cells in PBS for 20 minutes at room temperature. While 1ul FITC-annexin (BioLegend GmbH, Koblenz, Germany) and 1ul eBioscience™ 7-AAD Viability Staining Solution (Thermo Fisher Scientific, Eugene, USA) were added to stain tumor cells (100ul volume) for 15mins at room temperature and then were used to assay cell apoptosis. In addition, CellEvent™ Caspase-3/7 Green Flow Cytometry Assay Kit (Thermo Fisher Scientific, Eugene, USA) was used to further evaluate the apoptosis and caspase 3/7 activation level. 0.5µM CellEvent™ Caspase-3/7 Green Detection Reagent and 1µM SYTOX™ AADvanced™ Dead Cell Stain were utilized to stain tumor cells at room temperature for 1h and 5 mins respectively. In these three experiments, 0.5×10^4 K562 cells, 0.5×10^4 Jurkat cells and 0.3×10^4 SK-hep-1 cells were seeded in 96-well flat-bottom plates for 3 days. Of note, adherent cells (SK-hep-1) were added to the wells and meticrane was added 4 hours afterwards. Flow cytometry was performed for these three experiments.

Cytotoxicity assay of CIK cells

0.25µM CFSE was used to stain tumor cells (1×10^6) in 1ml PBS, 20 min at room temperature. Subsequently, 1×10^4 cells of K562 were seeded in 96-well flat-bottom plates and then meticrane and 10×10^4 CIK cells (4h co-culture time), 10×10^4 CIK cells (24h co-culture time) and 20×10^4 CIK cells (24h co-culture time) were added respectively. Likewise, 1×10^4 SK-hep-1 cells were seeded in 96-well flat-bottom plates and 4 hours later meticrane and 40×10^4 CIK cells (4h coculture time), 10×10^4 CIK cells (24h coculture time) and 20×10^4 CIK cells (24h coculture time) were added. Flow cytometry was used to test the cytotoxicity of CIKs against tumors at 4 and 24 hours of coculture. The cytotoxicity was calculated as following formula: cytotoxicity (%) = ((TC-TT)/TC) × 100. TC: percentage of live tumor cells in control tubes (tumor cells alone), TT: percentage of live tumor cells in test tubes (tumor cells + CIK cells).

RNA isolation and whole transcriptome analysis

K562 (1×10^5 cells), Jurakt (1×10^5 cells) and SK-hep-1 (0.6×10^5 cells) were seeded in six well plates. As previous described, meticrane was added promptly in K562 and Jurkat cells but in SK-hep-1 cells, it was introduced 4h later. RNA isolation was performed using the RNeasy plus mini kit (QIAGEN GmbH, Hilden, Germany) following the manufacturer's instructions. Whole transcriptome analysis (3'-mRNA sequencing) was performed at the NGS Core Facility in Bonn, Germany. The data was analyzed using Histat2 (mapping tool) and EdgeR2 (differential analysis tool). The cutoff value (logFC > 2 and FDR < 0.05) was

applied to select the differential genes between the untreated and treated meticrane groups. KEGG pathway enrichment analysis (R package: clusterProfiler) were performed on the basis of based on differential genes. The heatmap (R package: pheatmap) was used to show the comparative analysis of differential genes between the untreated and treated meticrane groups.

Identification of the potential targets of meticrane

To identify potential targets of meticrane, we used previously described methodology (15). Briefly, AML (Acute Myeloid Leukemia) and HCC (Hepatocellular carcinoma) specific gene expression data (\log_2 (FPKM+1)) (TCGA data from TCGA database, <https://portal.gdc.cancer.gov/>, project:TCGA-LAML and TCGA-LIHC) and survival data (TCGA data from Uscs Xena database, <https://xenabrowser.net/datapages/>, cohort: GDC TCGA Liver Cancer (LIHC) and GDC TCGA Acute Myeloid Leukemia (LAML)) were utilized to imitate the clinical model. Using the TCGA data, we identified genes relevant to survival based on the following criteria: KM curve ($p < 0.001$), Cox regression ($p < 0.001$) and the difference in five-year survival between the low and high gene expression groups of more than 10%. Based on the HR (hazard ratio) value from the Cox regression, we further distinguish between genes with a high risk (poor prognosis) ($HR > 1$) and those with a low risk (good prognosis) ($HR < 1$). We then overlap differentially expressed genes (RNA-sequence data) with prognostic genes from TCGA patients' data. In particular, overlapping of low risk group with up-regulated genes and a high-risk group with down-regulated genes induced by meticrane treatment. All the overlapping genes were used to build protein-protein interaction (string: <https://string-db.org/>) and KEGG analysis (R package: clusterProfiler).

Molecular docking and molecular dynamics (MD) simulation

In addition, molecular docking was used to further explore the potential targets of meticrane, particularly focusing on known immune checkpoint (CTLA-4, PD-1, PD-L1, LAG-3, TIM-3, B7-H4, TIGIT, CD73) and epigenetic targets (DNMT1, HDACs). For this purpose, the crystal structures of the corresponding proteins were first extracted from the protein database (www.rcsb.org) and the respective proteins CTLA-4/1I8L, PD-1/4ZQK, PD-L1/6R3K, LAG-3/7TZH, TIM-3/7M3Z, B7-H4/4GOS, TIGIT/5V52, CD73/6TWA, DNA methyltransferase 1/3PTA, and Histone deacetylases (HDAC2/7JS8, HDAC3/4A69, HDAC4/2VQJ, HDAC6/5EDU, HDAC7/3ZNR, HDAC8/7JVU and HDAC10/7U3M) were identified. Since for HDACs, three small molecules bound crystal structures were available, therefore, we used all of them to comprehensively analyze different binding modes of ligands in their respective pockets. The protein structures were prepared by using the protein preparation wizard (PPW) module of maestro (Schrodinger LLC, New York, NY, USA) was used to pre-process the structures (16–20). Then, the ligand (meticrane) was prepared

using Schrödinger suite (LLC, New York, NY, 2020) LIGPREP (module of maestro), which generates tautomers, and possible ionization states at the pH range 7 ± 2 using Epik (21) and also generates all the stereoisomers of the compound, if necessary (16). The optimization was done using the OPLS3 (Optimized Potentials for Liquid Simulations) force field (22). Finally, Glide module of Schrodinger was used to perform the molecular docking and Prime MM-GBSA for binding free energy quantification. The grids were generated using the centroid of co-crystals by using the Receptor Grid Generation panel in Glide. The most favorable ligand-receptor conformations for a drug complex provided by a docking study (18). Glide is a comprehensive and systematic search tool for the molecule of interest from the virtual libraries. The obtained docked poses were then subjected to short MD simulations to study their dynamicity in the pocket. Desmond v3.6 module from Schrodinger suite was used to perform the MD simulations. The systems were built *via* Systems builder using OPLS3 force field and solvated with TIP3P water solvent model. All the complexes were placed in the orthorhombic periodic boundary conditions with a size of repeating buffered units at 10Å. Counter ions were also added to neutralize the systems. An energy minimization step was done for each system for 100ps. The NPT ensemble was employed for the simulations with the Nose-Hoover chain thermostat and the martyna-tobias-klein barostat. RESPA integrator was used with a time step of 0.002ps. For short range coulombic interactions, a 9.0 Å cut-off was considered. Bonds to hydrogen were constrained using the MSHAKE algorithm of Desmond. The coordinates were saved at intervals of 10 ps.

Statistical analysis

All experiments were performed in triplicate and repeated thrice. Besides, the experiments involving CIK cells were performed with three independent donors. FACS data were analyzed using FlowJo V10.6 software (FlowJo, LLC, Ashland, Oregon, U.S.A.). The mean values and standard deviations were used in the figures to demonstrate the experimental data. Also, figures and statistical analyses including one-way or two-way analyses of variance (ANOVA) with Bonferroni's *post-hoc* test and T-tests were performed using GraphPad Prism v.8.0 (GraphPad Software, Inc., San Diego, CA, U.S.A.). For bioinformatic data, the statistical analyses and figures were performed by R software. A $p < 0.05$ was considered as significant. * $p < 0.05$; ** $p < 0.01$; *** $p < 0.001$; **** $p < 0.0001$; ns: not significant.

Results

Meticrane-induced alteration in the cell viability and proliferation is independent from the apoptosis signaling pathway

To investigate the anticancer effect of meticrane, all cancer cells were co-cultured with meticrane at a concentration of 0.06 to 1 mM at 72 h. The leukemia cells (K562 and Jurkat) were found to be more

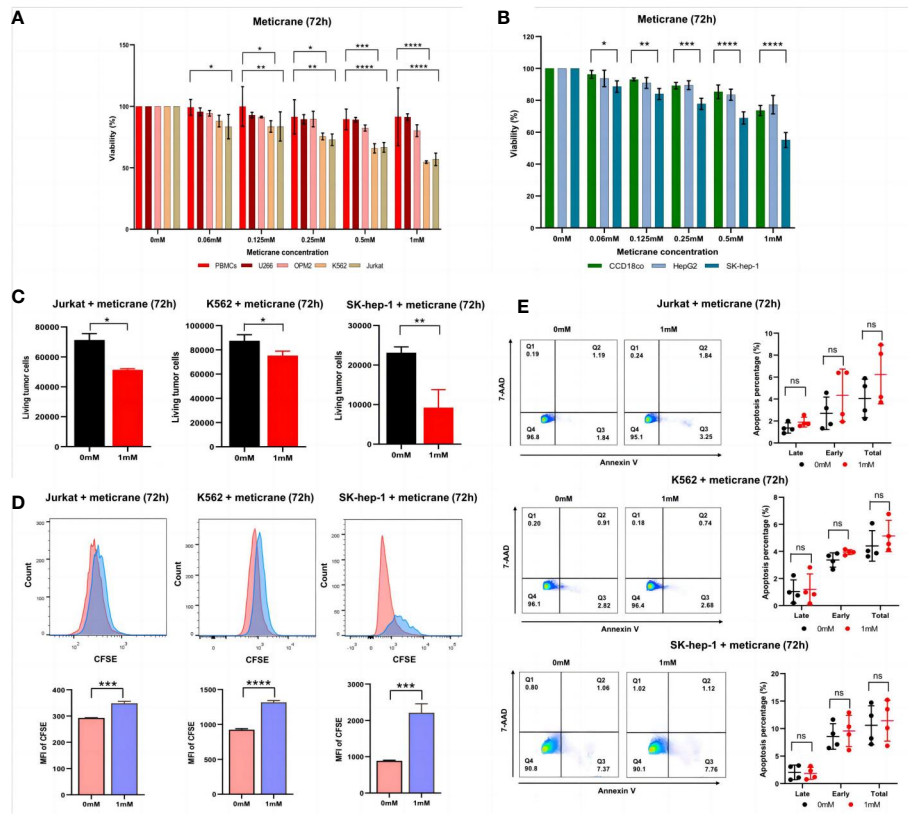


FIGURE 1

Effect of meticrane on the cell viability, alive cell number, proliferation and apoptosis of tumor cells. (A) CCK8 assay for cell viability for leukemia cell lines, myeloma cell lines and control cells. PBMCs (control cells), myeloma (U266 and OPM2) and leukemia (K562 and Jurkat) cells. P value were calculated by two-way ANOVA and Bonferroni's *post-hoc* test. All data were representative of at least three independent experiments ($n \geq 3$). (B) CCK8 assay for cell viability for liver cancer cell lines and control cells. CCD18co (control cells), and liver cancer (HepG2 and SK-hep-1) cells. P value were calculated by two-way ANOVA and Bonferroni's *post-hoc* test. All data were representative of at least three independent experiments ($n \geq 3$). (C) FACS assay for the relative alive cell number for Jurkat (left), K562 cells (middle) and SK-hep-1 cells (right). All data were representative of three independent experiments ($n = 3$). P value were calculated by T tests. (D) Proliferation of Jurkat (left), K562 cells (middle) and SK-hep-1 cells (right). Data are mean \pm SD of triplicate measurements; data are one representative of three independent experiments. T test were applied to calculate the p values. MFI, Mean Fluorescent Intensity. (E) The apoptosis of K562, Jurkat and SK-hep-1 cells. All data were representative of at four independent experiments ($n = 4$). P value were calculated by two-way ANOVA and Bonferroni's *post-hoc* test. * $p < 0.05$, ** $p < 0.01$, *** $p < 0.001$, **** $p < 0.0001$, ns, no significant.

sensitive to meticrane from 0.125 mM to 1 mM compared to the control cells (PBMCs) (Figure 1A). The cell viability was found to be decrease with increase in meticrane concentration in K562 (0.06mM: $p = 0.2384$, 0.125mM: $p = 0.0264$, 0.25mM: $p = 0.0323$, 0.5mM: $p = 0.0005$, 1mM: $p < 0.0001$) and Jurkat (0.06mM: $p = 0.0103$, 0.125mM: $p = 0.0073$, 0.25mM: $p = 0.0017$, 0.5mM: $p < 0.0001$, 1mM: $p < 0.0001$). However, myeloma cells (U266 and OPM2) (Figure 1A) showed no significant difference at any concentration compared to the controls (all p values at each concentration were more than 0.05). Likewise, in liver cells, SK-hep-1 cells showed significantly lower viability compared to the control cells (CCD18co cells), whereas HepG2 cells showed no significant difference (Figure 1B). The cell viability was found to be decrease with increase in meticrane concentration in SK-hep-1 (0.06mM: $p = 0.011$, 0.125mM: $p = 0.0025$, 0.25mM: $p = 0.0001$, 0.5mM: $p < 0.0001$, 1 mM: $p < 0.0001$) and HepG2 (all p values at each concentration were more than 0.05) (Figure 1B). Considering cell viability is directly correlated to the viable/alive cells, we next investigated and found that the number of alive K562 cells

($p = 0.026$), Jurkat cells ($p = 0.0013$), and SK-hep-1 cells ($p = 0.0011$) significantly decreased in the meticrane (1mM)-treated group compared with the untreated group after 72 h (Figure 1C), suggesting that meticrane could reduce the number of tumor cells. In addition, the MFI (Mean fluorescent intensity) of CFSE (Cell Trace carboxyl fluorescein succinimidyl ester) of K562 cells ($p < 0.0001$), Jurkat cells ($p = 0.0002$), and SK-hep-1 cells ($p = 0.0007$) was also found to be higher in the presence of meticrane (Figure 1D), suggesting that the proliferation of these cell were inhibited due to meticrane. Interestingly, no significant difference was observed between early and late apoptosis in all observed groups of K562 cells, Jurkat cells and SK-hep-1 cells by using Annexin V and 7AAD dyes (Figure 1E). Besides, we checked both apoptosis and caspase 3/7 activation level potentially caused by meticrane, and found no alterations by using CellEvent™ Caspase-3/7 Green Flow Cytometry Assay Kit (Supplementary Figure 1). Both two apoptosis experiments suggested that the strongly reduced cell viability is independent of the apoptosis-related signaling pathway. It can therefore be concluded that meticrane may

induce the alteration of cell viability and proliferation in selected hematologic and liver cancer cells, through independent of the apoptosis signaling pathway.

Meticrane showed additive/synergistic effect with epigenetic inhibitors

Whether the effects of meticrane led to the alteration in cell viability and proliferation in leukemia cells (K562 and Jurkat) and liver cancer cells (SK-hep-1) can be enhanced with known epigenetic inhibitors, we assayed both the DNMT1 inhibitor (5AC) and HDAC inhibitor (CUDC-101) in these cells for 72 h using CCK8 assay (Figures 2A, B). To ensure consistency, meticrane (125 μ M) was combined with 5AC (31.25nM-1000nM) and CUDC-101 (6.25nM-200nM) against K562 and Jurkat cells, whereas CUDC-101 (0.125 μ M-4 μ M) or 5AC (0.313 μ M-10 μ M) was optimized against SK-hep-1 cells. Of interest, in all cell lines, the

addition of 5AC in combination with meticrane showed significant differences in Jurkat cells (all $p < 0.0001$), K562 cells (1000nM: $p = 0.0033$, 31.25-500nM: all p values < 0.0001) and SK-hep-1 cells (0.313-1.25 μ M: all $p < 0.05$, 2.5 μ M: $p = 0.0014$) compared to the 5AC alone. Notably, in Jurkat cells, meticrane (125 μ M) in combination with 5AC (250nM: $p = 0.0499$, 500nM: $p = 0.001$ and 1000nM: $p < 0.0001$) showed higher inhibitory effect than meticrane alone (Figure 2A). This effect was also observed in K562 (125nM: $p = 0.0104$, 250nM: $p = 0.0004$, 500nM: $p < 0.0001$ and 1000nM: $p < 0.0001$) and SK-hep-1 cells (0.625 μ M: $p = 0.0006$, 1.25 μ M-10 μ M: all $p < 0.0001$). Like 5AC, CUDC-101 also in combination with meticrane showed significant differences in Jurkat cells (6.25nM: $p = 0.0005$, 12.5nM: $p = 0.0019$, 25nM: $p = 0.0018$, 50nM: $p = 0.0221$), K562 cells (6.25nM-25nM: all $p < 0.0001$, 50nM: $p = 0.0002$, 100nM: $p < 0.0001$, 200nM: $p = 0.0016$), and SK-hep-1 cells (0.125 μ M: $p < 0.0001$, 0.25 μ M: $p = 0.0001$, 0.5 μ M: $p = 0.0116$) compared to the CUDC-101 alone. The higher inhibitory effect of meticrane in combination with CUDC-101 was observed in Jurkat

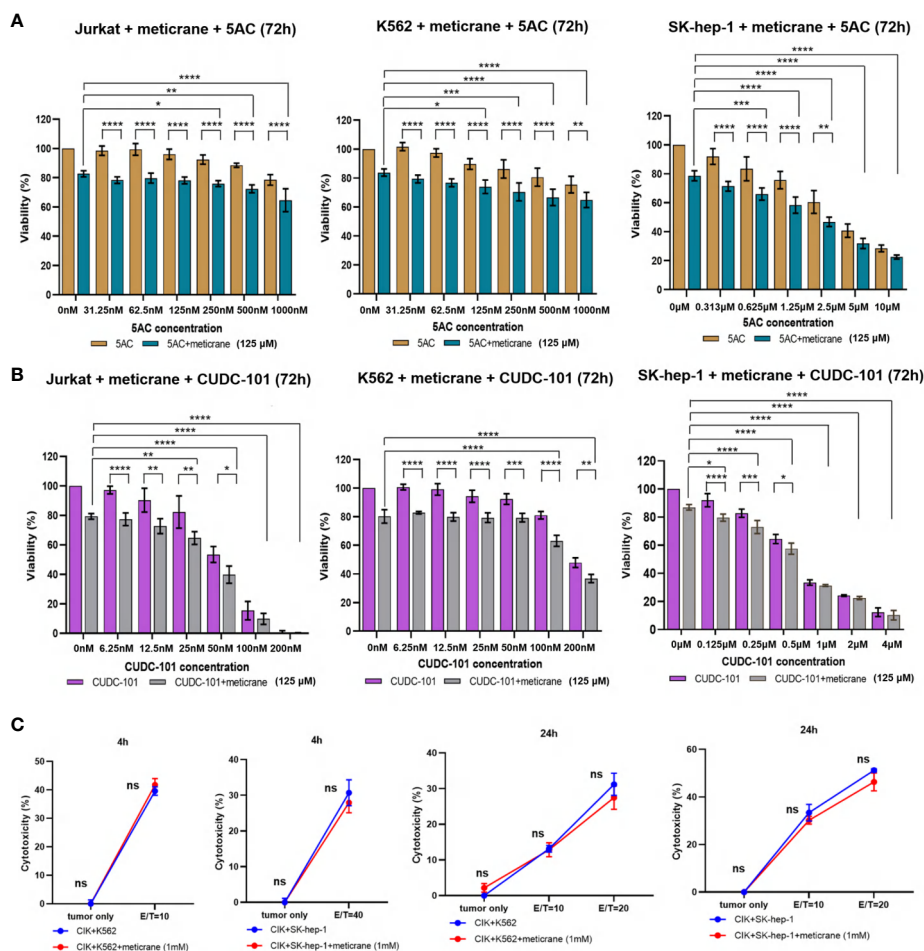


FIGURE 2

The combination effect of meticrane with epigenetic inhibitors or CIK cells. 5AC (A) or CUDC-101 (B) were used to test the cell viability (CCK8 assay) in Jurkat, K562 and SK-hep-1 cells. All data were representative of at least three independent experiments ($n \geq 3$). When comparing these two groups (no meticrane group vs. combined meticrane group), p -values were calculated using two-way ANOVA and Bonferroni's *post-hoc* test. When comparing the different dose in the group with meticrane, the p -value was calculated using a one-way ANOVA and the Bonferroni *post-hoc* test. (C) Cytotoxicity of CIK cells with/without meticrane against K562 and SK-hep-1 cells at 4 hours (left) and 24 hours (right) point time. Data are mean \pm SD of triplicate measurements; data are one representative of three independent experiments. T test (4h) and two-way ANOVA (Bonferroni's *post-hoc* test) (24h) were applied to calculate the p values. * $p < 0.05$, ** $p < 0.01$, *** $p < 0.001$, **** $p < 0.0001$. ns, no significant.

cells (25nM: $p=0.0033$, 50nM-200nM: all $p<0.0001$), K562 (100nM: $p<0.0001$, 200nM: $p<0.0001$) and Sk-hep-1 cells (0.125 μ M: $p=0.0126$, 0.25 μ M-4 μ M: $p<0.0001$) compared to meticrane alone. We also calculated the combination index Q values of meticrane with different concentrations of CUDC101 or 5AC on tumor cells (K562, Jurkat and SK-hep-1), and found mainly the additive/synergetic effects (Tables 1, 2).

Meticrane showed no compatibility with cytokine-induced killer cells

To further investigate the potential effect of meticrane with immunotherapy, cytokine-induced killer cells (CIKs) were assessed with meticrane. Meticrane (1mM) in combination with CIK cells was tested against K562 cells and SK-hep-1 cells. In particular, meticrane did not change the cytotoxicity of CIKs against K562 cells ($p=0.2391$) and SK-hep-1 cells ($p=0.424$) tested at time point 4h (Figure 2C). Due to this different sensitivity of CIKs against K562 and SK-hep-1 cells at 4h, we applied a different E/T ratio for K562 (E/T=10) and SK-hep-1 (E/T=40). Likewise, meticrane did not change the cytotoxicity of CIKs against K562 cells (E/T=10 $p=1$, E/T=20 $p=0.1548$) and SK-hep-1 cells (E/T=10 $p=0.344$, E/T=20 $p=0.0673$) tested at time point 24h (Figure 2C). Of note, as shown in the tumor only group in Figure 2C at 4h and 24 time point, meticrane alone (without CIKs) did not show cytotoxicity against

K562 (4 hours $p=1$, 24 hours $p=0.6757$) or SK-hep-1 cells (4 hours $p=1$, 24 hours $p=1$) at either 4 hours or 24 hours (Figure 2C). Overall, meticrane showed no compatibility with cytokine-induced killer cells.

Meticrane exerts no effect on cancer-associated signaling pathways in cancer cells

A genome-wide transcriptional analysis was performed to investigate the transcriptional changes in the cells treated with meticrane (Figures 3A-C). Based on differential genes between untreated and treated meticrane groups, we obtained meticrane induced significantly upregulated/downregulated genes from leukemia cell lines (Jurkat: 1500 up-regulated and 1519 down-regulated, Supplementary Table 1; K562: 1521 up-regulated and 1237 down-regulated, Supplementary Table 2) and liver cancer cell line (SK-hep-1: 1195 up-regulated and 1557 down-regulated, Supplementary Table 3). Using KEGG enrichment analysis to identify the ten most enriched metabolic pathways, we found that the leukaemia cell lines (Jurkat and K562) were highly enriched in oxidative phosphorylation, mTOR signalling, RNA degradation and regulation of cancer-related metabolic pathways. For the liver cancer cell line (SK-hep-1), there was significant enrichment in ferroptosis, focal adhesion and signaling pathways that play an

TABLE 1 Combination index Q of meticrane with CUDC101 in K562, Jurkat and SK-hep-1 cells.

Jurkat			K562			SK-hep-1		
meticrane	CUDC101	Index Q	meticrane	CUDC101	Index Q	meticrane	CUDC101	Index Q
125 μ M	0nM	1.00	125 μ M	0nM	1.00	125 μ M	0 μ M	1.00
125 μ M	6.25nM	0.99	125 μ M	6.25nM	0.90	125 μ M	0.125 μ M	1.02
125 μ M	12.5nM	0.96	125 μ M	12.5nM	0.98	125 μ M	0.25 μ M	0.96
125 μ M	25nM	1.02	125 μ M	25nM	0.85	125 μ M	0.5 μ M	0.96
125 μ M	50nM	1.05	125 μ M	50nM	0.80	125 μ M	1 μ M	0.97
125 μ M	100nM	1.03	125 μ M	100nM	1.05	125 μ M	2 μ M	0.98
125 μ M	200nM	1.00	125 μ M	200nM	1.03	125 μ M	4 μ M	1.01

TABLE 2 Combination index Q of meticrane with 5AC in K562, Jurkat and SK-hep-1 cells.

Jurkat			K562			SK-hep-1		
meticrane	5AC	Index Q	meticrane	5AC	Index Q	meticrane	5AC	Index Q
125 μ M	0nM	1.00	125 μ M	0nM	1.00	125 μ M	0 μ M	1.00
125 μ M	31.25nM	1.17	125 μ M	31.25nM	1.39	125 μ M	0.313 μ M	1.03
125 μ M	62.5nM	1.14	125 μ M	62.5nM	1.26	125 μ M	0.625 μ M	0.99
125 μ M	125nM	1.06	125 μ M	125nM	1.05	125 μ M	1.25 μ M	1.03
125 μ M	250nM	1.02	125 μ M	250nM	1.07	125 μ M	2.5 μ M	1.02
125 μ M	500nM	1.03	125 μ M	500nM	1.03	125 μ M	5 μ M	1.00
125 μ M	1000nM	1.01	125 μ M	1000nM	0.95	125 μ M	10 μ M	1.00

important role in cancer regulation, such as protein processing in the ribosome and endoplasmic reticulum. Thus, meticrane showed no direct/predominant effect on cancer-related signaling pathways in leukemia cell lines, and a distant impact (i.e., pathways not directly involved in cancer) to cancer in liver cancer cells.

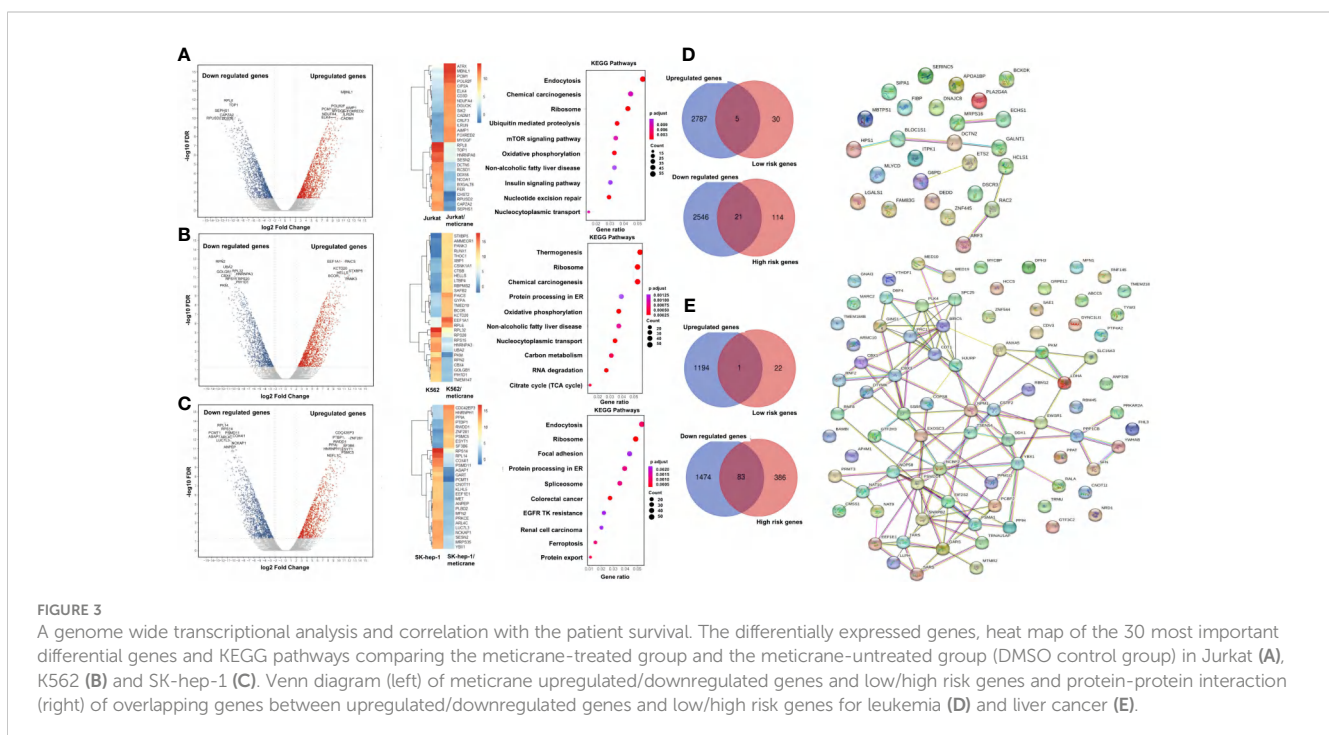
Meticrane induced differentially expressed genes showed association with survival-related genes in cancer

We identified survival relevant genes for AML (high risk genes: $n=135$ and low risk genes: $n=35$; [Supplementary Table 4](#)) and HCC (high risk genes: $n=469$ and low risk genes: $n=23$; [Supplementary Table 5](#)) were found using TCGA datasets. Subsequently, the low-risk genes were correlated with the up-regulated genes induced by meticrane (RNA-sequence) and the high-risk genes were correlated with the down-regulated genes induced by meticrane. In this pattern, we identified groups of overlapping genes in for AML (low-risk/up-regulated genes: $n=5$; high-risk/down-regulated genes: $n=21$) and HCC (low-risk/up-regulated genes: $n=1$; high-risk/down-regulated genes: $n=83$) ([Figures 3D, E](#); [Supplementary Table 6](#)). By combining our *in vitro* data and information from TCGA's publicly available clinical portal, we described 110 genes (AML=26 genes; HCC=84 genes) ([Supplementary Table 6](#)) as potential targets of meticrane in these two cancers. We then established PPI (protein-protein interaction, cutoff interaction value: 0.4.) on these genes and found moderate to weak interactions in HCC and AML, respectively ([Figures 3D, E](#)). Using KEGG analysis of these selective genes, we also found that they are specifically involved in non-cancer pathways ([Supplementary Figure 2](#)).

Molecular docking and molecular dynamics (MD) simulation analysis confirmed the binding affinity of meticrane with known oncological targets

To further explore the potential targets of meticrane, we performed a molecular docking analysis by aligning Meticrane against known immune checkpoints (CTLA-4, PD-1, PD-L1, LAG-3, TIM-3, B7-H4, TIGIT, CD73) and epigenetic targets (DNMT1, HDACs) ([Figure 4](#); [Supplementary Figure 3](#)). On the basis of molecular docking followed by MM-GBSA scores, it is evident that meticrane has considerable binding affinity against some oncological targets such as PD-L1, TIM-3, CD73, and HDACs (HDAC2, HDAC3, HDAC4, HDAC6, HDAC7, HDAC8 and HDAC10) ([Figure 4](#)). Given the small size of meticrane, the binding affinity score is considerable, suggesting that these proteins may be possible targets. As proof of principle, we selected HDAC6 for further analysis. Interestingly, when HDAC6 inhibitor (ACY1215) was combined with meticrane, a significantly high impact on the viability of tumor cells (K562, Jurkat and SK-hep-1) were observed ([Supplementary Figures 4A-C](#)). Additionally, we found that meticrane with ACY1215 has additive/synergistic effects against tumor cells, based on the combination index Q values ([Supplementary Figure 4D](#)).

To extend the analysis, we also performed MD simulations and investigated the dynamic behavior of the protein and ligands using the RMSD parameter, in which the structural deviations in the molecule are calculated over time with respect to the initial structure (docked pose). The RMSD of the ligands (plateau reached) confirms the stability of the meticran in the pocket of each protein, suggesting that these proteins may be of interest as



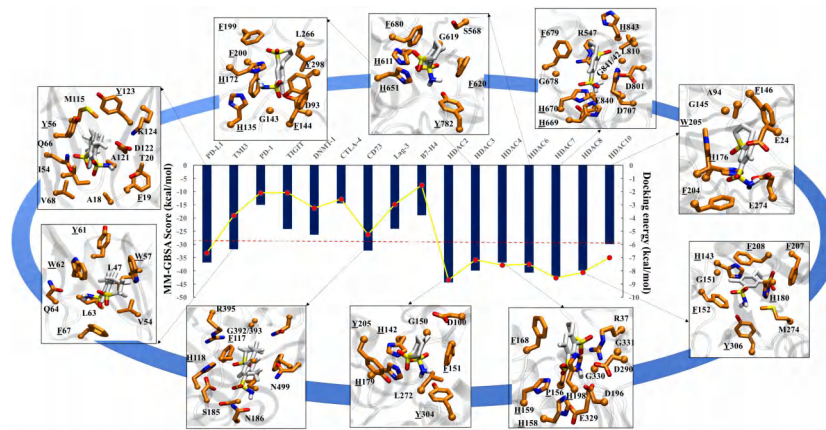


FIGURE 4

Molecular docking analysis for meticrane. Molecular docking of meticrane on established oncological targets is shown. The bi-axis docking energy and MM-GBSA scores (in kcal/mol) are marked. The cut-off is shown in a red dotted line. The interaction mapping of all targets with significant docking energy and MM-GBSA scores (\geq to cut-off) are highlighted. In the interaction map, the meticrane and amino acids of each protein are shown in licorice color and colored by atoms as C: white/orange, O: red, N: blue, S: yellow, respectively. From the interaction map the aromatic residues that appear to be essential for the binding and stability of the meticrane have been identified (highlighted with underlining).

potential targets for thorough experimental validation in the future (Supplemental Figure 5).

Discussion

Certainly, there are enormous number of chemotherapeutic agents and targeted anti-cancer drugs, however, their side effects on the patient's healthy cells/tissues are not negligible. Given that the development of new anti-tumor drugs requires extensive preclinical and clinical studies, drug repositioning (also known as “drug repurposing”) has emerged as a rapid alternative strategy, particularly related to non-oncology drugs (23). Moreover, several putative non-oncology drugs have been predicted, but their potential as future cancer therapeutics is unknown (24). Broadly, metformin is currently a typical example of a non-oncology anticancer drug (25), driven by the hypothesis of reducing the availability of glucose and insulin to slow down the tumor growth and progression. Herein, we tested another non-oncological drug named as meticrane, a thiazide diuretic commonly used to treat essential hypertension. Previously, meticrane in combination with CTLA-4 treatment was reported to improve the survival of mesothelioma mice (9), however, the anticancer effect of meticrane in tumors remained unexplored. In the current study, for the first time, we investigated the anti-cancer ability of meticrane in hematologic malignancies (myeloma and leukemia) and liver cancer cell lines.

We first cultured meticrane with cancer cells and found that leukemia cells (K562 and Jurkat) were more sensitive, whereas myeloma cells (U266 and OPM2) lacked a similar response. Similarly, some liver cancer cells (SK-hep-1) responded more effectively to meticrane, whereas others did not (HepG2). Notably, all the cell lines included in this study have a very distinctive (epi-)genetic profile, e.g., K562 (adult female/53 years, TP53 mutation), Jurkat (young male/14 years, TP53, BAX,

NOTCH1, MSH1/6, INPP5D mutations), U266 (adult male/53 years, TP53, BRAF, TRAF3, MSH6 mutations), OPM2 (adult female/56 years, TP53, SMAD2, CDKN2A, FGFR3 mutations), SK-hep-1 (adult male/52 years, BRAF, CDKN2A mutations), and HepG2 (young male/15 years, TERT, NRAS mutations). Thus, we confirmed that meticrane indeed has an anti-cancer potential that specifically targets certain genetic constellations. Certainly, some discrepancies in the experiments are expected owing to heterogeneity among cancer cell lines in addition to (epi-)genomic factors (26). In addition, we also tested and confirmed that meticrane has the potential to significantly reduce the number of tumor cells and proliferation. Particularly, these effects were validated in three cell lines (K562, Jurkat and SK-hep-1). We also examined whether apoptosis-related signaling pathways (cell death) might contribute to this noticeable cytotoxic effect, but confirmed that no evidence of apoptosis was detectable in K562, Jurkat, or SK-hep-1 cells, suggesting that it may inhibit cancer cell proliferation in an apoptosis-independent manner. In fact, some previous evidence suggests that a few compounds can cause cancer cell death *via* an apoptosis-independent pathway (27, 28). Whether meticrane would be of greater benefit to patients, who do not respond to clinical drugs due to apoptosis resistance, will be of future interest.

Next, we combined meticrane with the established epigenetic inhibitors CUCD-101 (HDACi) and 5AC (DNMTi), as epigenetic alterations are also known to influence numerous aspects of cancer and such inhibitors have already been tested in multiple cancer/clinical studies (29). Noticeably, meticrane in combination with CUCD-101 or 5AC showed a higher inhibitory effect in hematological malignancies (K562 and Jurkat cells) and in liver cancer (SK-hep-1) cells compared to meticrane or epigenetic inhibitors alone. The combination of meticrane and epigenetic inhibitors (CUCD-101 or 5AC) showed additive/synergistic effects on K562, Jurkat and SK-hep-1 cells. Therefore, this combo (meticrane+epigenetic inhibitors) might be a possible replacement for toxic substances used for cancer treatment, however, *in-vivo*

studies are warranted in this context. Motivated by the optimistic results attained with a cocktail of meticrane and epigenetic inhibitors for anticancer efficacy, we subsequently tested its suitability for immunotherapy against cancers, in particular, cytokine-induced killer (CIK) cell therapy. Being a pioneer of CIK cell therapy (30), we have already demonstrated the favorable effect of CIK cells with known cancer inhibitors (e.g. PD-1/PD-L1) (31) and even epigenetic compounds (e.g. HDAC) (32). Intriguingly, meticrane showed no response to the cytotoxicity of CIKs against K562 cells and Sk-hep-1 cells over 4-24 hours of treatment. At this point, we cannot conclude whether similar effect will also prevail for other immunomodulatory effects of CIK cells when used under *in vivo* conditions. To our knowledge, this is the very first study to test any non-oncology drug against CIK cells. To gain better insight into the transcriptional role of meticrane, we performed genome-wide transcriptional analyses in both untreated and treated groups of meticrane in Jurkat, K562 and SK-hep-1 cells. Interestingly, we identified both up-regulated and down-regulated genes in all experimental groups, showed no direct/predominant effect on cancer-related signaling pathways in leukemia cell lines, and a distant impact to cancer in liver cancer cells. This suggests that meticrane can induce changes in cancer cells (as confirmed by the changes in cell viability and proliferation), but in a passive manner. As a proof of concept, we also overlap the obtained meticrane induced differentially expressed genes with the cancer specific survival data from the publicly available TCGA dataset and found a correlation among them. Therefore, it is reasonable to speculate that meticrane is involved in some anticancer pathways that are passively involved in targeting cancer cells and may be considered as compatible with other clinically safe drugs, particularly epigenetic inhibitors. These findings also prompted us to conduct molecular docking analysis in order to further explore the potential targets of meticrane. We specifically focused on known immune checkpoints (CTLA-4, PD-1, PD-L1, LAG-3, TIM-3, B7-H4, TIGIT, CD73) and epigenetic targets (DNMT1, HDACs). Of interest, we found considerable binding affinity scores of meticrane against PD-L1, TIM-3, CD73, and HDACs. To validate, we focused on HDAC6 for further analysis, and found a significantly high impact on the viability of tumor cells when HDAC6 inhibitor (ACY1215) was combined with the meticrane. Since meticrane showed additive/synergistic effects with CUDC101, 5AC and ACY1215 in our analysis, this could partly explain its positive molecular binding affinity with these epigenetic target proteins. Certainly, additional analyses for other putative targets are warranted. On a broader view, it is reasonable to speculate that meticrane may not alter any specific cancer-related pathway, but may exert its distant effects on the cancer cells (passively) *via* well-known immune-regulatory/epigenetic signaling pathways, preferably *via* targeting PD-L1, TIM-3, CD73, and HDACs.

It is equally important to address the limitations and future prospects of our (similar) studies, for instance, 1) As we have observed in case of meticrane, other non-oncology drugs may also not have direct targets associated with cancer, and therefore

experiments like RNA sequencing (whole transcriptome analysis) studies following co-cultures in cancer cells may not be sufficient to draw any conclusions. 2) It is entirely possible that these drugs show anticancer activity only at high doses, so screening with variable concentrations (min to max) is recommended. At least in the case of meticrane, synthesis of other next-generation compounds (based on its structure) with a stronger tendency to inhibit the proliferation of cancer cells may solve this problem to some extent. 3) The genetic/epigenetic background of the cancer type and even gender differences may lead to different outcomes with these drugs in clinics. Specifically, when it is also known about the considerable overlapping between gene expression variation and the association of altered mutational pathways across the cancer genome (33, 34). Therefore, larger panels of cancer cell lines with multiple genetic constellations are necessary to confirm their potential mode of action. 4) Considering that cancer patients have a limited therapeutic window, it will be a significant question to follow whether non-oncology drugs (presumably alone) are sufficient to prolong the survival, especially in patients without any signs of cancer for a certain period of time after the treatment. 5) Such drugs may not be appropriate for all cancer immunotherapy types, hence, a critical selection of specific immunotherapy (broadly activating the immune system and/or precisely targets of the tumor) should be pre-addressed. Overall, we were able to show that meticrane, a non-oncology drug, exhibits anticancer potential with epigenetic inhibitors *in-vitro*, but not with cytokine-induced killer (CIK) cells.

Conclusions

Non-oncology drug (meticrane) effectively synergizes with epigenetic inhibitors in leukemia and liver cancer cells. Though we have demonstrated its anticancer ability, its mechanistic inference is still unclear. In the current study, we also expressed some important concerns encountered during the meticrane testing, which are also relevant to other non-oncology drugs when considering their future clinical or preclinical use.

Data availability statement

The data supporting the findings of this study are available from the corresponding author [I.G.H.S-W] on request.

Author contributions

Conceptualization, YW, AS, and IS-W; methodology, YW, YY, HJL, HDL, LM, SA, and CZ; validation, YW, FG and PC; writing—original draft preparation, YW, AS, and IS-W; project administration, AS and IS-W; funding acquisition, IS-W. All authors contributed to the article and approved the submitted version.

Funding

The CIO Aachen Bonn Köln Düsseldorf is kindly supported by the Deutsche Krebshilfe.

Conflict of interest

The authors declare that the research was conducted in the absence of any commercial or financial relationships that could be construed as a potential conflict of interest.

Publisher's note

All claims expressed in this article are solely those of the authors and do not necessarily represent those of their affiliated organizations, or those of the publisher, the editors and the reviewers. Any product that may be evaluated in this article, or claim that may be made by its manufacturer, is not guaranteed or endorsed by the publisher.

Supplementary material

The Supplementary Material for this article can be found online at: <https://www.frontiersin.org/articles/10.3389/fonc.2023.1157366/full#supplementary-material>

SUPPLEMENTARY FIGURE 1

Evaluating apoptosis and Caspase3/7 activation by using CellEvent™ Caspase-3/7 Green Flow Cytometry Assay Kit

SUPPLEMENTARY FIGURE 2

KEGG enrichment analysis of overlapping genes found between meticrane induced differentially expressed genes and survival-related genes in cancer.

SUPPLEMENTARY FIGURE 3

Molecular docking analysis.

SUPPLEMENTARY FIGURE 4

The combination effect of meticrane with ACY1215 (selective HDAC6 inhibitor). The viability of Jurkat (A), K562 (B) and SK-hep-1 (C) cells in presence of ACY1215 with/without meticrane. D) Combination index Q of Meticrane and ACY1215 on K562, Jurkat and SK-hep-1 cells.

SUPPLEMENTARY FIGURE 5

Molecular dynamics

SUPPLEMENTARY TABLE 1

Meticrane induced differentially expressed genes in Jurkat.

SUPPLEMENTARY TABLE 2

Meticrane induced differentially expressed genes in K562.

SUPPLEMENTARY TABLE 3

Meticrane induced differentially expressed genes in SK-hep-1.

SUPPLEMENTARY TABLE 4

Survival-related genes in AML.

SUPPLEMENTARY TABLE 5

Survival-related genes in HCC.

SUPPLEMENTARY TABLE 6

Overlapping genes between meticrane induced differentially expressed genes and survival-related genes in cancers.

References

- Zhang Z, Zhou L, Xie N, Nice EC, Zhang T, Cui Y, et al. Overcoming cancer therapeutic bottleneck by drug repurposing. *Signal transduction targeted Ther* (2020) 5(1):113. doi: 10.1038/s41392-020-00213-8
- Papapetropoulos A, Szabo C. Inventing new therapies without reinventing the wheel: the power of drug repurposing. *Br J Pharmacol* (2018) 175(2):165–7. doi: 10.1111/bph.14081
- Kasznicki J, Sliwinska A, Drzewoski J. Metformin in cancer prevention and therapy. *Ann Trans Med* (2014) 2(6):57. doi: 10.3978/j.issn.2305-5839.2014.06.01
- Zi F, Zi H, Li Y, He J, Shi Q, Cai Z. Metformin and cancer: an existing drug for cancer prevention and therapy. *Oncol Lett* (2018) 15(1):683–90. doi: 10.3892/ol.2017.7412
- Fu L, Jin W, Zhang J, Zhu L, Lu J, Zhen Y, et al. Repurposing non-oncology small-molecule drugs to improve cancer therapy: current situation and future directions. *Acta Pharm Sin B* (2022) 12(2):532–57. doi: 10.1016/j.apsb.2021.09.006
- Pushpakom S, Iorio F, Eyers PA, Escott KJ, Hopper S, Wells A, et al. Drug repurposing: progress, challenges and recommendations. *Nat Rev Drug Discovery* (2019) 18(1):41–58. doi: 10.1038/nrd.2018.168
- Majchrzak-Celińska A, Warych A, Szoszkiewicz M. Novel approaches to epigenetic therapies: from drug combinations to epigenetic editing. *Genes* (2021) 12(2). doi: 10.3390/genes12020208
- Sharma A, Liu H, Herwig-Carl MC, Chand Dakal T, Schmidt-Wolf IGH. Epigenetic regulatory enzymes: mutation prevalence and coexistence in cancers. *Cancer Invest* (2021) 39(3):257–73. doi: 10.1080/07357907.2021.1872593
- Lesterhuis WJ, Rinaldi C, Jones A, Rozali EN, Dick IM, Khong A, et al. Network analysis of immunotherapy-induced regressing tumours identifies novel synergistic drug combinations. *Sci Rep* (2015) 5:12298. doi: 10.1038/srep12298
- Schmidt-Wolf IG, Negrin RS, Kiem HP, Blume KG, Weissman IL. Use of a acid Mouse/Human lymphoma model to evaluate cytokine-induced killer cells with potent antitumor cell activity. *J Exp Med* (1991) 174(1):139–49. doi: 10.1084/jem.174.1.139
- Pinho MP, Lepski GA, Rehder R, Chauca-Torres NE, Evangelista GCM, Teixeira SF, et al. Near-complete remission of glioblastoma in a patient treated with an allogenic dendritic cell-based vaccine: the role of tumor-specific Cd4+T-cell cytokine secretion pattern in predicting response and recurrence. *Int J Mol Sci* (2022) 23(10). doi: 10.3390/ijms23105396
- Zhang Y, Wu X, Sharma A, Weiher H, Schmid M, Kristiansen G, et al. Anti-Cd40 predominates over anti-Ctla-4 to provide enhanced antitumor response of dc-cik cells in renal cell carcinoma. *Front Immunol* (2022) 13:925633. doi: 10.3389/fimmu.2022.925633
- Garofano F, Sharma A, Abken H, Gonzalez-Carmona MA, Schmidt-Wolf IGH. A low dose of pure cannabidiol is sufficient to stimulate the cytotoxic function of cik cells without exerting the downstream mediators in pancreatic cancer cells. *Int J Mol Sci* (2022) 23(7). doi: 10.3390/ijms23073783
- Sun X, Fan T, Sun G, Zhou Y, Huang Y, Zhang N, et al. 2-Deoxy-D-Glucose increases the sensitivity of glioblastoma cells to bcnu through the regulation of glycolysis, ros and ers pathways: *In vitro* and *in vivo* validation. *Biochem Pharmacol* (2022) 199:115029. doi: 10.1016/j.bcp.2022.115029
- Wang Y, Setiawan MF, Liu H, Dakal TC, Liu H, Ge F, et al. Regulator of G protein signaling 20 correlates with long intergenic non-coding rna (Lincrnas) harboring oncogenic potential and is markedly upregulated in hepatocellular carcinoma. *Biology* (2022) 11(8). doi: 10.3390/biology11081174
- Mittal L, Kumari A, Srivastava M, Singh M, Asthana S. Identification of potential molecules against covid-19 main protease through structure-guided virtual screening approach. *J biomol structure dynamics* (2021) 39(10):3662–80. doi: 10.1080/07391102.2020.1768151
- Mittal L, Tonk RK, Awasthi A, Asthana S. Targeting cryptic-orthosteric site of pd-L1 for inhibitor identification using structure-guided approach. *Arch Biochem biophys* (2021) 713:109059. doi: 10.1016/j.abb.2021.109059
- Panwar S, Kumari A, Kumar H, Tiwari AK, Tripathi P, Asthana S. Structure-based virtual screening, molecular dynamics simulation and *in vitro* evaluation to

- identify inhibitors against nampt. *J biomol structure dynamics* (2022) 40(20):10332–44. doi: 10.1080/07391102.2021.1943526
19. Tyagi R, Srivastava M, Jain P, Pandey RP, Asthana S, Kumar D, et al. Development of potential proteasome inhibitors against mycobacterium tuberculosis. *J biomol structure dynamics* (2022) 40(5):2189–203. doi: 10.1080/07391102.2020.1835722
20. Srivastava M, Mittal L, Kumari A, Asthana S. Molecular dynamics simulations reveal the interaction fingerprint of remdesivir triphosphate pivotal in allosteric regulation of sars-Cov-2 rdrp. *Front Mol Biosci* (2021) 8:639614. doi: 10.3389/fmolb.2021.639614
21. Greenwood JR, Calkins D, Sullivan AP, Shelley JC. Towards the comprehensive, rapid, and accurate prediction of the favorable tautomeric states of drug-like molecules in aqueous solution. *J computer-aided Mol design* (2010) 24(6-7):591–604. doi: 10.1007/s10822-010-9349-1
22. Harder E, Damm W, Maple J, Wu C, Reboul M, Xiang JY, et al. Opls3: a force field providing broad coverage of drug-like small molecules and proteins. *J Chem Theory Comput* (2016) 12(1):281–96. doi: 10.1021/acs.jctc.5b00864
23. Turabi KS, Deshmukh A, Paul S, Swami D, Siddiqui S, Kumar U, et al. Drug repurposing-an emerging strategy in cancer therapeutics. *Naunyn-Schmiedeberg's Arch Pharmacol* (2022) 395(10):1139–58. doi: 10.1007/s00210-022-02263-x
24. Corsello SM, Nagari RT, Spangler RD, Rossen J, Kocak M, Bryan JG, et al. Discovering the anti-cancer potential of non-oncology drugs by systematic viability profiling. *Nat Cancer* (2020) 1(2):235–48. doi: 10.1038/s43018-019-0018-6
25. Skuli SJ, Alomari S, Gaitsch H, Bakayoko A, Skuli N, Tyler BM. Metformin and cancer, an ambiguanidous relationship. *Pharm (Basel Switzerland)* (2022) 15(5). doi: 10.3390/ph15050626
26. Sharma A, Reutter H, Ellinger J. DNA Methylation and bladder cancer: where genotype does not predict phenotype. *Curr Genomics* (2020) 21(1):34–6. doi: 10.2174/1389202921666200102163422
27. Yang J, Zhou Y, Cheng X, Fan Y, He S, Li S, et al. Isogambogenic acid induces apoptosis-independent autophagic cell death in human non-Small-Cell lung carcinoma cells. *Sci Rep* (2015) 5:7697. doi: 10.1038/srep07697
28. O'Sullivan-Coyne G, O'Sullivan GC, O'Donovan TR, Piwocka K, McKenna SL. Curcumin induces apoptosis-independent death in oesophageal cancer cells. *Br J Cancer* (2009) 101(9):1585–95. doi: 10.1038/sj.bjc.6605308
29. Cheng Y, He C, Wang M, Ma X, Mo F, Yang S, et al. Targeting epigenetic regulators for cancer therapy: mechanisms and advances in clinical trials. *Signal transduction targeted Ther* (2019) 4:62. doi: 10.1038/s41392-019-0095-0
30. Sharma A, Schmidt-Wolf IGH. 30 years of CIK cell therapy: recapitulating the key breakthroughs and future perspective. *J Exp Clin Cancer Res CR* (2021) 40(1):388. doi: 10.1186/s13046-021-02184-2
31. Li Y, Sharma A, Bloemendal M, Schmidt-Wolf R, Kornek M, Schmidt-Wolf IGH. Pd-1 blockade enhances cytokine-induced killer cell-mediated cytotoxicity in b-cell non-Hodgkin lymphoma cell lines. *Oncol Lett* (2021) 22(2):613. doi: 10.3892/ol.2021.12874
32. Stephan D, Weiher H, Schmidt-Wolf IGH. Cik cells and hdac inhibitors in multiple myeloma. *Int J Mol Sci* (2017) 18(5). doi: 10.3390/ijms18050945
33. Liu H, Li H, Luo K, Sharma A, Sun X. Prognostic gene expression signature revealed the involvement of mutational pathways in cancer genome. *J Cancer* (2020) 11(15):4510–20. doi: 10.7150/jca.40237
34. Sharma A, Wüllner U, Schmidt-Wolf IGH, Maciaczyk J. Marginalizing the genomic architecture to identify crosstalk across cancer and neurodegeneration. *Front Mol Neurosci* (2023) 16:1155177. doi: 10.3389/fnmol.2023.1155177

3.3 Publication 3: Computational analysis of heat shock proteins and ferroptosis-associated lncRNAs to predict prognosis in acute myeloid leukemia patients

Fangfang Ge^{1†} , Yulu Wang^{1†} , Amit Sharma^{1,2†} , Ulrich Jaehde ³ , Markus Essler⁴ , Matthias Schmid⁵ and Ingo G. H. Schmidt-Wolf ^{1 *}

¹Department of Integrated Oncology, Center for Integrated Oncology (CIO), University Hospital Bonn, Bonn, Germany

²Department of Neurosurgery, University Hospital Bonn, Bonn, Germany

³Department of Clinical Pharmacy, Institute of Pharmacy, University of Bonn, Bonn, Germany

⁴Department of Nuclear Medicine, University Hospital Bonn, Bonn, Germany

⁵Institute for Medical Biometry, Informatics and Epidemiology, University Hospital Bonn, Bonn, Germany



OPEN ACCESS

EDITED BY

Wei Li,
First Affiliated Hospital of Zhengzhou
University, China

REVIEWED BY

Yongping Song,
First Affiliated Hospital of Zhengzhou
University, China
Zhongxing Jiang,
First Affiliated Hospital of Zhengzhou
University, China

*CORRESPONDENCE

Ingo G. H. Schmidt-Wolf,
✉ ingo.schmidt-wolf@ukbonn.de

[†]These authors share first authorship

RECEIVED 06 May 2023

ACCEPTED 06 July 2023

PUBLISHED 01 August 2023

CITATION

Ge F, Wang Y, Sharma A, Jaehde U,
Essler M, Schmid M and
Schmidt-Wolf IGH (2023), Computational
analysis of heat shock proteins and
ferroptosis-associated lncRNAs to
predict prognosis in acute myeloid
leukemia patients.
Front. Genet. 14:1218276.
doi: 10.3389/fgene.2023.1218276

COPYRIGHT

© 2023 Ge, Wang, Sharma, Jaehde,
Essler, Schmid and Schmidt-Wolf. This is
an open-access article distributed under
the terms of the [Creative Commons
Attribution License \(CC BY\)](https://creativecommons.org/licenses/by/4.0/). The use,
distribution or reproduction in other
forums is permitted, provided the original
author(s) and the copyright owner(s) are
credited and that the original publication
in this journal is cited, in accordance with
accepted academic practice. No use,
distribution or reproduction is permitted
which does not comply with these terms.

Computational analysis of heat shock proteins and ferroptosis-associated lncRNAs to predict prognosis in acute myeloid leukemia patients

Fangfang Ge^{1†}, Yulu Wang^{1†}, Amit Sharma^{1,2†}, Ulrich Jaehde³,
Markus Essler⁴, Matthias Schmid⁵ and Ingo G. H. Schmidt-Wolf^{1*}

¹Department of Integrated Oncology, Center for Integrated Oncology (CIO), University Hospital Bonn, Bonn, Germany, ²Department of Neurosurgery, University Hospital Bonn, Bonn, Germany, ³Department of Clinical Pharmacy, Institute of Pharmacy, University of Bonn, Bonn, Germany, ⁴Department of Nuclear Medicine, University Hospital Bonn, Bonn, Germany, ⁵Institute for Medical Biometry, Informatics and Epidemiology, University Hospital Bonn, Bonn, Germany

Owing to their functional diversity in many cancers, long noncoding RNAs (lncRNAs) are receiving special attention. lncRNAs not only function as oncogenes or tumor suppressors by participating in various signaling pathways but also serve as predictive markers for various types of cancer, including acute myeloid leukemia (AML). Considering this, we investigated lncRNAs that may act as a mediator between two processes, i.e., heat shock proteins and ferroptosis, which appear to be closely related in tumorigenesis. Using a comprehensive bioinformatics approach, we identified four lncRNAs (AL138716.1, AC000120.1, AC004947.1, and LINC01547) with prognostic value in AML patients. Of interest, two of them (AC000120.1 and LINC01547) have already been reported to be AML-related, and AC004947.1 is considered to have oncogenic potential. In particular, the signature obtained showed a lower survival probability with high-risk patients, and *vice versa*. To our knowledge, this is the first predictive model of lncRNA that may correlate with the processes of heat shock proteins and ferroptosis in AML. Nevertheless, validation using patient samples is warranted.

KEYWORDS

acute myeloid leukemia, heat shock proteins, ferroptosis, long noncoding RNAs, prognosis

Introduction

It has been almost two decades since gene expression-based prognostic classification has been introduced in acute myeloid leukemia (AML). Undeniably, several approved approaches ranging from coding (Li et al., 2020a; Li et al., 2020b) to noncoding, including micro-RNA and long noncoding RNA (lncRNA) expression, have been successfully used to model patients' stratifications in AML (Wallace and O'Connell, 2017; Gourvest et al., 2019; Singh et al., 2021). This, in turn, also raises the possibility of further integrating and understanding the unrelated molecular processes involved in different types of cancer, including AML.

In particular, lncRNAs have received considerable attention in recent years due to their involvement in developmental processes and various diseases, including AML. For

instance, one study investigated the differential expression profiles of lncRNAs in AML patients by microarray and found that SNHG5 significantly regulates chemotherapy resistance in AML through the miR-32/DNAJB9 axis (Wang et al., 2020). Underexpression of LINC00649 has been reported to be an unfavorable prognostic marker in acute myeloid leukemia (Guo et al., 2020). Garzon et al. revealed that some deregulated lncRNAs were associated with recurrent mutations and clinical outcome in AML patients (Garzon et al., 2014). Serum LINC00899 was predicted to be a potential and useful noninvasive biomarker for the early clinical detection and prognosis of AML (Wang et al., 2018). Interestingly, several lncRNA-based integrated models have been developed for the stratification of AML patients (Liu et al., 2021; Zhu et al., 2023). Recently, an integrated prognostic signature encompassing five immune-related protein-coding genes and an immune-related lncRNA has been successfully constructed to predict the survival and stratification of AML patients (Zhao et al., 2022). Notably, the expression of heat shock proteins (HSPs) is associated with major adverse prognostic factors in AML (Thomas et al., 2005), and some HSP90 inhibitors have been confirmed to be effective agents against primary AML (Flandrin et al., 2008; Lazenby et al., 2015). Likewise, research on ferroptosis-related processes and clinical outcomes in AML is gaining momentum (Zheng et al., 2021; Cui et al., 2022). In addition, some pieces of evidence suggest a link among oncogenes, HSPs, and ferroptosis. For instance, members of the HSP family, such as HSP72/73, HSP70, and HSP90, have been linked to TP53 mutations in numerous cancers (Lane et al., 1993; Sun et al., 1997; Calderwood et al., 2006). Similarly, mutations in RAS and TP53 have been demonstrated as being associated with both HSPs and ferroptosis (Ye et al., 2020; Chen et al., 2021).

Considering that a link between HSPs and ferroptosis in AML has been recently suspected (Dai and Hu, 2022; Liu et al., 2022; Aolyamat et al., 2023), herein, we investigated lncRNAs that may act as mediators between two processes like HSPs and ferroptosis in AML. To our knowledge, this is the first computational study integrating these two processes, i.e., HSP and ferroptosis.

Materials and methods

Data generation for AML patients from The Cancer Genome Atlas database

Transcriptomic profiling data for AML patients were obtained from The Cancer Genome Atlas (TCGA) database (<https://portal.gdc.cancer.gov/repository>, TCGA-LAML), while clinical data (cytogenetic risk, age, blast cells, bone marrow blast cells, hemoglobin, leucocytes, FAB classification, and gender) and survival data for AML patients were downloaded from UCSC Xena (<https://xena.ucsc.edu/>). From the TCGA-LAML dataset, we extracted the gene expression of 97 HSP genes (Supplementary Table S1), 268 ferroptosis genes (Supplementary Table S1), and lncRNAs. Overall, 150 patients were included in our study. By overlapping gene expression data with survival data, 131 patients were included for further analysis. Of these, 84 patients had mutation data and 127 patients had clinical data.

Identification of HSP and ferroptosis-associated lncRNAs (HSP/ferroptosis-lncRNAs) and construction of a novel prognostic signature

According to Pearson's correlation analysis, lncRNAs related to HSP genes (HSP-associated lncRNAs) and ferroptosis genes (ferroptosis-associated lncRNAs) were considered on the basis of the following standard: Pearson's analysis: $|R| > 0.6$ and $p < 0.001$. lncRNAs overlapping between HSPs and ferroptosis-related lncRNAs were designated as HSP-dependent and ferroptosis-related lncRNAs (HSP/ferroptosis-lncRNAs). A total of 131 patients (gene expression and survival data were included) were randomly assigned to a training cohort ($n = 66$) and a validation cohort ($n = 65$). A new signature was then determined in the training cohort using the aforementioned HSP/ferroptosis-lncRNAs. In brief, 64 survival-related HSP/ferroptosis-lncRNAs were determined by univariable Cox regression analysis in the training cohort. Cox regression analysis with least absolute shrinkage and selection operator (LASSO) was then used to further test the survival-associated lncRNAs. Based on 10-fold cross-validation and lambda.min values, five lncRNAs were obtained. Multivariate Cox regression analysis based on the minimum value of the Akaike information criterion (AIC) was used to generate a prognostic signature of HSP/ferroptosis-lncRNAs. The signature risk score of each patient was calculated via the following formula: $\text{risk score} = \sum_1^n \text{Coe } f_i \times \text{Exp } r_i$ (Coe f_i = coefficient, Exp r_i = expression value of HSP dependent ferroptosis related lncRNA). After summarizing the risk scores for the 66 patients, the median risk score was used as a cutoff point to classify them into high- and low-risk groups. It is worth noting that the same cutoff value was also used in the test and overall groups. In addition, a chi-squared test was used to confirm the unbiasedness of the clinical baseline data between the validation (test and overall cohorts) and training cohorts.

Evaluation of the prognostic signature of the four lncRNAs

The training, test, and overall cohorts were assessed for predictive ability between the high- and low-risk groups using Kaplan–Meier (KM) curves. Receiver operating characteristic (ROC) curves and a concordance index (C-index) were introduced to further validate the predictive ability of the signature in the overall cohort. The CPH function from the 'rms' R package was used to perform C-index analysis. Univariable and multivariate Cox regression analyses were used to examine potential independent predictors of survival in the overall cohort by combining signature and clinical characteristics. In addition, this signature was applied to the overall cohort to assess its prognostic potential in subgroups of individual clinical characteristics. Of note, the cutoff values for continuous clinical characteristics were age/60 years, blast cells/median value, bone marrow/median value, hemoglobin/median value, and leucocytes/median value, respectively, while subgroups of the remaining clinical characteristics were cytogenetic risk (favorable/normal vs. poor), FAB classification (non-M3 vs. M3), and sex (male vs. female).

Functional enrichment analysis

We compared the gene expression of the high-risk and low-risk groups to obtain differential genes that must meet the following criterion: false discovery rate (FDR) < 0.05 and log₂-fold change (log₂FC) > 1. Then, Gene Ontology (GO) enrichment analysis was used to identify biological processes (BPs), cellular components (CCs), and molecular functions (MFs). The Kyoto Encyclopedia of Genes and Genomes (KEGG) analysis was used to explore potential biological signaling pathways.

Investigating the association of immune function, Tumor Immune Dysfunction and Exclusion, and tumor mutation burden using the obtained signature

Single-sample gene set enrichment analysis (ssGSEA) was used to assess the different immune functions between the high-risk and low-risk groups. The Tumor Immune Dysfunction and Exclusion (TIDE) score can help physicians select patients who are best-suited to receive immune checkpoint therapy, so we calculated the TIDE score of AML patients in TCGA. The TIDE algorithm was used to calculate the TIDE score, and we compared the differential TIDE values between the high- and low-risk groups using the Wilcoxon rank-sum test. We further implemented the R package “maftools” to visualize the mutation profiles of AML patients. The first 16 mutated

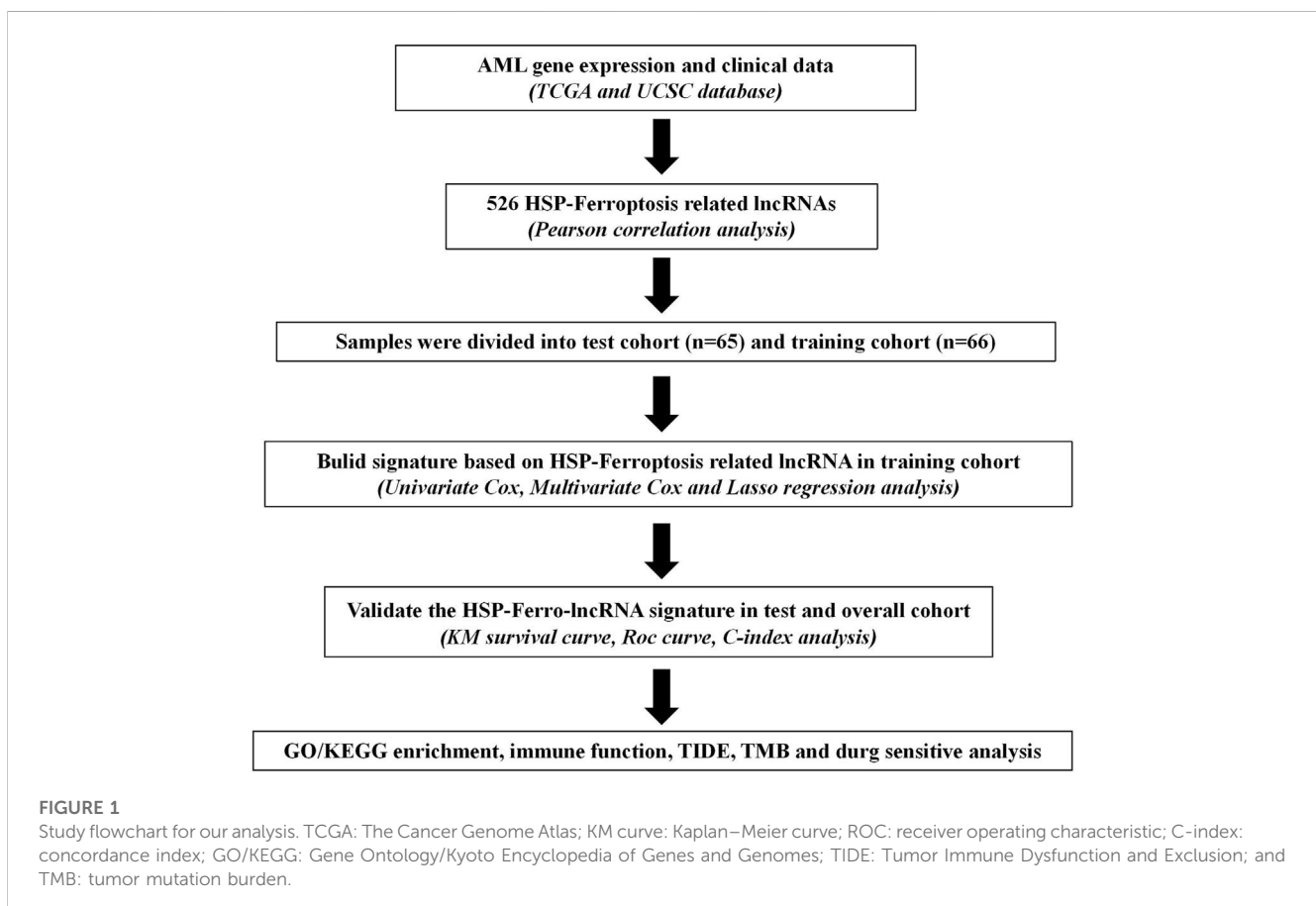
genes were *TP53*, *TTN*, *IDH2*, *NPM1*, *DNMT3A*, *FLT3*, *ASXL1*, *KIT*, *PAN2*, *FAT2*, *IDH1*, *IQCN*, *KRAS*, *MUC16*, *RUNX1*, and *BCORL1*. The difference in the tumor mutation burden (TMB) between the high- and low-risk groups was compared using the Wilcoxon rank-sum test. The differences in survival probability between the high-TMB and low-TMB groups are also presented using KM curves. The optimal cutoff value for the TMB was determined using the `surv_cutpoint` function in R.

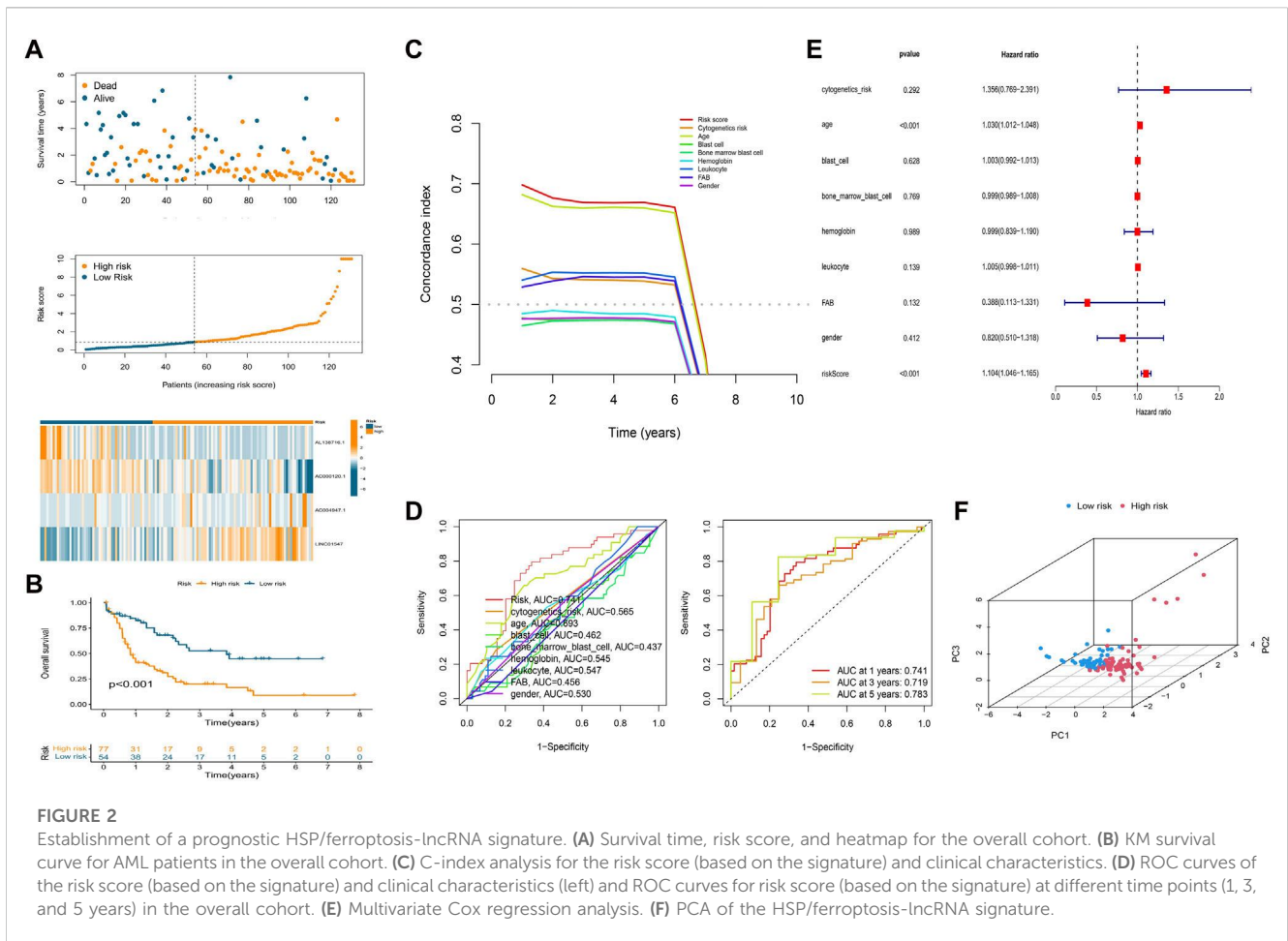
IC₅₀ scores

The determination of the half-maximal inhibitory concentration (IC₅₀) serves as a crucial parameter for assessing the effectiveness of and response to a drug treatment. In our study, we utilized the “pRRophetic” package to predict the clinical chemotherapeutic response for each sample.

Statistical analysis

Statistical analyses were performed using R software. Pearson’s correlation analysis, LASSO Cox regression, univariable and multivariable Cox regression, Kaplan–Meier curves, ROC curves, C-index, and Wilcoxon rank-sum test were used to analyze our study data. $p < 0.05$ was considered significant. * $p < 0.05$; ** $p < 0.01$; and *** $p < 0.001$; ns: not significant.





Results

Establishing a signature from HSP/ferroptosis-associated lncRNAs (HSP/ferroptosis-lncRNAs) in AML patients

The flowchart of this study is given in Figure 1. We extracted HSP, ferroptosis, and lncRNA gene expression from the RNA-seq data of AML patients from the TCGA database. Using Pearson’s correlation analysis ($|R| > 0.6$ and $p < 0.001$), 713 lncRNAs associated with HSP genes and 1,537 lncRNAs associated with ferroptosis genes were identified (Supplementary Table S2, 3). Overlapping 526 lncRNAs from the HSP-associated and ferroptosis-associated lncRNAs were determined as HSP/ferroptosis-lncRNAs (Supplementary Table S4). Subsequently, 131 patients (gene expression and survival data) were randomized to the training and test cohorts in a 1:1 ratio. We then

determined the prognostic signature in the training group. First, in combination with survival data, we used univariable Cox regression to find the top 64 lncRNAs that were associated with survival time (Supplementary Table S5). To further test the lncRNAs for survival, we used LASSO Cox regression and obtained five lncRNAs (AL138716.1, AC000120.1, AC004947.1, AC020934.2, and LINC01547) (Supplementary Figure S1). In addition, multivariate Cox regression analysis was performed to generate a novel prognostic signature containing four lncRNAs associated with HSP/ferroptosis (AL138716.1, AC000120.1, AC004947.1, and LINC01547) (Table 1). As shown in Supplementary Table S6, all clinical factors were unbiasedly distributed between the training and test cohorts, which was confirmed by using the chi-squared test method (p -values > 0.05).

Evaluating and confirming the prognosis of the signature

We calculated the risk score of each patient using the formula given in Materials and Methods. According to the median value of the risk score of the patients in the training cohort, we classified the patients in the three cohorts (training, test, and overall cohorts) into high- and low-risk groups. The risk level, survival status, and survival time between the high- and low-risk groups in these three cohorts are shown in Figure 2 and Supplementary Figure S2. The expression of the four

TABLE 1 Multivariate Cox regression analysis.

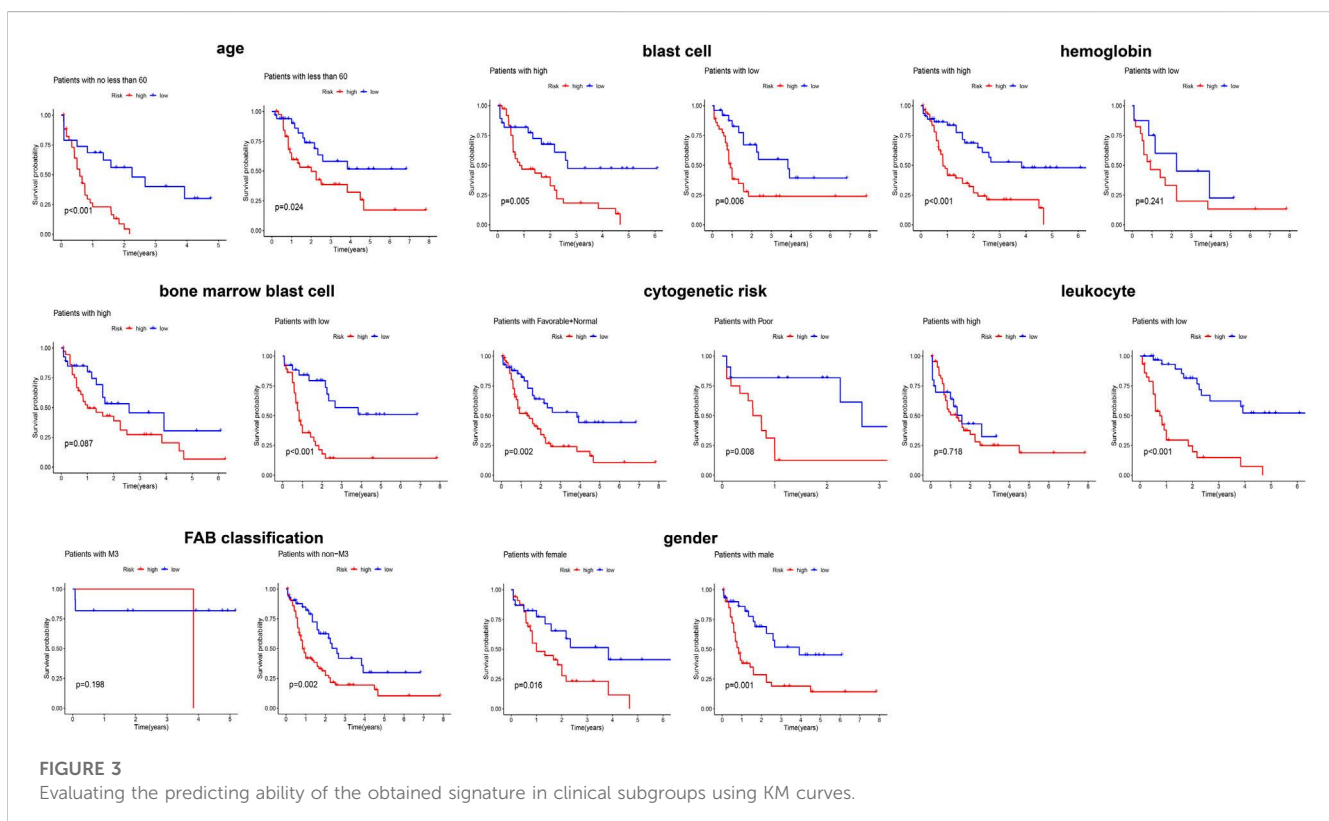
lncRNA	Coefficient
AL138716.1	-0.936
AC000120.1	-1.149
AC004947.1	0.658
LINC01547	0.798

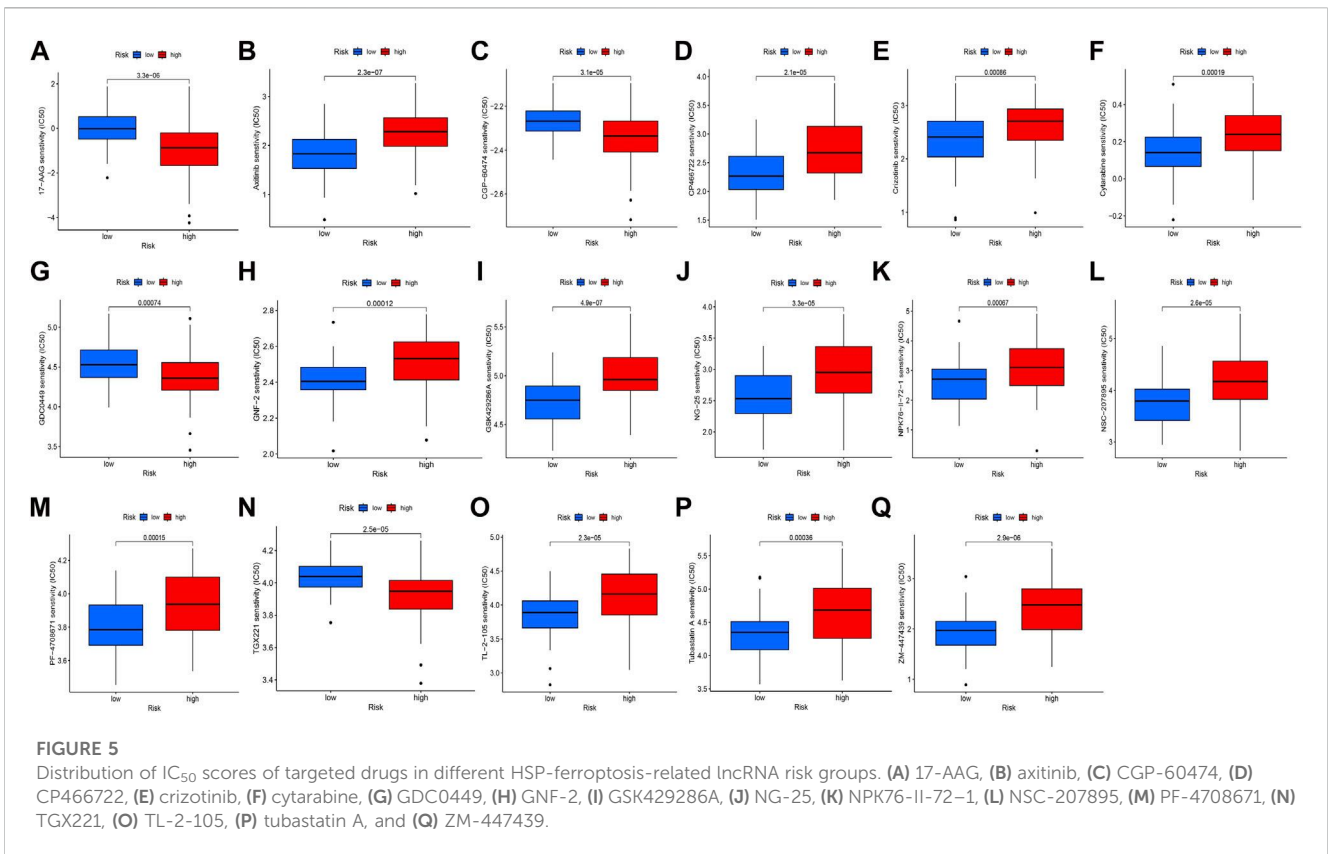
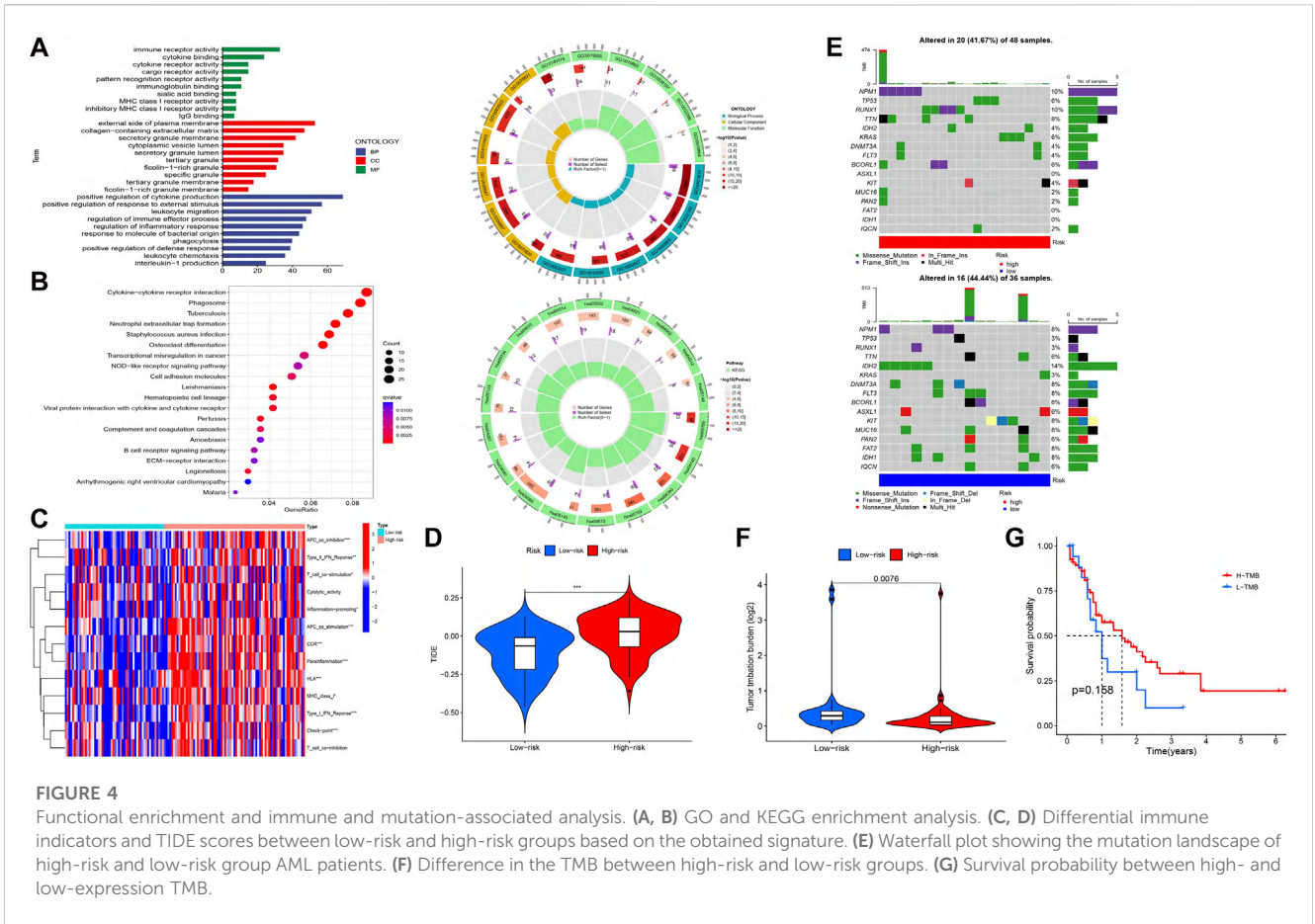
lncRNAs associated with HSP and ferroptosis for each patient in the different cohorts is shown as a heatmap (Figure 2A and Supplementary Figure S2A). Survival analysis (KM method) showed that the OS of the low-risk group was longer than that of the high-risk group in the training cohort ($p < 0.001$), test cohort ($p = 0.046$), and overall cohort ($p < 0.001$) (Figure 2B and Supplementary Figure S2B). The prognostic significance of the signature was further confirmed using the ROC curve and C-index analysis in the overall cohort. As shown in Figure 2C, the risk score based on our signature and age showed values greater than 0.65 for the C-index method, and the risk score is higher than the age. Moreover, compared with other clinical characteristics, the risk score has the highest AUC (0.741) in the ROC curve (Figure 2D). In addition, the AUC values of the ROC curve at different time points were all above 0.700 at 1 year (AUC = 0.741), 3 years (AUC = 0.719), and 5 years (AUC = 0.783) (Figure 2D). Thus, the signature represents a robust model for predicting survival in AML patients.

Univariable cox regression was used to confirm that the risk score (based on the signature), FAB classification, and age are factors that can predict survival in AML patients (Supplementary Figure S2C). In addition, by combining the risk score (signature-based) and clinical characteristics, we confirmed the risk score and age to be independent predictors of survival in AML patients using multivariate Cox regression (Figure 2E). PCA was then performed to test the ability to cluster the high- and low-risk patients in different groups including the HSP/ferroptosis-lncRNA signature, overall gene expression profile, HSP genes, HSP-associated lncRNAs, ferroptosis genes, ferroptosis-associated lncRNAs, and

HSP-associated and ferroptosis-associated lncRNAs. Supplementary Figure S3 and Figure 2F show that the HSP/ferroptosis-lncRNA signature group showed a significant distribution between the high- and low-risk subgroups, whereas the other groups were relatively dispersed between the high- and low-risk subgroups. These results showed that the prognostic signature can discriminate well between high- and low-risk groups.

Given that elderly patients, patients with high leukocyte value and/or poor cytogenetics risk, etc., have poor prognosis in clinic, we further assessed the predictive ability of the obtained signature in clinical subgroups using KM curves (Figure 3). We divided the clinical characteristics into the following subgroups: sex (male and female), age (≥ 60 and < 60), FAB (M3 and non-M3) and cytogenetic risk (favorable + normal and poor), blast cells (high and low), bone marrow blast cells (high and low), hemoglobin (high and low), and leucocytes (high and low). Of note, the classification of blast cells, bone marrow blast cells, hemoglobin, and leucocytes into high and low groups was based on their median value. After applying the obtained signature to classify the patients into low and high risk, the differential survival probability between low- and high-risk patients was shown as gender (male, $p = 0.001$), gender (female, $p = 0.016$), age (≥ 60 , $p < 0.001$), age (< 60 , $p = 0.024$), FAB (M3 group, $p = 0.198$), FAB (non-M3, $p = 0.002$), cytogenetic risk (favorable + normal, $p = 0.002$), cytogenetic risk (poor, $p = 0.008$), blast cells (high, $p = 0.005$), blast cells (low, $p = 0.006$), bone marrow blast cells (high, $p = 0.087$), bone marrow blast cells (low, $p < 0.001$), hemoglobin (high, $p < 0.001$), hemoglobin





(low, $p = 0.241$), leucocytes (high, $p = 0.781$), and leucocytes (low, $p < 0.001$) in Figure 3. Overall, the signature has prognostic ability in most clinical subgroups.

Correlation of functional enrichment, immune function, mutations, and TIDE analysis with the obtained signature

To elucidate the relationship between the signature and potential function (BP, CC, MF, and pathway), we performed functional enrichment analysis using the GO and KEGG method (Figures 4A,B). Interestingly, the enrichment analysis revealed the involvement of many immune-related BPs, MFs, and pathways for the signature. To examine changes in immune markers between the high- and low-risk groups based on our signature, we used the ssGSEA and Wilcoxon rank-sum test (Figure 4C). The results showed that APC inhibition/stimulation, interferon (IFN) type I/II responses, chemokine receptor (CCR), para-inflammation, human leukocyte antigen (HLA), major histocompatibility complex (MHC) class I, checkpoint, T-cell stimulation, and promotion of inflammation were significantly more active in the high-risk group than in the low-risk group. Thus, this signature is implicated in the immune progression/functioning in AML patients. Considering this, we further investigated the association of the immune checkpoint blockade with the signature using TIDE analysis (Figure 4D). The high-risk group showed a high TIDE score compared to the low-risk group, suggesting a lower sensitivity to immune checkpoint inhibitors in the high-risk group, which could help in predicting ICI treatment in the clinic for patients classified based on the signature.

Given that gene mutations are an important part of AML, we analyzed the mutation data in our study. The 16 most mutated genes from 84 samples (samples that contained gene mutation data) were used in a high-risk group (48 samples) and a low-risk group (36 samples) to assess the differential mutation landscapes, as shown in Figure 4E. In particular, the mutation rates of the NPM1 and RUNX1 genes in the high-risk group and the IDH2 gene in the low-risk group were 10%, 10%, and 14%, respectively. As shown in Figure 4F, the TMB estimates in the low-risk group exceeded those in the high-risk group ($p = 0.0076$). However, there was no difference in survival time between the high- and low-risk groups with respect to the TMB (Figure 4G).

IC₅₀ scores

In our study, we examined the differences in the IC₅₀ scores for chemotherapy between high- and low-risk groups based on the obtained signature. Specifically, we observed that the IC₅₀ values for axitinib, CP466722, crizotinib, cytarabine, GNF-2, GSK429286A, NK-25, NPK76-II-72-1, NSC-207895, PF-4708671, TL-2-105, tubastatin, and ZM-447439 were higher in the high-risk group. Conversely, the IC₅₀ values for 17-AAG, CGP-60474, GDC0449, and TGX221 were lower in the high-risk group (Figure 5). These findings support the notion that there is a statistically significant difference in the distribution of IC₅₀ values for targeted agents among high- and low-risk groups based on the obtained signature.

Discussion

Although studies in recent decades have improved our understanding of AML, the underlying pathogenesis of this lethal disease has not yet been fully elucidated. With the development of NGS technologies, more and more AML-related mechanisms have emerged, including the eventual contribution of long noncoding RNAs (lncRNAs) (Mer et al., 2018; Liu et al., 2019; Mishra et al., 2022). In fact, several studies have established lncRNA-based prognostic models for clinical characterization in AML patients (Zhao et al., 2021; Ding et al., 2022; Li et al., 2022; Zhang et al., 2022). Independently, an association of HSPs (Li and Ge, 2021) and ferroptosis-related lncRNAs (Zheng et al., 2021) has been demonstrated in AML. Given that HSPs and ferroptosis appear to be closely linked to tumorigenesis (Liu et al., 2022), using a comprehensive bioinformatics approach, we sought to identify lncRNAs that may overlap with these processes with predictive relevance for AML patients.

To determine this, we extracted the HSP-, ferroptosis-, and lncRNA-related gene expression data of AML patients using the TCGA database. Using Pearson's correlation analysis, we identified overlapping lncRNAs (termed HSP/ferroptosis-lncRNAs), and subsequent analysis revealed four lncRNAs associated with HSP/ferroptosis genes (AL138716.1, AC000120.1, AC004947.1, and LINC01547) as a prognostic signature. In particular, AC000120.1 has been recently reported in a prediction model based on seven cuproptosis-related lncRNAs for AML prognosis (Zhu et al., 2023). Similarly, LINC01547 has been reported in m6A-related lncRNAs associated with prognosis and immune response in AML patients (Li et al., 2021). While AC004947.1 has shown oncogenic potential (Zhao et al., 2020), AL138716.1 has not yet been reported in studies. Notably, when we tested the obtained signature to classify AML patients, we found that high-risk patients had a lower survival probability compared to the low-risk group, indicating the prognostic ability of the signature in AML, and the following analysis confirms that the signature is a robust independent factor for AML patients. In addition, the prognostic ability also presents its potential predicting ability in different clinical subgroups.

Both GO and KEGG analysis provided immune-related evidence in AML. Some immune indicators in possible different between low-risk and high-risk group. Moreover, the high-risk group showed a high TIDE score, indicating a lower sensitivity to immune checkpoint inhibitors in the high-risk group, potentially helping to predict ICI treatment in the clinic for patients classified on the basis of the signature. Overall, these lines of evidence revealed the relation of the obtained signature with immune response. The differential landscapes of gene mutation and tumor mutational burden were found between high- and low-risk groups, which may partly contribute to the prognostic ability of our signature. Furthermore, our study contributes valuable insights into the varying treatment sensitivity among AML patients by conducting drug sensitivity analysis for the high-risk and low-risk groups based on the HSP-ferroptosis-lncRNA status.

It is also worth noting the limitation to this study, as the analysis relies purely on comprehensive bioinformatics and requires effective experimental validation. Nevertheless, two out of four lncRNAs in our signature have been proven in AML, thus providing evidence that our predictive model of lncRNA may correlate with the processes of HSPs and ferroptosis in AML.

Data availability statement

The original contributions presented in the study are included in the article/Supplementary Material; further inquiries can be directed to the corresponding author. Publicly datasets utilized in this study can be accessed via The Cancer Genome Atlas (<https://portal.gdc.cancer.gov/>, Project: TCGA-LAML) and Uscs Xena (<https://xenabrowser.net/datapages/>, Cohort: GDC TCGA Acute Myeloid Leukemia (LAML)).

Ethics statement

Written informed consent was obtained from the individual(s) for the publication of any potentially identifiable images or data included in this article.

Author contributions

FG, YW, and IS-W were responsible for the conceptualization of the project. FG contributed to data curation, analysis and validation of the data, methodology, and writing of the original draft. YW was responsible for data curation, methodology, and editing and reviewing the manuscript. AS and IS-W participated in supervision and reviewing and editing the manuscript. UJ, ME, and MS participated in reviewing and editing the manuscript. All authors contributed to the article and approved the submitted version.

References

- Aolyamat, I., Hatmal, M. M., and Olaimat, A. N. (2023). The emerging role of heat shock factor 1 (HSF1) and heat shock proteins (HSPs) in ferroptosis. *Pathophysiology* 30, 63–82. doi:10.3390/pathophysiology30010007
- Calderwood, S. K., Khaleque, M. A., Sawyer, D. B., and Ciocca, D. R. (2006). Heat shock proteins in cancer: Chaperones of tumorigenesis. *Trends Biochem. Sci.* 31, 164–172. doi:10.1016/j.tibs.2006.01.006
- Chen, X., Kang, R., Kroemer, G., and Tang, D. (2021). Broadening horizons: The role of ferroptosis in cancer. *Nat. Rev. Clin. Oncol.* 18, 280–296. doi:10.1038/s41571-020-00462-0
- Cui, Z., Fu, Y., Yang, Z., Gao, Z., Feng, H., Zhou, M., et al. (2022). Comprehensive analysis of a ferroptosis pattern and associated prognostic signature in acute myeloid leukemia. *Front. Pharmacol.* 13, 866325. doi:10.3389/fphar.2022.866325
- Dai, Y., and Hu, L. (2022). HSPB1 overexpression improves hypoxic-ischemic brain damage by attenuating ferroptosis in rats through promoting G6PD expression. *J. Neurophysiol.* 128, 1507–1517. doi:10.1152/jn.00306.2022
- Ding, W., Ling, Y., Shi, Y., and Zheng, Z. (2022). DesA prognostic risk model of lncRNAs in patients with acute myeloid leukemia based on TCGA data. *Front. Bioeng. Biotechnol.* 10, 818905. doi:10.3389/fbioe.2022.818905
- Flandrin, P., Guyotat, D., Duval, A., Cornillon, J., Tavernier, E., Nadal, N., et al. (2008). Significance of heat-shock protein (HSP) 90 expression in acute myeloid leukemia cells. *Cell. Stress Chaperones* 13, 357–364. doi:10.1007/s12192-008-0035-3
- Garzon, R., Volinia, S., Papaioannou, D., Nicolet, D., Kohlschmidt, J., Yan, P. S., et al. (2014). Expression and prognostic impact of lncRNAs in acute myeloid leukemia. *Proc. Natl. Acad. Sci. U. S. A.* 111, 18679–18684. doi:10.1073/pnas.1422050112
- Gourvest, M., Brousset, P., and Bousquet, M. (2019). Long noncoding RNAs in acute myeloid leukemia: Functional characterization and clinical relevance. *Cancers (Basel)* 11, 1638. doi:10.3390/cancers11111638
- Guo, C., Gao, Y.-Y., Ju, Q.-Q., Zhang, C.-X., Gong, M., and Li, Z.-L. (2020). LINC00649 underexpression is an adverse prognostic marker in acute myeloid leukemia. *BMC Cancer* 20, 841. doi:10.1186/s12885-020-07331-0
- Lane, D. P., Midgley, C., and Hupp, T. (1993). Tumour suppressor genes and molecular chaperones. *Philos. Trans. R. Soc. Lond. B Biol. Sci.* 339, 369–372; discussion 372–373. doi:10.1098/rstb.1993.0036
- Lazenby, M., Hills, R., Burnett, A. K., and Zabkiewicz, J. (2015). The HSP90 inhibitor ganetespib: A potential effective agent for acute myeloid leukemia in combination with cytarabine. *Leuk. Res.* 39, 617–624. doi:10.1016/j.leukres.2015.03.016
- Li, J., and Ge, Z. (2021). High HSPA8 expression predicts adverse outcomes of acute myeloid leukemia. *BMC Cancer* 21, 475. doi:10.1186/s12885-021-08193-w
- Li, H., Sharma, A., Luo, K., Qin, Z. S., Sun, X., and Liu, H. (2020a). DeconPeaker, a deconvolution model to identify cell types based on chromatin accessibility in ATAC-seq data of mixture samples. *Front. Genet.* 11, 392. doi:10.3389/fgene.2020.00392
- Li, H., Sharma, A., Ming, W., Sun, X., and Liu, H. (2020b). A deconvolution method and its application in analyzing the cellular fractions in acute myeloid leukemia samples. *BMC Genomics* 21, 652. doi:10.1186/s12864-020-06888-1
- Li, D., Liang, J., Cheng, C., Guo, W., Li, S., Song, W., et al. (2021). Identification of m6A-related lncRNAs associated with prognoses and immune responses in acute myeloid leukemia. *Front. Cell. Dev. Biol.* 9, 770451. doi:10.3389/fcell.2021.770451
- Li, R., Wu, S., Wu, X., Zhao, P., Li, J., Xue, K., et al. (2022). Immune-related lncRNAs can predict the prognosis of acute myeloid leukemia. *Cancer Med.* 11, 888–899. doi:10.1002/cam4.4487
- Liu, Y., Cheng, Z., Pang, Y., Cui, L., Qian, T., Quan, L., et al. (2019). Role of microRNAs, circRNAs and long noncoding RNAs in acute myeloid leukemia. *J. Hematol. Oncol.* 12, 51. doi:10.1186/s13045-019-0734-5
- Liu, C.-Y., Guo, H.-H., Li, H.-X., Liang, Y., Tang, C., and Chen, N.-N. (2021). Identification of the 7-lncRNA signature as a prognostic biomarker for acute myeloid leukemia. *Dis. Markers* 2021, 8223216. doi:10.1155/2021/8223216
- Liu, Y., Zhou, L., Xu, Y., Li, K., Zhao, Y., Qiao, H., et al. (2022). Heat shock proteins and ferroptosis. *Front. Cell. Dev. Biol.* 10, 864635. doi:10.3389/fcell.2022.864635
- Mer, A. S., Lindberg, J., Nilsson, C., Klevebring, D., Wang, M., Grönberg, H., et al. (2018). Expression levels of long non-coding RNAs are prognostic for AML outcome. *J. Hematol. Oncol.* 11, 52. doi:10.1186/s13045-018-0596-2
- Mishra, S., Liu, J., Chai, L., and Tenen, D. G. (2022). Diverse functions of long noncoding RNAs in acute myeloid leukemia: Emerging roles in pathophysiology, prognosis, and treatment resistance. *Curr. Opin. Hematol.* 29, 34–43. doi:10.1097/MOH.0000000000000692

Funding

The Center for Integrated Oncology (CIO) Aachen Bonn Köln Düsseldorf was kindly supported by the Deutsche Krebshilfe (Grant No. 70113470).

Conflict of interest

The authors declare that the research was conducted in the absence of any commercial or financial relationships that could be construed as a potential conflict of interest.

Publisher's note

All claims expressed in this article are solely those of the authors and do not necessarily represent those of their affiliated organizations, or those of the publisher, the editors, and the reviewers. Any product that may be evaluated in this article, or claim that may be made by its manufacturer, is not guaranteed or endorsed by the publisher.

Supplementary material

The Supplementary Material for this article can be found online at: <https://www.frontiersin.org/articles/10.3389/fgene.2023.1218276/full#supplementary-material>

- Singh, V. K., Thakral, D., and Gupta, R. (2021). Regulatory noncoding RNAs: Potential biomarkers and therapeutic targets in acute myeloid leukemia. *Am. J. Blood Res.* 11, 504–519.
- Sun, X. F., Zhang, H., Carstensen, J., Jansson, A., and Nordenskjöld, B. (1997). Heat shock protein 72/73 in relation to cytoplasmic p53 expression and prognosis in colorectal adenocarcinomas. *Int. J. Cancer* 74, 600–604. doi:10.1002/(sici)1097-0215(19971219)74:6<600:aid-ijc7>3.0.co;2-y
- Thomas, X., Campos, L., Mounier, C., Cornillon, J., Flandrin, P., Le, Q.-H., et al. (2005). Expression of heat-shock proteins is associated with major adverse prognostic factors in acute myeloid leukemia. *Leuk. Res.* 29, 1049–1058. doi:10.1016/j.leukres.2005.02.010
- Wallace, J. A., and O'Connell, R. M. (2017). MicroRNAs and acute myeloid leukemia: Therapeutic implications and emerging concepts. *Blood* 130, 1290–1301. doi:10.1182/blood-2016-10-697698
- Wang, Y., Li, Y., Song, H.-Q., and Sun, G.-W. (2018). Long non-coding RNA LINC00899 as a novel serum biomarker for diagnosis and prognosis prediction of acute myeloid leukemia. *Eur. Rev. Med. Pharmacol. Sci.* 22, 7364–7370. doi:10.26355/eurrev_201811_16274
- Wang, D., Zeng, T., Lin, Z., Yan, L., Wang, F., Tang, L., et al. (2020). Long non-coding RNA SNHG5 regulates chemotherapy resistance through the miR-32/DNAJB9 axis in acute myeloid leukemia. *Biomed. Pharmacother.* 123, 109802. doi:10.1016/j.biopha.2019.109802
- Ye, Z., Liu, W., Zhuo, Q., Hu, Q., Liu, M., Sun, Q., et al. (2020). Ferroptosis: Final destination for cancer? *Cell. Prolif.* 53, e12761. doi:10.1111/cpr.12761
- Zhang, L., Ke, W., Hu, P., Li, Z., Geng, W., Guo, Y., et al. (2022). N6-Methyladenosine-Related lncRNAs are novel prognostic markers and predict the immune landscape in acute myeloid leukemia. *Front. Genet.* 13, 804614. doi:10.3389/fgene.2022.804614
- Zhao, T., Khadka, V. S., and Deng, Y. (2020). Identification of lncRNA biomarkers for lung cancer through integrative cross-platform data analyses. *Aging (Albany NY)* 12, 14506–14527. doi:10.18632/aging.103496
- Zhao, C., Wang, Y., Tu, F., Zhao, S., Ye, X., Liu, J., et al. (2021). A prognostic autophagy-related long non-coding RNA (ARlncRNA) signature in acute myeloid leukemia (AML). *Front. Genet.* 12, 681867. doi:10.3389/fgene.2021.681867
- Zhao, C., Wang, Y., Sharma, A., Wang, Z., Zheng, C., Wei, Y., et al. (2022). Identification of the integrated prognostic signature associated with immunorelevant genes and long non-coding RNAs in acute myeloid leukemia. *Cancer Invest.* 40, 663–674. doi:10.1080/07357907.2022.2096230
- Zheng, Z., Wu, W., Lin, Z., Liu, S., Chen, Q., Jiang, X., et al. (2021). Identification of seven novel ferroptosis-related long non-coding RNA signatures as a diagnostic biomarker for acute myeloid leukemia. *BMC Med. Genomics* 14, 236. doi:10.1186/s12920-021-01085-9
- Zhu, Y., He, J., Li, Z., and Yang, W. (2023). Cuproptosis-related lncRNA signature for prognostic prediction in patients with acute myeloid leukemia. *BMC Bioinforma.* 24, 37. doi:10.1186/s12859-023-05148-9

3.4 Publication 4: Immunoautophagy-Related Long Noncoding RNA (IAR-lncRNA) Signature Predicts Survival in Hepatocellular Carcinoma

Yulu Wang ^{1,†}, **Fangfang Ge** ^{1,†}, Amit Sharma ^{1,2,†}, Oliver Rudan ¹, Maria F. Setiawan ¹,
Maria A. Gonzalez-Carmona ³, Miroslaw T. Kornek ³, Christian P. Strassburg ³,
Matthias Schmid ⁴ and Ingo G. H. Schmidt-Wolf ^{1,*}

¹Center for Integrated Oncology (CIO), Department of Integrated Oncology, University Hospital of Bonn, 53127 Bonn, Germany; Yulu.Wang@ukbonn.de (Y.W.); Fangfang.Ge@ukbonn.de (F.G.); Amit.Sharma@ukbonn.de (A.S.); oliver.rudan@ukbonn.de (O.R.); Maria_fitria.setiawan@ukbonn.de (M.F.S.)




²Department of Neurosurgery, University Hospital of Bonn, 53127 Bonn, Germany

³Department of Internal Medicine I, University Hospital of Bonn, 53127 Bonn, Germany; maria.gonzalez-carmona@ukbonn.de (M.A.G.-C.); Miroslaw_theodor.kornek@ukbonn.de (M.T.K.); christian.strassburg@ukbonn.de (C.P.S.)

⁴Institute of Medical Biometry, Informatics and Epidemiology, University Hospital of Bonn, 53127 Bonn, Germany; matthias.schmid@ukbonn.de

Article

Immunoautophagy-Related Long Noncoding RNA (IAR-lncRNA) Signature Predicts Survival in Hepatocellular Carcinoma

Yulu Wang ^{1,†}, Fangfang Ge ^{1,†}, Amit Sharma ^{1,2,†} , Oliver Rudan ¹, Maria F. Setiawan ¹, Maria A. Gonzalez-Carmona ³ , Mirosław T. Kornek ³ , Christian P. Strassburg ³, Matthias Schmid ⁴ and Ingo G. H. Schmidt-Wolf ^{1,*}

- ¹ Center for Integrated Oncology (CIO), Department of Integrated Oncology, University Hospital of Bonn, 53127 Bonn, Germany; Yulu.Wang@ukbonn.de (Y.W.); Fangfang.Ge@ukbonn.de (F.G.); Amit.Sharma@ukbonn.de (A.S.); oliver.rudan@ukbonn.de (O.R.); Maria_fitria.setiawan@ukbonn.de (M.F.S.)
- ² Department of Neurosurgery, University Hospital of Bonn, 53127 Bonn, Germany
- ³ Department of Internal Medicine I, University Hospital of Bonn, 53127 Bonn, Germany; maria.gonzalez-carmona@ukbonn.de (M.A.G.-C.); Mirosław_theodor.kornek@ukbonn.de (M.T.K.); christian.strassburg@ukbonn.de (C.P.S.)
- ⁴ Institute of Medical Biometry, Informatics and Epidemiology, University Hospital of Bonn, 53127 Bonn, Germany; matthias.schmid@ukbonn.de
- * Correspondence: ingo.schmidt-wolf@ukbonn.de; Tel.: +49-(0)-228-287-17050
- † These authors have contributed equally as co-first authors.



Citation: Wang, Y.; Ge, F.; Sharma, A.; Rudan, O.; Setiawan, M.F.; Gonzalez-Carmona, M.A.; Kornek, M.T.; Strassburg, C.P.; Schmid, M.; Schmidt-Wolf, I.G.H. Immunoautophagy-Related Long Noncoding RNA (IAR-lncRNA) Signature Predicts Survival in Hepatocellular Carcinoma. *Biology* **2021**, *10*, 1301. <https://doi.org/10.3390/biology10121301>

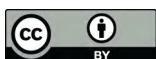
Academic Editor: Georg Damm

Received: 4 November 2021

Accepted: 7 December 2021

Published: 9 December 2021

Publisher's Note: MDPI stays neutral with regard to jurisdictional claims in published maps and institutional affiliations.



Copyright: © 2021 by the authors. Licensee MDPI, Basel, Switzerland. This article is an open access article distributed under the terms and conditions of the Creative Commons Attribution (CC BY) license (<https://creativecommons.org/licenses/by/4.0/>).

Simple Summary: Hepatocellular carcinoma (HCC) is the most common type of primary liver cancer, which is more prevalent in adults. Herein, we established the first immuno-autophagy-related long non-coding RNA (IARlncRNA) signature displaying a prognostic ability among HCC patient groups.

Abstract: Background: The dysregulation of autophagy and immunological processes has been linked to various pathophysiological conditions, including cancer. Most notably, their particular involvement in hepatocellular carcinoma (HCC) is becoming increasingly evident. This has led to the possibility of developing a prognostic signature based on immuno-autophagy-related (IAR) genes. Given that long non-coding RNAs (lncRNAs) also play a special role in HCC, a combined signature utilizing IAR genes and HCC-associated long noncoding RNAs (as IARlncRNA) may potentially help in the clinical scenario. Method: We used Pearson correlation analysis, Kaplan–Meier survival curves, univariate and multivariate Cox regression, and ROC curves to generate and validate a prognostic immuno-autophagy-related long non-coding RNA (IARlncRNA) signature. The Chi-squared test was utilized to investigate the correlation between the obtained signature and the clinical characteristics. CIBERSORT algorithms and the Wilcoxon rank sum test were applied to investigate the correlation between signature and infiltrating immune cells. GO and KEGG analyses were performed to derived signature-dependent pathways. Results: Herein, we build an IAR-lncRNA signature (as first in the literature) and demonstrate its prognostic ability in hepatocellular carcinoma. Primarily, we identified three IARlncRNAs (MIR210HG, AC099850.3 and CYTOR) as unfavorable prognostic determinants. The obtained signature predicted the high-risk HCC group with shorter overall survival, and was further associated with clinical characteristics such as tumor grade ($t = 10.918$, $p = 0.001$). Additionally, several infiltrating immune cells showed varied fractions between the low-risk group and the high-risk HCC groups in association with the obtained signature. In addition, pathways analysis described by the signature clearly distinguishes both risk groups in HCC. Conclusions: The immuno-autophagy-related long non-coding RNA (IARlncRNA) signature we established exhibits a prognostic ability in hepatocellular carcinoma. To our knowledge, this is the first attempt in the literature to combine three determinants (immune, autophagy and lncRNAs), thus requiring molecular validation of this obtained signature in clinical samples.

Keywords: liver cancer; hepatocellular carcinoma; lncRNAs; autophagy; biomarker; kyoto encyclopedia of genes and genomes; prognosis; signature; immune genes

1. Introduction

Autophagy as a conserved process captures and degrades intracellular components primarily to maintain metabolism and cellular homeostasis. Dysregulation of this process has been linked to several pathophysiological conditions, such as cancer and neurodegenerative diseases [1,2]. Particularly in hepatocellular carcinoma (HCC), autophagy has been shown to play a role by promoting the metastatic colonization of HCC cells [3].

HCC, the most common malignancy of the liver, is currently the fourth leading cause of cancer-related death worldwide [4]. Primary risk factors for the development of HCC include chronic liver disease and cirrhosis, most of which are caused by chronic viral hepatitis (B + C) and excessive alcohol consumption. Several genetic and epigenetic factors have also been implicated in the molecular pathogenesis of HCC [5]. Considering the overlap of mutational pathways in cancers [6], studies have also prompted the analysis of the prognostic potential of certain genes across the spectrum of multiple cancers, including HCC [7]. Likewise, the relative contribution of autophagy in HCC is becoming increasingly apparent; for instance, Wu et al. showed that autophagic degradation machinery and the cell-cycle regulator cyclin D1 are linked to HCC tumorigenesis [8]. It has also been discussed that activation of autophagy decreases the expression of oncogenic microRNA-224, and thus impedes tumorigenesis in hepatitis B virus-related HCC [9]. Of interest, several compounds have been shown to exert antitumor effects in liver cancer via autophagy [10–12]. In the context of autophagy-related genes (ATG), lower expression was previously observed in HCC, which was predicted to contribute to tumor growth and the poor prognosis of the disease [13,14]. Of interest, there have been few recent attempts to identify a prognostic signature of ATGs in HCC [15,16]. Besides this, immunoautophagy-related genes (IARGs) were also recently evaluated for their potential prognostic significance in HCC patients [17]. Considering that long non-coding RNAs (lncRNAs) also play a special role in cancer, their ability to regulate tumor growth by modulating autophagy in liver, bladder, and pancreatic cancers has already been implicated [18,19]. In HCC, a study discussed the potential involvement of lncRNA HULC (highly upregulated in liver cancer) in the autophagy and chemoresistance of HCC cells [20]. Similarly, the lncRNA SNHG1 has been shown to induce resistance to the drug sorafenib in HCC through activation of the Akt pathway [21]. Recently, the prognostic value of an autophagy-related lncRNA signature in HCC has been discussed [22].

Considering this plethora of literature, we have attempted to combine immune-, autophagy, and noncoding RNAs to generate immunoautophagy-related long noncoding RNA (IAR-lncRNA). Herein, we build an IAR-lncRNA signature (first in the literature) and demonstrate its prognostic ability in hepatocellular carcinoma.

2. Materials and Methods

2.1. Gene Expression Data and Clinicopathological Characteristics

Gene expression data (workflow type: HTSeq—FPKM) and associated clinical information of patients with hepatocellular carcinoma of the liver (HCC) were downloaded from UCSC Xena (<https://xena.ucsc.edu/>, accessed on 22 October 2021). The reference database was the GDC TCGA Liver Cancer (LIHC) dataset, which contains 374 tumor samples with comprehensive gene expression data. Of these, 371 samples were from primary tumors (mainly used in this study), and the remaining 3 samples were from recurrent tumors (3 samples from 2 patients), which were excluded from the analysis. Only 365 samples have both gene expression data and survival data (survival time and survival status). Based on the available clinical characteristics, only 163 samples were further processed for the clinical comparisons. In total, 210 genes involved in autophagy were retrieved from the Human Autophagy Database (HADb, <http://autophagy.lu/clustering/index.html>, accessed on 22 May 2021). A total of 1344 immune-related genes were retrieved from Immport Shared Data (<https://www.immport.org/shared/home>, accessed on 27 June

2021). We focused our analysis on 371 HCC samples, excluding recurrent samples due to their peculiar clinical/biological characteristics. $\log_2(\text{FPKM} + 1)$ gene expression data were applied to obtain AR genes, IR genes and lncRNAs. Due to the sizes of genes and lncRNAs, the average gene expression ($\log_2(\text{FPKM} + 1)$) of AR genes and IR genes (no more than 0) and lncRNAs (no more than 0.5) was excluded. \log_2 was further applied for the gene expression data ($\log_2(\text{FPKM} + 1)$) in order to obtain fitting normalized distribution. Since lncRNAs were expressed at relatively low levels, the correlation of gene (AR and IR) expression ($\log_2(\log_2(\text{FPKM} + 1) + 1)$) and lncRNA expression ($\log_2(\text{FPKM} + 1)$) was used to establish AR- and IR-related lncRNAs. lncRNA expression ($\log_2(\log_2(\text{FPKM} + 1) + 1)$) data were subsequently used in statistical analyses.

2.2. Development of the Prognostic Immuno-Autophagy-Related lncRNAs Signature

Univariate Cox regressions were applied to select survival-related autophagy genes and immune genes, which were based on p -values < 0.01 . Then the correlation between lncRNAs and survival-related autophagy genes was determined by Pearson correlation analysis. lncRNAs with correlation coefficients $|R| > 0.4$ and p values < 0.01 were considered autophagy-related. The correlation between lncRNAs and survival-related immune genes was determined by Pearson correlation analysis. lncRNAs with correlation coefficients $|R| > 0.6$ and p values < 0.01 were defined as immune-related. Thus, we obtained autophagy-related lncRNAs (ARlncRNAs) and immune-related lncRNAs (IRlncRNAs) for the further steps. Next, we determined the lncRNA was associated with immunoautophagy (IARlncRNA) if the lncRNA belonged to both ARlncRNAs and IRlncRNAs concurrently. Then, univariate Cox regression was performed to select survival-related IARlncRNA. Subsequently, multivariate Cox regression analysis was performed based on the lowest Akaike information criterion (AIC) to determine the optimal prognostic signature. Risk scores were calculated using the following formula: $(\beta_{\text{gene 1}} \times \text{exp}_{\text{gene 1}}) + (\beta_{\text{gene 2}} \times \text{exp}_{\text{gene 2}}) + \dots + (\beta_{\text{gene } n} \times \text{exp}_{\text{gene } n})$. Here, exp_{gene} represents the expression of lncRNA. Of note, the cutoff value for the high-risk group and the low-risk group was the median risk score. The differential expressions of the lncRNAs in signature between high- and low-risk groups were assessed by Wilcoxon rank sum test.

2.3. Prognostic Ability of Immuno-Autophagy-Related lncRNAs Signature

The Kaplan–Meier survival curve was applied to investigate the survival rate between high-risk and low-risk groups, and $p < 0.05$ was considered as a significant difference. Subsequently, an ROC curve was performed to test the predicting value of the signature. Univariate Cox regression and multivariate Cox regression were used to assess the independent ability of the signature, primarily based on $p < 0.05$ when clinical features (age, gender, Child–Pugh classification, AFP, fibrosis, grade and stage) were considered.

2.4. Correlation between Immune Cells and Signature

CIBERSORT analysis was performed to explore the percentages of 22 immune cells in each patient. Wilcoxon rank-sum test was used to determine the varying of immune cells in low- and high-risk groups ($p < 0.05$).

2.5. GO and KEGG Analysis

Differential genes were found between the low-risk group and the high-risk group based on \log_2 fold change ($\log_{\text{FC}} > 1$) and false discovery rate (FDR) < 0.05 using the Wilcoxon rank sum test. Subsequently, these genes were included in GO and KEGG analyses using the R package “clusterProfiler” to explore pathways, which were selected with a q value < 0.05 .

2.6. Statistical Analysis

Pearson correlation analysis, Chi-squared test, Wilcoxon rank sum test, Cox regression, Kaplan–Meier curves, survival status, heat map, ROC curve, cibersort algorithm, GO

analysis and KEGG analysis were performed using R software. The coexpression network between genes (ARgenes and IRgenes) along with an lncRNA coexpression network was illustrated using CYTOSCAPE software.

3. Results

3.1. Correlating Autophagy-Related Genes and Immune-Related Genes with lncRNAs

We first derived autophagy-related genes from the Human Autophagy Database (HADb, <http://autophagy.lu/clustering/index.html>, accessed on 22 May 2021) and immune-related genes from the Immport Shared Data (<https://www.immport.org/shared/home>, accessed on 27 June 2021). Subsequently, the gene expression datasets of LIHC (GDC TCGA Liver Cancer (LIHC)) were downloaded from the UCSC Xena. Next, we extracted the lncRNA genes, autophagy-related (AR) genes and immune-related (IR) genes corresponding to HCC from the TCGA data. First, univariate Cox regressions were performed to select survival-related AR genes and IR genes. Subsequently, Pearson correlation was used to confirm the correlation between autophagic genes and lncRNA ($|R| > 0.4$ and p -value < 0.01), in addition to the correlation between immune-related genes and lncRNA ($|R| > 0.6$ and p -value < 0.01). Using these parameters, a total of 244 ARlncRNAs (Supplementary File S1) and 36 IRlncRNAs (Supplementary File S2) was identified. When combined, the ARlncRNAs and IRlncRNAs yielded 36 IARlncRNAs. The overview of the complete strategy is shown in a flowchart (Figure S1).

3.2. A Signature Involving 3 Immuno-Autophagy-Related lncRNAs with Prognostic Potential

The aforementioned 36 immuno-autophagy-related lncRNAs were analyzed in combination with clinical survival data. Univariate Cox regression analysis was performed with a p -value of less than 0.01, resulting in the mapping of 10 lncRNAs (BACE1-AS, MIR210HG, AC073896.4, AC099850.3, AC026401.3, MAPKAPK5-AS1, LINC01018, CYTOR, AC115619.1, and F11-AS1) (Figure 1A). In addition, we used a multivariate Cox regression analysis based on the lowest Akaike information criterion (AIC) to determine the β -values that were subsequently used to calculate the risk scores. The analysis revealed three immunoautophagy-related lncRNAs (MIR210HG, AC099850.3, and CYTOR) as the strongest candidates with prognostic potential (Table S1). The correlation between the IARlncRNA of the obtained signature and the genes (AR genes and IR genes) is shown in Figure 1C. Of interest, all these genes showed high expression in the high-risk group (Figure 1B), and were considered unfavorable prognostic determinants (Figure 1D).

3.3. Validating the Prognostic Potential of Immuno-Autophagy-Related lncRNA Signature in Low- and High-Risk HCC Groups

Next, we determined the functionality of the obtained signature within the low-risk group and high-risk group HCC patients (Figure 2). The scatter plot shows that both survival rates and survival time were lower in the high-risk group compared to the low-risk group (Figure 2A).

Additionally, an expression pattern between lncRNAs and signature risk was observed in the heat map (Figure 2A). The Kaplan–Meier survival curve showed a significant difference in overall survival between the low-risk and high-risk groups (Figure 2B). Notably, the high-risk group showed shorter overall survival compared with the low-risk group. In addition, we performed univariable (Figure 2C) and multivariable Cox (Figure 2D) regression analyses to identify independent prognostic factors with clinical characteristics, and found that age, stage, and risk score were independent predictive determinants of survival in HCC patients. Additionally, an ROC curve was used to confirm the model, for which the AUC values of the risk score for the prediction times of 1, 2, and 3 years were 0.746, 0.700, and 0.674, respectively, for each prediction time (Figure 2E).

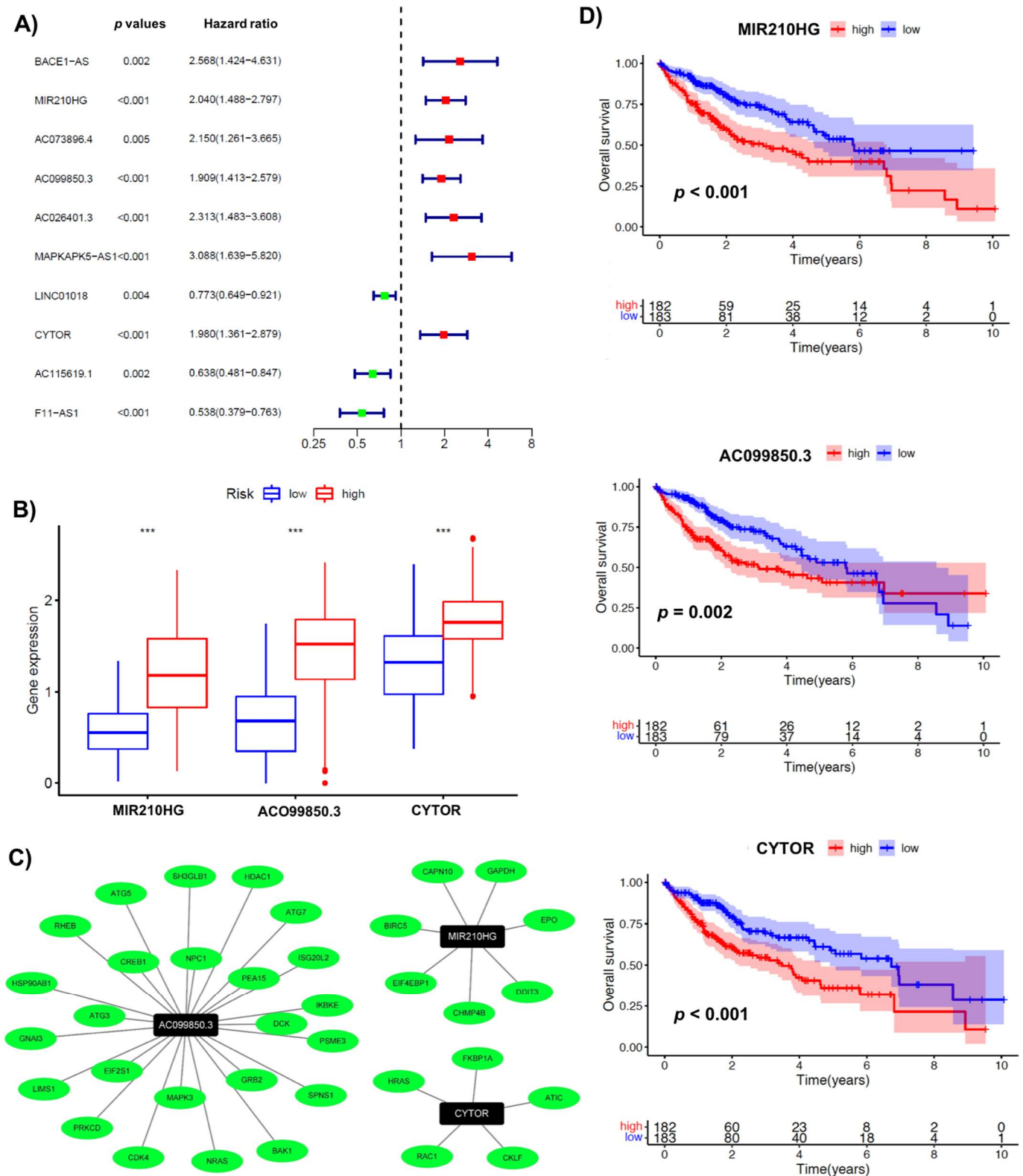
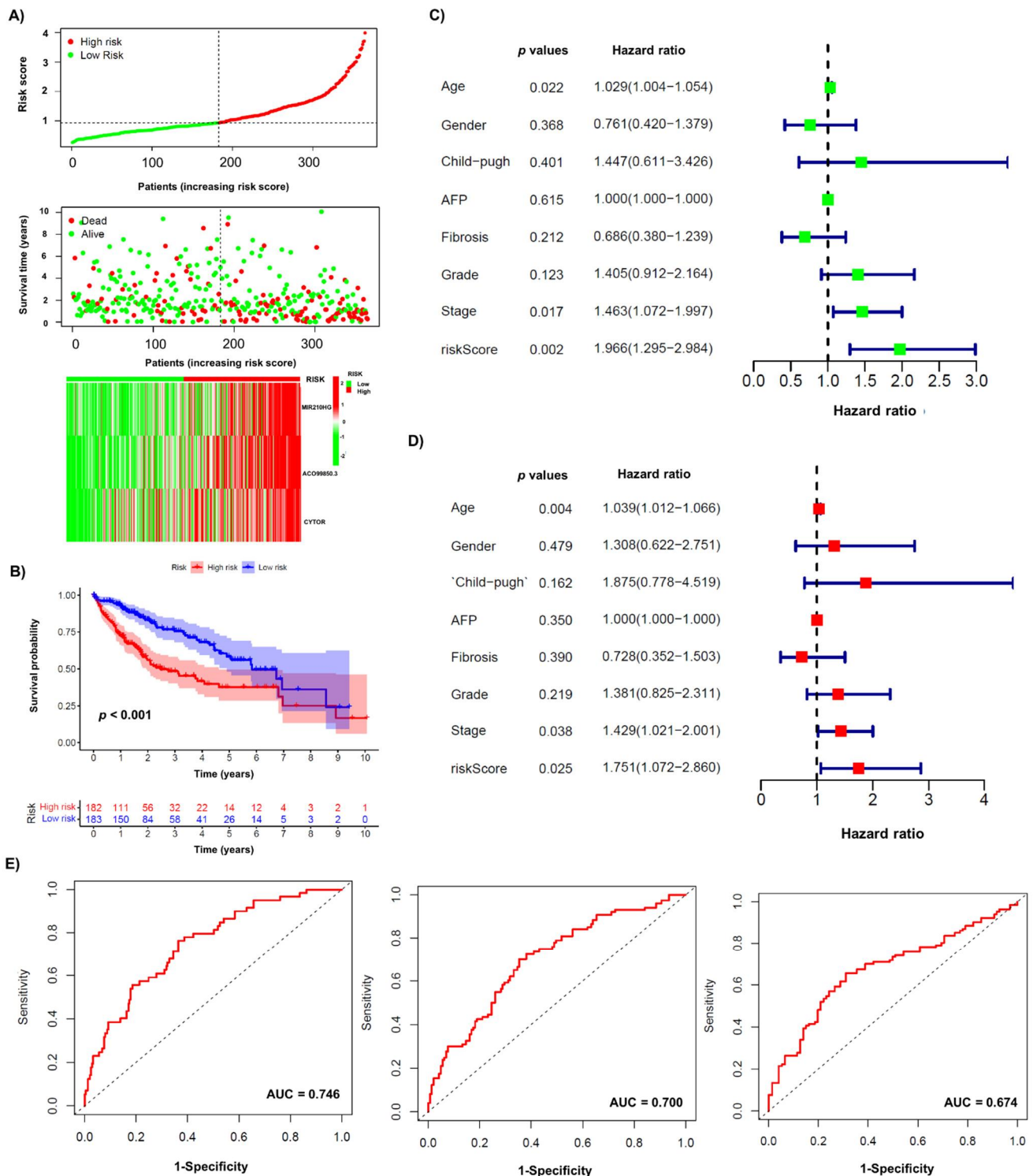


Figure 1. Identification of immuno-autophagy-related lncRNAs with prognostic potential. (A) Univariate Cox regression analysis: ten survival-related IARlncRNAs. (B) The differential gene expression of IARlncRNAs between high- and low-risk groups. (C) A network of prognostic lncRNA (black nodes) with co-expressed genes (green) in HCC. (D) Kaplan–Meier survival curves for 3 IARlncRNAs (MIR210HG, ACO99850.3, and CYTOR) associated with HCC. *** $p < 0.001$.



3.4. Association of Immuno-Autophagy-Related lncRNA Signature with Clinical Characteristics

To determine the association between immuno-autophagy-related lncRNA signature and clinical characteristics, we divided each feature into two groups, such as age (over/under 65 years), gender (male/female), grade (G1–G2/G3–G4), stage (I–II/III–IV), Child–Pugh classification (A/B + C), AFP/alpha-fetoprotein (over/under 400 ng/mL) and fibrosis (with/without) status of patients (Table 1). The analysis showed that a high-risk score was associated significantly with the higher grade ($t = 10.918$, $p = 0.001$).

Table 1. The relation between risk of signature with clinical features.

	Risk	Total	High Risk	Low Risk	t	p Value
Age	<65	95 (58.28%)	46 (63.89%)	49 (53.85%)	1.280	0.258
	≥65	68 (41.72%)	26 (36.11%)	42 (46.15%)		
Gender	Female	50 (30.67%)	24 (33.33%)	26 (28.57%)	0.234	0.629
	Male	113 (69.33%)	48 (66.67%)	65 (71.43%)		
Child–Pugh	A	147 (90.18%)	64 (88.89%)	83 (91.21%)	0.053	0.819
	B + C	16 (9.82%)	8 (11.11%)	8 (8.79%)		
AFP	≥400	30 (18.4%)	17 (23.61%)	13 (14.29%)	1.748	0.186
	<400	133 (81.6%)	55 (76.39%)	78 (85.71%)		
Fibrosis	Fibrosis	113 (69.33%)	50 (69.44%)	63 (69.23%)	0	1
	No Fibrosis	50 (30.67%)	22 (30.56%)	28 (30.77%)		
Grade	G1–G2	99 (60.74%)	33 (45.83%)	66 (72.53%)	10.918	0.001 **
	G3–G4	64 (39.26%)	39 (54.17%)	25 (27.47%)		
Stage	Stage I–II	131 (80.37%)	57 (79.17%)	74 (81.32%)	0.021	0.885
	Stage III–IV	32 (19.63%)	15 (20.83%)	17 (18.68%)		

** $p < 0.01$.

3.5. Association of Infiltrating Immune Cells and Obtained Signature

Considering the obtained signature involved both immune and autophagy determinants, its relationship with immune infiltration cells was investigated. The relative percentages of 22 immune cells in each patient are shown in Figure S2. The distribution of these cells in risk groups is shown in Figure 3A. The Wilcoxon rank sum test was applied to determine the difference between each immune cell in the low- and high-risk groups (Figure 3B). Interestingly, B cells (naïve, $p < 0.01$; memory, $p < 0.01$), T cells CD4 memory (resting, $p = 0.007$; activated, $p < 0.001$), T cells follicular helpers ($p < 0.001$), NK cells resting ($p = 0.018$), macrophages M0 ($p < 0.001$), macrophages M2 ($p = 0.034$) and mast cells resting ($p = 0.015$) were significantly different between low- and high-risk groups.

3.6. GO and KEGG Pathway Enrichment Analysis of the Obtained Signature

We further investigated the cellular and molecular pathways associated with the obtained signature. The differential genes between high- and low-risk groups are listed in Supplementary File S3. The biological/cellular processes obtained from GO analysis (Figure S3) show that the signature is mainly associated with mitosis and chromosome segregation. Additionally, the molecular function of the signature was related to tubulin binding and kinase activity. The KEGG analysis shows that the signature is clearly associated with seven signaling pathways, including cell cycle, oocyte meiosis, progesterone-mediated oocyte maturation, p53 signaling pathway, human T-cell leukemia virus 1 infection, cellular senescence, and human immunodeficiency virus 1 (Figure 3C).

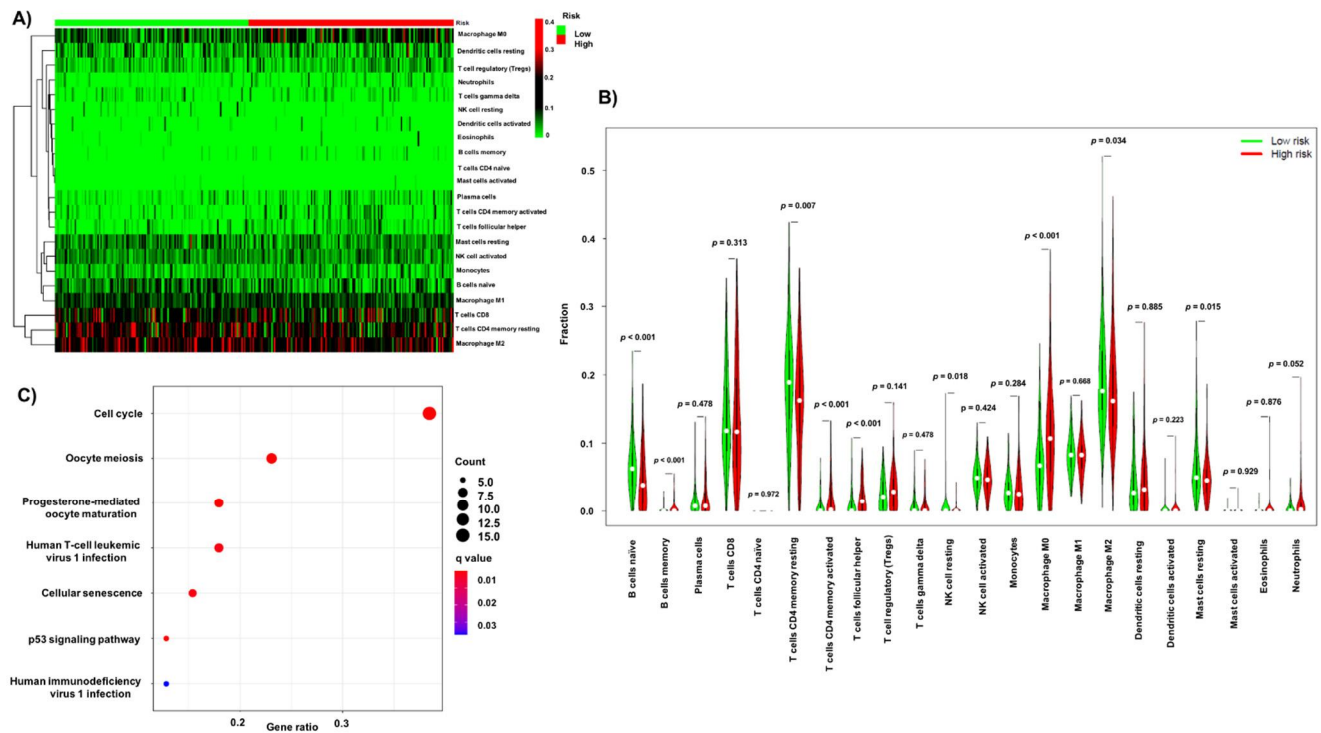


Figure 3. The relationship between immuno-autophagy-related lncRNA signature, infiltration immune cells and potential pathways. (A) Heatmap of 22 immune cells in high-/low-risk group. (B) The fractions of immune cells in high- and low-risk group. (C) KEGG analysis.

4. Discussion

Cancer is a relatively complex disease [6,23], driven primarily by genetic/epigenetic processes that help these cells to proliferate and fuel cancer progression. Overall, the dynamics of dysregulated mechanisms involving several key cellular signaling pathways act as a critical factor for the slow to fast progression of this disease. Among them, autophagy and immune-related processes also play a crucial role in both promoting and suppressing tumor growth. Likewise, the peculiar contribution of long non-coding RNA (lncRNA) can also not be excluded. To date, several prognostic signatures involving autophagy-related (AR) and immune-related (IR) genes have been shown [24–26], and some have even attempted to combine them with lncRNAs [27,28]. However, to date, no combinatorial signature utilizing IR, AR and lncRNAs has been shown.

With a special focus on hepatocellular carcinoma (HCC), herein, we sought to investigate a possible immuno-autophagy-related long non-coding RNA (IARlncRNA) signature, primarily to predict survival in HCC patients. At first, we selected survival-related IR and AR genes, and combined them lncRNAs to identify ARlncRNAs and IRlncRNAs datasets. Following this, specific sets of ARlncRNAs ($n = 244$) and IRlncRNAs ($n = 36$) were generated, and then a preliminary signature of IARlncRNAs ($n = 36$) was derived from the aforementioned data sets. Among them, 10 IARlncRNAs (BACE1-AS, MIR210HG, AC073896.4, AC099850.3, AC026401.3, MAPKAPK5-AS1, LINC01018, CYTOR, AC115619.1, and F11-AS1) were found to be associated with survival. Of importance, three of them (MIR210HG, AC099850.3, and CYTOR) displayed a robust prognostic signature with unfavorable prognosis. Previously, these three IARlncRNAs had all been implicated in HCC; for instance, it has been shown that the silencing of MIR210HG expression leads to the inhibition of HCC tumor growth [29]. Similarly, CYTOR has been shown to promote HCC proliferation, and its disruption inhibited HCC growth [30,31]. Additionally, AC099850.3 has been shown to increase proliferation and migration in HCC [32], thus providing strong evidence for the utility of our prognostic signature in the clinical spectrum of HCC patients.

We next determined the functionality of the obtained signature within the HCC patient groups, and found that both survival rates and survival time were significantly low in the high-risk group. In addition, an inverse expression pattern was observed in lncRNAs and risk groups. Of interest, among several clinical characteristics, risk score was found to be an independent predictive determinant of survival in HCC patients. We also examined the relationship between the obtained signature and the infiltrating immune cells. The analysis showed that a higher proportion of naïve B cells, resting memory CD4 T cells, resting NK cells, M2 macrophages, and resting mast cells predominated in the low-risk group, whereas the proportion of memory B cells, activated memory CD4 T cells, follicular helper T cells, and M0 macrophages was specific for the high-risk group. GO analysis showed that differential gene expressions between risk groups were significantly enriched in biological processes (mitosis and chromosome segregation), cellular components (chromosomes), and molecular functions (tubulin binding and kinase activity). In addition, seven defined signaling pathways (cell cycle, oocyte meiosis, progesterone-mediated oocyte maturation, p53 signaling pathway, human T-cell leukemia virus 1 infection, cellular senescence, and human immunodeficiency virus 1) were found to be associated with the obtained signature. To our knowledge, we have presented for the first time an immuno-autophagy-related long non-coding RNA (IARlncRNA) signature prognostic ability in hepatocellular carcinoma. It is worth mentioning that molecular validation of this obtained signature using clinical samples is required. Prognostic models for HCC based on lncRNAs have also been reported previously. For instance, a recent study identified five autophagy-related long non-coding RNAs (AR-lncRNAs) (including TMCC1-AS1, PLBD1-AS1, MKLN1-AS, LINC01063, and CYTOR) for HCC patients from the TCGA database [27]. Likewise, one independent study described four-immune-related-lncRNA signatures for predicting the prognosis and guiding the application of immunotherapy in HCC [33]. However, it is worth mentioning that the heterogeneity within clinical samples submitted to repositories (as previously described by Sharma et al. [34]) and especially the selection of different computational analytical methods makes these predictive markers less effective in the clinical environment. In the present study, we have provided a detailed description of the methods used in our analysis, which offers a platform for methodological compression to enable similar analyses in HCC or in other cancers.

5. Conclusions

The immuno-autophagy-related long non-coding RNA (IARlncRNA) signature we established exhibits a prognostic ability in hepatocellular carcinoma.

Supplementary Materials: The following are available online at <https://www.mdpi.com/article/10.3390/biology10121301/s1>, Supplementary File S1, Supplementary File S2, Supplementary File S3, Table S1: Information of multivariable Cox regression, Figure S1: Flow chart illustrating the defined strategy in the study, Figure S2: Percentage of infiltration immune cells in patients, Figure S3: GO analysis.

Author Contributions: Conceptualization, Y.W., A.S. and I.G.H.S.-W.; statistical analysis, Y.W. and F.G.; formal analysis, Y.W., F.G., A.S., O.R. and M.F.S.; writing—original draft preparation, Y.W., A.S. and I.G.H.S.-W.; writing—review and editing, all co-authors; supervision, M.A.G.-C., M.T.K., C.P.S., M.S. and I.G.H.S.-W.; project administration, I.G.H.S.-W. All authors have read and agreed to the published version of the manuscript.

Funding: This research received no external funding.

Institutional Review Board Statement: Not applicable.

Informed Consent Statement: Not applicable.

Data Availability Statement: The data set in this study can be found at <https://xenabrowser.net/datapages/> as accessed on 22 October 2021. The TCGA-LIHC dataset is GDC TCGA Liver Cancer (LIHC) (14 datasets).

Acknowledgments: Not applicable.

Conflicts of Interest: The authors declare no conflict of interest.

References

- Chavez-Dominguez, R.; Perez-Medina, M.; Lopez-Gonzalez, J.S.; Galicia-Velasco, M.; Aguilar-Cazares, D. The Double-Edge Sword of Autophagy in Cancer: From Tumor Suppression to Pro-tumor Activity. *Front. Oncol.* **2020**, *10*, 578418. [[CrossRef](#)] [[PubMed](#)]
- Nixon, A.R. The role of autophagy in neurodegenerative disease. *Nat. Med.* **2013**, *19*, 983–997. [[CrossRef](#)]
- Peng, Y.-F.; Shi, Y.-H.; Shen, Y.-H.; Ding, Z.-B.; Ke, A.-W.; Zhou, J.; Qiu, S.-J.; Fan, J. Promoting Colonization in Metastatic HCC Cells by Modulation of Autophagy. *PLoS ONE* **2013**, *8*, e74407. [[CrossRef](#)] [[PubMed](#)]
- O'Connor, S.; Ward, J.W.; Watson, M.; Momin, B.; Richardson, L.C. Hepatocellular carcinoma—United States, 2001–2006. *MMWR Morb. Mortal. Wkly. Rep.* **2010**, *59*, 517–520.
- Liu, M.; Jiang, L.; Guan, X.-Y. The genetic and epigenetic alterations in human hepatocellular carcinoma: A recent update. *Protein Cell* **2014**, *5*, 673–691. [[CrossRef](#)] [[PubMed](#)]
- Liu, H.; Li, H.; Luo, K.; Sharma, A.; Sun, X. Prognostic gene expression signature revealed the involvement of mutational pathways in cancer genome. *J. Cancer* **2020**, *11*, 4510–4520. [[CrossRef](#)]
- Sharma, A.; Biswas, A.; Liu, H.; Sen, S.; Paruchuri, A.; Katsonis, P.; Lichtarge, O.; Dakal, T.C.; Maulik, U.; Gromiha, M.M.; et al. Mutational Landscape of the BAP1 Locus Reveals an Intrinsic Control to Regulate the miRNA Network and the Binding of Protein Complexes in Uveal Melanoma. *Cancers* **2019**, *11*, 1600. [[CrossRef](#)]
- Wu, S.-Y.; Lan, S.-H.; Wu, S.-R.; Chiu, Y.-C.; Lin, X.-Z.; Su, I.-J.; Tsai, T.-F.; Yen, C.-J.; Lu, T.-H.; Liang, F.-W.; et al. Hepatocellular carcinoma-related cyclin D1 is selectively regulated by autophagy degradation system. *Hepatology* **2018**, *68*, 141–154. [[CrossRef](#)]
- Lan, S.; Wu, S.; Zucchini, R.; Lin, X.; Su, I.; Tsai, T.; Lin, Y.; Wu, C.; Liu, H. Autophagy suppresses tumorigenesis of hepatitis B virus-associated hepatocellular carcinoma through degradation of microRNA-224. *Hepatology* **2014**, *59*, 505–517. [[CrossRef](#)]
- Chu, Y.-L.; Ho, C.-T.; Chung, J.-G.; Rajasekaran, R.; Sheen, L.-Y. Allicin Induces p53-Mediated Autophagy in Hep G2 Human Liver Cancer Cells. *J. Agric. Food Chem.* **2012**, *60*, 8363–8371. [[CrossRef](#)]
- Liu, X.-W.; Cai, T.-Y.; Zhu, H.; Cao, J.; Su, Y.; Hu, Y.-Z.; He, Q.-J.; Yang, B. Q6, a novel hypoxia-targeted drug, regulates hypoxia-inducible factor signaling via an autophagy-dependent mechanism in hepatocellular carcinoma. *Autophagy* **2013**, *10*, 111–122. [[CrossRef](#)]
- Hsieh, S.-L.; Chen, C.-T.; Wang, J.-J.; Kuo, Y.-H.; Li, C.-C.; Wu, C.-C. Sedanolide induces autophagy through the PI3K, p53 and NF- κ B signaling pathways in human liver cancer cells. *Int. J. Oncol.* **2015**, *47*, 2240–2246. [[CrossRef](#)] [[PubMed](#)]
- Shi, Y.-H.; Ding, Z.-B.; Zhou, J.; Qiu, S.-J.; Fan, J. Prognostic significance of Beclin 1-dependent apoptotic activity in hepatocellular carcinoma. *Autophagy* **2009**, *5*, 380–382. [[CrossRef](#)] [[PubMed](#)]
- Ding, Z.-B.; Shi, Y.-H.; Zhou, J.; Qiu, S.-J.; Xu, Y.; Dai, Z.; Shi, G.-M.; Wang, X.-Y.; Ke, A.-W.; Wu, B.; et al. Association of Autophagy Defect with a Malignant Phenotype and Poor Prognosis of Hepatocellular Carcinoma. *Cancer Res.* **2008**, *68*, 9167–9175. [[CrossRef](#)]
- Luo, Y.; Liu, F.; Han, S.; Qi, Y.; Hu, X.; Zhou, C.; Liang, H.; Zhang, Z. Autophagy-Related Gene Pairs Signature for the Prognosis of Hepatocellular Carcinoma. *Front. Mol. Biosci.* **2021**, *8*, 670241. [[CrossRef](#)]
- Song, Z.; Zhang, G.; Yu, Y.; Li, S. A Prognostic Autophagy-Related Gene Pair Signature and Small-Molecule Drugs for Hepatocellular Carcinoma. *Front. Genet.* **2021**, *12*, 689801. [[CrossRef](#)] [[PubMed](#)]
- Sun, Z.; Lu, Z.; Li, R.; Shao, W.; Zheng, Y.; Shi, X.; Li, Y.; Song, J. Construction of a Prognostic Model for Hepatocellular Carcinoma Based on Immunoautophagy-Related Genes and Tumor Microenvironment. *Int. J. Gen. Med.* **2021**, *14*, 5461–5473. [[CrossRef](#)]
- Xin, X.; Wu, M.; Meng, Q.; Wang, C.; Lu, Y.; Yang, Y.; Li, X.; Zheng, Q.; Pu, H.; Gui, X.; et al. Long noncoding RNA HULC accelerates liver cancer by inhibiting PTEN via autophagy cooperation to miR15a. *Mol. Cancer* **2018**, *17*, 1–16. [[CrossRef](#)]
- Ying, L.; Huang, Y.; Chen, H.; Wang, Y.; Xia, L.; Chen, Y.; Liu, Y.; Qiu, F. Downregulated MEG3 activates autophagy and increases cell proliferation in bladder cancer. *Mol. Biosyst.* **2012**, *9*, 407–411. [[CrossRef](#)]
- Xiong, H.; Ni, Z.; He, J.; Jiang, S.; Li, X.; Gong, W.; Zheng, L.; Chen, S.; Li, B.; Zhang, N.; et al. LncRNA HULC triggers autophagy via stabilizing Sirt1 and attenuates the chemosensitivity of HCC cells. *Oncogene* **2017**, *36*, 3528–3540. [[CrossRef](#)]
- Li, W.; Dong, X.; He, C.; Tan, G.; Li, Z.; Zhai, B.; Feng, J.; Jiang, X.; Liu, C.; Jiang, H.; et al. LncRNA SNHG1 contributes to sorafenib resistance by activating the Akt pathway and is positively regulated by miR-21 in hepatocellular carcinoma cells. *J. Exp. Clin. Cancer Res.* **2019**, *38*, 1–13. [[CrossRef](#)]
- Yang, S.; Zhou, Y.; Zhang, X.; Wang, L.; Fu, J.; Zhao, X.; Yang, L. The prognostic value of an autophagy-related lncRNA signature in hepatocellular carcinoma. *BMC Bioinform.* **2021**, *22*, 1–16. [[CrossRef](#)] [[PubMed](#)]
- Sharma, A.; Liu, H.; Herwig-Carl, M.C.; Dakal, T.C.; Schmidt-Wolf, I.G.H. Epigenetic Regulatory Enzymes: Mutation Prevalence and Coexistence in Cancers. *Cancer Investig.* **2021**, *39*, 257–273. [[CrossRef](#)] [[PubMed](#)]
- Mao, D.; Zhang, Z.; Zhao, X.; Dong, X. Autophagy-related genes prognosis signature as potential predictive markers for immunotherapy in hepatocellular carcinoma. *PeerJ* **2020**, *8*, e8383. [[CrossRef](#)] [[PubMed](#)]
- Li, L.; Xia, S.; Shi, X.; Chen, X.; Shang, D. The novel immune-related genes predict the prognosis of patients with hepatocellular carcinoma. *Sci. Rep.* **2021**, *11*, 1–14. [[CrossRef](#)]
- Dai, Y.; Qiang, W.; Lin, K.; Gui, Y.; Lan, X.; Wang, D. An immune-related gene signature for predicting survival and immunotherapy efficacy in hepatocellular carcinoma. *Cancer Immunol. Immunother.* **2020**, *70*, 967–979. [[CrossRef](#)]

27. Deng, X.; Bi, Q.; Chen, S.; Chen, X.; Li, S.; Zhong, Z.; Guo, W.; Li, X.; Deng, Y.; Yang, Y. Identification of a Five-Autophagy-Related-lncRNA Signature as a Novel Prognostic Biomarker for Hepatocellular Carcinoma. *Front. Mol. Biosci.* **2021**, *7*. [[CrossRef](#)]
28. Xu, Q.; Wang, Y.; Huang, W. Identification of immune-related lncRNA signature for predicting immune checkpoint blockade and prognosis in hepatocellular carcinoma. *Int. Immunopharmacol.* **2021**, *92*, 107333. [[CrossRef](#)]
29. Wang, Y.; Li, W.; Chen, X.; Li, Y.; Wen, P.; Xu, F. MIR210HG predicts poor prognosis and functions as an oncogenic lncRNA in hepatocellular carcinoma. *Biomed. Pharmacother.* **2019**, *111*, 1297–1301. [[CrossRef](#)]
30. Hu, B.; Yang, X.-B.; Yang, X.; Sang, X.-T. LncRNA CYTOR affects the proliferation, cell cycle and apoptosis of hepatocellular carcinoma cells by regulating the miR-125b-5p/KIAA1522 axis. *Aging* **2020**, *13*, 2626–2639. [[CrossRef](#)]
31. Tian, Q.; Yan, X.; Yang, L.; Liu, Z.; Yuan, Z.; Zhang, Y. lncRNA CYTOR promotes cell proliferation and tumor growth via miR-125b/SEMA4C axis in hepatocellular carcinoma. *Oncol. Lett.* **2021**, *22*, 1–12. [[CrossRef](#)] [[PubMed](#)]
32. Wu, F.; Wei, H.; Liu, G.; Zhang, Y. Bioinformatics Profiling of Five Immune-Related lncRNAs for a Prognostic Model of Hepatocellular Carcinoma. *Front. Oncol.* **2021**, *11*, 667904. [[CrossRef](#)] [[PubMed](#)]
33. Li, M.; Liang, M.; Lan, T.; Wu, X.; Xie, W.; Wang, T.; Chen, Z.; Shen, S.; Peng, B. Four Immune-Related Long Non-coding RNAs for Prognosis Prediction in Patients with Hepatocellular Carcinoma. *Front. Mol. Biosci.* **2020**, *7*, 566491. [[CrossRef](#)] [[PubMed](#)]
34. Sharma, A.; Reutter, H.; Ellinger, J. DNA Methylation and Bladder Cancer: Where Genotype does not Predict Phenotype. *Curr. Genom.* **2020**, *21*, 34–36. [[CrossRef](#)]

4. Discussion

4.1 Main findings

Cancer immunotherapy encompasses a diverse array of strategies, spanning categories such as checkpoint inhibitors, lymphocyte-activating cytokines, CAR T cells, other cell-based therapies, agonistic antibodies targeting co-stimulatory receptors, cancer vaccines, oncolytic viruses, and biologics (Riley et al., 2019). These modalities specifically modulate the immune response to foster recognition and attack against cancer cells (Kennedy and Salama, 2020). Despite notable strides in the field of immunotherapy, its clinical implementation continues to confront significant challenges concerning both efficacy and safety. The pursuit of effecting cancer immunotherapy in a more controlled and secure manner is a pivotal objective. This innovative approach holds the potential to extend the therapeutic reach of these interventions to a broader patient cohort, simultaneously ameliorating concerns of treatment-related toxicity. In synopsis, this study is oriented towards addressing the following inquiries within the context of hematological malignancies (specifically Burkitt's lymphoma and acute myeloid leukemia) and liver cancer: 1) Elucidating the dynamics of tumor cell eradication and the intricate mechanisms underlying the synergy achieved through the co-administration of conventional anti-tumor agents and non-tumor pharmaceuticals with cytokine-induced killer (CIK) cells. 2) Investigating the plausible association between long non-coding RNAs (lncRNAs) as prospective prognostic markers and their correlation with survival outcomes in the spectrum of cancer patients.

In the first publication, In light of the persistent challenges posed by Burkitt's lymphoma (BL) as a formidable hematological malignancy, our study delves into the potential therapeutic avenue forged through the synergistic integration of HSP90 inhibitors and cytokine-induced killer (CIK) cells. To address this inquiry, we initiated our investigation by assessing the viability of BL cells (BL41 and Raji) under the influence of two distinct HSP90 inhibitors (17-DMAG and ganetespib) in conjunction with CIK cells, leading to the discernment of a robust synergistic effect across all permutations. The NKG2D/NKG2DL axis stands acknowledged as pivotal in CIK cell-mediated anticancer responses, with MICA/B emerging as the predominant NKG2D ligand on tumor cell surfaces (Fan et al., 2017; Nwangwu et al., 2017; Wu et al., 2020, 2021b). Our focus then shifted to

evaluating MICA/B expression on BL cell surfaces and appraising potential modifications resulting from HSP90 inhibitors. The findings unequivocally demonstrated that neither HSP90 inhibitor exerted any discernible influence on MICA/B expression levels in BL cells. Intriguingly, our investigations unveiled that CIK cells, when combined with HSP90 inhibitors, precipitated an early apoptotic response within BL cells. Furthermore, heightened Fas expression on the surfaces of BL cells was associated with the instigation of apoptosis reliant on caspase 3/7 activity. These observations suggest the plausibility of the Fas/FasL pathway, in lieu of the NKG2D/NKG2D pathway, serving as an alternative mechanism underlying CIK cell-mediated cytotoxicity (in the presence of HSP90) against BL cells.

In the second publication, Our research is concentrated on the exploration of the prospective application of non-oncology drugs in conjunction with epigenetic agents for the management of hematological malignancies (including leukemia and multiple myeloma) as well as liver cancer. Within this investigative framework, meticrane, a Thiazide diuretic traditionally employed for essential hypertension, emerges as a subject of scrutiny due to its underexplored anticancer properties. Consequently, our study endeavors to elucidate the anticancer potential of meticrane in the context of hematological malignancies and hepatocarcinoma cell lines. Preliminary results indicate that meticrane, administered in isolation or in combination with cytokine-induced killer (CIK) cells, demonstrated limited or negligible efficacy in treating leukemia, myeloma, and hepatocellular carcinoma cells. Subsequent investigations sought to evaluate the cumulative effects achieved through the co-administration of meticrane with established epigenetic agents. These combinations of meticrane and epigenetic inhibitors exhibited discernible additive or even synergistic impacts on leukemia and liver cancer cells, thereby potentially mitigating the inherent toxicity often associated with standalone epigenetic drug regimens in clinical settings. Noteworthy is the observation that meticrane displayed a fractionally significant binding affinity compared to a majority of HDACs. In summation, our investigation centered on meticrane, a non-oncological drug with clinical applications, in tandem with epigenetic inhibitors as a prospective contender for combination therapy.

In the third publication, There is a need to develop markers to select cases that are expected to benefit before or early in treatment and to improve the therapeutic effect of combination therapy with other molecularly targeted agents. several studies have established lncRNA-based prognostic models for clinical characterization in AML patients (Wang et al., 2020a; Zhao et al., 2021; Zhang et al., 2022). In light of these considerations, we embarked on an inquiry into long non-coding RNAs (lncRNAs) that could potentially serve as mediators bridging two converging processes: heat shock proteins and ferroptosis. These processes hold a discernible interconnectedness in the context of tumorigenesis. Employing an exhaustive bioinformatics approach, we successfully identified four distinct lncRNAs (AL138716.1, AC000120.1, AC004947.1, and LINC01547) bearing significant prognostic implications in the milieu of acute myeloid leukemia (AML) patients. Notably, within this group, two lncRNAs (AC000120.1 and LINC01547) have been previously associated with AML, reinforcing their relevance in this context, while AC004947.1 is noted for its oncogenic potential (Zhu et al., 2023). The resulting signature unveiled a distinct survival trajectory, with high-risk patients exhibiting diminished survival probabilities, and conversely, low-risk patients displaying more favorable outcomes. Importantly, we believe our work marks the first endeavor to devise a predictive model centered around lncRNAs that potentially underlie the intersection of heat shock proteins and ferroptosis within the framework of AML.

In our fourth publication, with a particular focus on hepatocellular carcinoma (HCC), this article attempts to investigate possible immunoautophagy-associated long noncoding RNA (lncRNA) signatures, primarily for predicting survival in HCC patients. Drawing from the repertoire of these lncRNAs, we devised a predictive model comprising three specific lncRNAs, namely MIR210HG, AC099850.3, and CYTOR. This meticulously constructed signature emerged as an independent and robust prognostic determinant for clinical prognosis in hepatocellular carcinoma (HCC) patients. Remarkably, the influence of these three lncRNAs (MIR210HG, AC099850.3, and CYTOR) integrated within the signature extended to the modulation of liver cancer's proliferative and growth dynamics (Wang et al., 2019; Wu et al., 2021a; Liu and Geng, 2022). Collectively, our findings shed light on the intricate interrelationship between lncRNAs and the survival outcomes of cancer patients, thereby suggesting their potential as viable targets for therapeutic interventions aimed at enhancing clinical outcomes in the realm of cancer patients.

4.2 Future perspectives

In this thesis, our investigation represents an inaugural endeavor in demonstrating that the incorporation of HSP90 inhibitors can synergistically enhance the cytotoxic potency of cytokine-induced killer (CIK) cells. This augmentation is achieved via the mediation of the Fas/FasL signaling cascade, which subsequently instigates caspase3/7-dependent apoptotic pathways. While deeper insights can potentially be gleaned from subsequent *in vivo* experiments, our current preclinical study marks a pioneering attempt to elucidate the compatibility of cancer immunotherapy involving CIK cells in tandem with HSP90 inhibitors, specifically within the context of Burkitt's lymphoma. The functional aspect of the cytotoxicity of CIK cells via the NKG2D/NKG2DL signaling pathway and/or Fas/FasL signaling has also been widely discussed in the literature, especially for NKG2D/NKG2DL in hematological malignancies (Laport et al., 2011). The utilization of HSP90 inhibitors in conjunction with cytokine-induced killer (CIK) cells can potentially be extended to encompass the treatment of additional hematological malignancies, including but not limited to acute myeloid leukemia (AML), multiple myeloma (MM), chronic myeloid leukemia (CML), chronic lymphocytic leukemia (CLL), and non-Hodgkin's lymphoma. This expanded scope aims to assess the potential of HSP90 inhibitors in augmenting the cytotoxicity of CIK cells and to delve into the underlying mechanistic intricacies governing this synergy. Histone deacetylases (HDACs) constitute a class of epigenetic enzymes that have garnered substantial attention as potential anti-tumor therapeutic targets (Wang et al., 2020b; Ramaiah et al., 2021; Roca et al., 2022; Tang et al., 2022). Emerging research has unveiled an expanding array of non-histone proteins that serve as substrates for HDACs, encompassing a diverse spectrum from molecular chaperones to cytoskeletal proteins and transcription factors. Notably, within this landscape, heat shock protein 90 (Hsp90) emerges as an indispensable molecular chaperone within eukaryotic systems. Recently, investigations have unveiled intricate and significant interactions between Hsp90 and HDACs, further accentuating the complexity of their interplay (Li et al., 2022a). Looking ahead, the prospective availability of dual inhibitors, exemplified by HSP90-HDAC inhibitors, holds the promise of further refining the cytotoxic efficacy of CIK cells in the milieu of Burkitt's lymphoma, thereby contributing to a more comprehensive understanding of this therapeutic approach.

Leveraging openly accessible RNA sequencing datasets in conjunction with clinical information, this dissertation successfully delineates a distinctive cohort of long non-coding RNAs (lncRNAs) intricately linked to the survival outcomes of two distinct cancers, namely acute myeloid leukemia (AML) and hepatocellular carcinoma (HCC). These identified lncRNAs exhibit the potential to serve as discerning classifiers for the stratification of cancer patients upon initial diagnosis. It is pertinent to acknowledge a noteworthy constraint inherent in this thesis, whereby the analysis is primarily founded on comprehensive bioinformatics approaches, necessitating the imperative of rigorous experimental validation for substantiation and robustness. Furthermore, they furnish valuable insights into potential epigenetic targets, thereby presenting novel vistas for the development of cancer therapies. The cumulative strengths of these findings distinctly amplify the dissertation's significance, fortifying its potential contributions to the realm of cancer research and therapeutic advancements.

4.3 References

- Riley, R.S.; June, C.H.; Langer, R.; Mitchell, M.J. Delivery Technologies for Cancer Immunotherapy. *Nat Rev Drug Discov* **2019**, *18*, 175–196, doi:10.1038/s41573-018-0006-z.
- Kennedy, L.B.; Salama, A.K.S. A Review of Cancer Immunotherapy Toxicity. *CA Cancer J Clin* **2020**, *70*, 86–104, doi:10.3322/caac.21596.
- Wu, X.; Zhang, Y.; Li, Y.; Schmidt-Wolf, I.G.H. Increase of Antitumoral Effects of Cytokine-Induced Killer Cells by Antibody-Mediated Inhibition of MICA Shedding. *Cancers (Basel)* **2020**, *12*, 1818, doi:10.3390/cancers12071818.
- Fan, X.-Y.; Wang, P.-Y.; Zhang, C.; Zhang, Y.-L.; Fu, Y.; Zhang, C.; Li, Q.-X.; Zhou, J.-N.; Shan, B.-E.; He, D.-W. All-Trans Retinoic Acid Enhances Cytotoxicity of CIK Cells against Human Lung Adenocarcinoma by Upregulating MICA and IL-2 Secretion. *Sci Rep* **2017**, *7*, 16481, doi:10.1038/s41598-017-16745-z.
- Nwangwu, C.A.; Weiher, H.; Schmidt-Wolf, I.G.H. Increase of CIK Cell Efficacy by Upregulating Cell Surface MICA and Inhibition of NKG2D Ligand Shedding in Multiple Myeloma. *Hematol Oncol* **2017**, *35*, 719–725, doi:10.1002/hon.2326.
- Wu, X.; Sharma, A.; Oldenburg, J.; Weiher, H.; Essler, M.; Skowasch, D.; Schmidt-Wolf, I.G.H. NKG2D Engagement Alone Is Sufficient to Activate Cytokine-Induced Killer Cells While 2B4 Only Provides Limited Coactivation. *Front Immunol* **2021**, *12*, 731767, doi:10.3389/fimmu.2021.731767.
- Zhao, C.; Wang, Y.; Tu, F.; Zhao, S.; Ye, X.; Liu, J.; Zhang, J.; Wang, Z. A Prognostic Autophagy-Related Long Non-Coding RNA (ARlncRNA) Signature in Acute Myeloid Leukemia (AML). *Front Genet* **2021**, *12*, 681867, doi:10.3389/fgene.2021.681867.
- Zhang, L.; Ke, W.; Hu, P.; Li, Z.; Geng, W.; Guo, Y.; Song, B.; Jiang, H.; Zhang, X.; Wan, C. N6-Methyladenosine-Related LncRNAs Are Novel Prognostic Markers and

- Predict the Immune Landscape in Acute Myeloid Leukemia. *Front Genet* **2022**, *13*, 804614, doi:10.3389/fgene.2022.804614.
- Wang, D.; Zeng, T.; Lin, Z.; Yan, L.; Wang, F.; Tang, L.; Wang, L.; Tang, D.; Chen, P.; Yang, M. Long Non-Coding RNA SNHG5 Regulates Chemotherapy Resistance through the MiR-32/DNAJB9 Axis in Acute Myeloid Leukemia. *Biomed Pharmacother* **2020**, *123*, 109802, doi:10.1016/j.biopha.2019.109802.
- Zhu, Y.; He, J.; Li, Z.; Yang, W. Cuproptosis-Related LncRNA Signature for Prognostic Prediction in Patients with Acute Myeloid Leukemia. *BMC Bioinformatics* **2023**, *24*, 37, doi:10.1186/s12859-023-05148-9.
- Liu, Y.; Geng, X. Long Non-Coding RNA (LncRNA) CYTOR Promotes Hepatocellular Carcinoma Proliferation by Targeting the MicroRNA-125a-5p/LASP1 Axis. *Bioengineered* **2022**, *13*, 3666–3679, doi:10.1080/21655979.2021.2024328.
- Wang, Y.; Li, W.; Chen, X.; Li, Y.; Wen, P.; Xu, F. MIR210HG Predicts Poor Prognosis and Functions as an Oncogenic LncRNA in Hepatocellular Carcinoma. *Biomed Pharmacother* **2019**, *111*, 1297–1301, doi:10.1016/j.biopha.2018.12.134.
- Wu, F.; Wei, H.; Liu, G.; Zhang, Y. Bioinformatics Profiling of Five Immune-Related LncRNAs for a Prognostic Model of Hepatocellular Carcinoma. *Front Oncol* **2021**, *11*, 667904, doi:10.3389/fonc.2021.667904.
- Laport, G.G.; Sheehan, K.; Baker, J.; Armstrong, R.; Wong, R.M.; Lowsky, R.; Johnston, L.J.; Shizuru, J.A.; Miklos, D.; Arai, S.; et al. Adoptive Immunotherapy with Cytokine-Induced Killer Cells for Patients with Relapsed Hematologic Malignancies after Allogeneic Hematopoietic Cell Transplantation. *Biol Blood Marrow Transplant* **2011**, *17*, 1679–1687, doi:10.1016/j.bbmt.2011.05.012.
- Tang, C.; Wang, X.; Jin, Y.; Wang, F. Recent Advances in HDAC-Targeted Imaging Probes for Cancer Detection. *Biochim Biophys Acta Rev Cancer* **2022**, *1877*, 188788, doi:10.1016/j.bbcan.2022.188788.

- Ramaiah, M.J.; Tangutur, A.D.; Manyam, R.R. Epigenetic Modulation and Understanding of HDAC Inhibitors in Cancer Therapy. *Life Sci* **2021**, *277*, 119504, doi:10.1016/j.lfs.2021.119504.
- Roca, M.S.; Moccia, T.; Iannelli, F.; Testa, C.; Vitagliano, C.; Minopoli, M.; Camerlingo, R.; De Riso, G.; De Cecio, R.; Bruzzese, F.; et al. HDAC Class I Inhibitor Domatinostat Sensitizes Pancreatic Cancer to Chemotherapy by Targeting Cancer Stem Cell Compartment via FOXM1 Modulation. *J Exp Clin Cancer Res* **2022**, *41*, 83, doi:10.1186/s13046-022-02295-4.
- Wang, X.; Waschke, B.C.; Woolaver, R.A.; Chen, S.M.Y.; Chen, Z.; Wang, J.H. HDAC Inhibitors Overcome Immunotherapy Resistance in B-Cell Lymphoma. *Protein Cell* **2020**, *11*, 472–482, doi:10.1007/s13238-020-00694-x.
- Li, C.; Tu, J.; Han, G.; Liu, N.; Sheng, C. Heat Shock Protein 90 (Hsp90)/Histone Deacetylase (HDAC) Dual Inhibitors for the Treatment of Azoles-Resistant *Candida Albicans*. *Eur J Med Chem* **2022**, *227*, 113961, doi:10.1016/j.ejmech.2021.113961.

5. Acknowledgements

My four years in Bonn encompassed profoundly transformative experiences that have left an indelible mark on my personal and academic journey. Expressing my profound gratitude is imperative for the immense growth and learning I have undergone, both in the realm of scientific inquiry and life's broader dimensions. I take this opportunity to extend my heartfelt appreciation to every individual who has contributed to the realization of this paper.

Foremost, I extend my gratitude to my esteemed supervisor, Prof. Dr. Ingo Schmidt-Wolf, whose acceptance of me as his doctoral student marked a pivotal juncture. His unwavering support in guiding my scientific exploration, invaluable discussions, and astute suggestions have been instrumental. Additionally, I am indebted to him for imparting the essence of scientific inquiry and fostering my growth as a researcher. My gratitude extends to my second supervisor, Prof. Dr. Ulrich Jaehde, for his insightful discussions and invaluable recommendations present in the annual committee report. His support in reviewing this paper stands as a testament to his dedication. The role of Prof. Markus Essler and Prof. Matthias Schmid in my thesis committee is deeply appreciated.

I acknowledge Amit Sharma for his constructive suggestions that enhanced my English writing, Yulu Wang for his unwavering support in my research and personal life, and the indispensable assistance of Dagmar Bolz and Tanja Schuster during my Ph.D. journey. I recognize Fitria Setiawan and Oliver Rudan for their impeccable organization and seamless lab coordination. The support and camaraderie of my Chinese colleagues (Xiaolong Wu, Ying Zhang, Peng Chen, Yutao Li) enriched my work and daily life, which I am profoundly grateful for.

Lastly, but importantly, My heartfelt appreciation is reserved for my cherished parents and friends, whose steadfast belief in me and unwavering spiritual and life support have illuminated my path. Your enduring love and unwavering commitment have played a pivotal role in shaping the trajectory of my Ph.D. journey.

In conclusion, the time spent in Bonn has been a privilege and an education, for which I am immensely thankful.